AD-A167 801   RUNWAY RUBBER REMOVAL SPECIFICATION DEVELOPMENT: FIELD   1/2
EVALUATION RESULTS. (U) NEW MEXICO ENGINEERING RESEARCH
INST ALBUQUERQUE R A GRAUL ET AL. JUL 85
UNCLASSIFIED   NMERI-WA5-6-(5.04) DOT/FAA/PM-85/32   F/G 1/5   NL

DOT/FAA/PM-85/32
ESL-TR-85-63

Program Engineering
and Maintenance Service
Washington, D.C. 20591

AD-A167 801

Runway Rubber Removal
Specification Development:
Field Evaluation Results
and Data Analysis

②

Richard A. Graul
Lary R. Lenke

New Mexico Engineering
  Research Institute
Box 25, University of New Mexico
Albuquerque, New Mexico 87131

July 1985

Interim Report
(July 1984 to July 1985)

DTIC
ELECTE
S MAY 1 3 1986
D
D

DTIC FILE COPY

U.S. Department
of Transportation
**Federal Aviation
Administration**

Department of Defense
**USAF Engineering & Services
Center**

86 5 13 039

NOTICE

This document is disseminated under the sponsorship of the Department of Transportation in the interest of information exchange. The United States Government assumes no liability for the contents or use thereof.

The United States Government does not endorse products or manufacturers. Trade or manufacturer's names appear herein solely because they are considered essential to the object of this report.

1. Report No.	2. Government Accession No.	3. Recipient's Catalog No.
DOT/FAA/PM-85/32	ADA 167801	

4. Title and Subtitle	5. Report Date
Runway Rubber Removal Specification Development: Field Evaluation Results and Data Analysis	July 1985
	6. Performing Organization Code
	NMERI WA5-6-(5.04)

7. Author's)	8. Performing Organization Report No.
Richard A. Graul, Lary R. Lenke	ESL-TR-85-63

9. Performing Organization Name and Address	10. Work Unit No. (TRAIS)
New Mexico Engineering Research Institute Box 25, University of New Mexico Albuquerque, New Mexico 87131 and *	
	11. Contract or Grant No.
	F29601-84-C-0080

12. Sponsoring Agency Name and Address	13. Type of Report and Period Covered
U.S. Department of Transportation Federal Aviation Administration Program Engineering and Maintenance Service Washington, D.C. 20591	Interim Report July 1984 - July 1985
	14. Sponsoring Agency Code
	APM 740

15. Supplementary Notes

*Headquarters Air Force Engineering and Services Center
Tyndall AFB FL 32403-6001

16. Abstract

The phenomenon of runway touchdown zone rubber buildup is a potentially hazardous problem. Rubber buildup covers the runway surface and occludes the surface texture. This results in a reduced wet friction coefficient between the runway and the aircraft tires.

Presently, methods and equipment available for evaluating the wet friction coefficient are expensive and require highly trained personnel. Therefore, most airport and airbase managers rely exclusively on visual impressions of rubber buildup in lieu of quantitative measurements.

The use of pavement surface texture measurements is generally thought capable of determining pavement friction levels. This report discusses use of four economical texture measurement techniques and their relationship to friction levels as determined by the Mu-Meter.

Good correlations were obtained by relating pavement surface texture measurements to friction. However, predictive errors preclude the use of these models in lieu of friction measurements for use in rubber removal guidelines. Keywords;

17. Key Words	18. Distribution Statement
Runway Pavement Texture Measurement Friction Friction Measurement Rubber Buildup Mu-Meter Rubber Removal Stereophotography; Hydroplaning	This document is available to the public through the National Technical Information Service Springfield, Virginia 22161

19. Security Classif. (of this report)	20. Security Classif. (of this page)	21. No. of Pages	22. Price
UNCLASSIFIED	UNCLASSIFIED	106	

Form DOT F 1700.7 (8-72)   Reproduction of completed page authorized

A

PREFACE

The authors extend their appreciation to the following individuals at the New Mexico Engineering Research Institute for their help during the field validation study. The authors wish to thank: Mr. S. Scales, Mr. V. Cassino, Mr. J. Parra, and Mr. D. L. Standiford for their help during the field testing.

Additional appreciation is extended to: Professors Clifford Qualls and Edward Bedrick of the University of New Mexico Department of Mathematics and Statistics for their helpful insights into the analysis of this data; the FAA Technical Center for use of the Mu Meter and tow vehicle during this research effort, the various airport and airbase managers and rubber removal contractors for their cooperation; and the various members of ASTM E-17 for their help and guidance in understanding tire-pavement traction.

i
(The reverse of this page is blank.)

TABLE OF CONTENTS

LIST OF FIGURES

LIST OF FIGURES (CONCLUDED)

LIST OF TABLES

(The reverse of this page is blank.)

OBJECTIVE

The objective of this effort is to develop a procedures for determining when runway rubber removal is needed and when rubber has been satisfactorily removed. These developed procedures were correlated in a designed field equipment with friction measurements obtained using a self-watering Mu-Meter. The results of this correlation study are to be used in the development of contract specifications for runway rubber removal.

BACKGROUND

The higher operational speeds and heavier gross weights of modern aircraft require high shear forces generated at the tire-pavement interface for safe operation. These shear forces are dependent upon the available tire-pavement friction. Dry friction between the tire and clean pavement does not present a problem, because of the chemical and physical properties of the tire rubber and the mechanical properties of the tire structure. However, once a lubricant, most commonly water from rainfall, is introduced at this interface, a serious loss of friction can occur. This loss of friction can be slight, as on a damp pavement when the operator must reduce frictional demand during maneuvering to maintain directional control, or significant, as in the case of hydroplaning where the operator loses directional control of the vehicle.

Once a contaminant other than rain water is placed upon the pavement, the operational characteristics of the pavement change. Specifically, on a runway, rubber deposits formed by landing aircraft can dramatically reduce the wet frictional performance of the runway touchdown zone pavement. Since these touchdown zones are subjected to impact of the tires during landing, a certain amount of rubber is transferred from the tire to the pavement as a result of heat and abrasion produced when the aircraft tires spin up. This rubber is deposited on the pavement surface as thin layers that adhere to the pavement materials. As subsequent rubber deposits increase the buildup to a significant thickness, several problems appear. They are (1) obliteration of pavement markings, (2) accumulation of loose debris on the runway surface, and (3) reduced wet frictional levels. Maintenance action is required to eliminate or reduce these problems to an acceptable level. Painting of pavement markings is a regular activity at all active airports; periodic sweeping of runways removes the loose debris; and rubber removal may restore the pavement's frictional properties (Reference 1).

Currently both the United States Air Force (USAF) and the Federal Aviation Administration (FAA) periodically recommend removal of runway touchdown-zone rubber deposits. Presently, the airport or base pavement engineer must rely heavily upon visual impressions or experience or both to determine when rubber removal is required and when removal of rubber has adequately improved the pavement's frictional characteristics. Unfortunately, test results obtained by the USAF indicate that this visual/experience method of inspecting rubber deposits does not correlate well with the frictional results obtained with a Mu-Meter (Reference 2). Since the Mu-Meter or other tire-pavement friction measurement equipment is expensive and requires highly trained

personnel, it is unavailable at many airfields. As a result, a cost-effective rubber-removal program is impractical without guidelines indicating when rubber buildup is sufficient to warrant removal.

The New Mexico Engineering Research Institute (NMERI) was tasked to develop an alternate procedure to quantify amounts of rubber buildup and their effect upon the frictional characteristics of the runway pavement. This project was subdivided into the following five phases.

Phase I--Rubber Buildup Criteria and Evaluation Procedure Development

This phase consisted of a review of existing techniques for evaluating surface friction. Based upon this review, five evaluation procedures were selected which require little special training, are insensitive to operator change, and are cost effective (less than $10,000 per installation for implementation).

Phase II--Rubber Removal Techniques and Equipment Review

Phase II required review and research of existing rubber removal techniques. Evaluation of effectiveness, cost, simplicity, safety, and environmental effects was ascertained when the reviewed techniques are applied solely to porous friction surfaces (PFS).

Phase III--Rubber Buildup Parameters Development

Phase III required the field testing of the evaluation procedures selected in Phase I. This evaluation was conducted before and after rubber removal at selected airports and air bases. Friction measurements using the Mu-Meter along with the five candidate procedures were obtained with subsequent analysis and correlation. The field testing was conducted for various surface types including portland cement concrete (PCC), asphalt concrete (AC) and PFS pavements.

Phase IV--Rubber Removal Specifications Development

This phase incorporates the results of Phases I and III into a concise specification for rubber-removal contracts. The intent of this specification is to eliminate the undesirable attributes of existing visual/experience methods for determining rubber removal quality. Thus an efficient rubber removal program may be initiated.

Phase V--Permeability Equipment Evaluation for Porous Friction Surfaces

Phase V required a review of existing techniques for evaluating permeability of porous friction surfaces. Based upon this review, the application of these techniques was evaluated, and measurement techniques recommended for use on PFS.

Phases I, II, and V have been completed and are reported upon elsewhere (References 3, 1, and 4). Phase IV is currently in progress and will be reported upon at a later date.

SCOPE

This report is a discussion of Phase III. Included are a review of tire-pavement friction theory, both theoretical and empirical, and description of selected field test techniques and design of the field evaluation experiment. Following this review, a description of test sites, test distributions, regression modelling of Mu-Meter friction levels using pavement surface texture measurements, and the results of this analysis are presented.

SECTION II
TIRE-PAVEMENT FRICTION

THEORETICAL BACKGROUND

The development of friction between an aircraft tire and the runway pavement is a complex phenomenon. As stated in an earlier report by the authors (Reference 3), many factors influence the aircraft-wet pavement performance. Yager (Reference 5) describes these factors in the flowchart shown in Figure 1. This flowchart emphasizes the effects of principal weather, aircraft runway, and pilot factors which interact to affect the aircraft ground-handling performance during wet runway conditions. To ensure ground handling performance on wet runways, several approaches are necessary to reduce the severity of the problem. These include continued pilot education and training, implementation of procedures to monitor wet runway conditions, implementation of procedures to notify pilots when slippery runway conditions exist, improvement of antiskid brake systems and prompt remedial treatment of runway drainage problems. It is also clear that the quality of the pavement, from a surface texture standpoint, must be ensured at the design, construction and maintenance levels as changes continuously occur throughout the life of the pavement.

Tire-pavement friction is formed by a combination of adhesional and hysteretic friction. Kummer (Reference 6) pictorially represents these components in Figure 2. The adhesional component depends on both the surface area of bonding and the intensity of the bonding, while the hysteretic friction is generated by the surface roughness. To develop a better understanding of these mechanisms, a historical overview of each will be given.

Adhesional Friction Theories

In 1968 Schallamach (Reference 7) presented a review of adhesional friction. In this article, he stressed the importance of the rate temperature equivalence principle first proposed by Williams, Landel, and Ferry (Reference 8). This principle expressed by the Williams, Landel, and Ferry (WLF) equation allows for horizontal shifts in friction versus sliding speeds plots that help researchers correct for temperature and develop "friction master curves." An example of these curves is given in Figure 3 (Reference 9). These master curves are unique for any combination of rubber and surface. For many years researchers have tried unsuccessfully to develop a theory of adhesional friction which models these curves.

Various theoretical models have been used in developing a theory of adhesional friction. Schallamach (Reference 10) used a concept of molecular bonding, akin to Van der Waals bonds, but considered their making and breaking as separately activated processes. A newly formed bond does not sustain any force until a relative displacement occurs, at which time the bond breaks and a new unstressed bond is formed. This explains the slip-stick mechanism of adhesional friction but does not explain friction at either very low or very high frequencies. Also the peak value is related to an adhesional energy concept that depends on both the surface and the rubber.

4
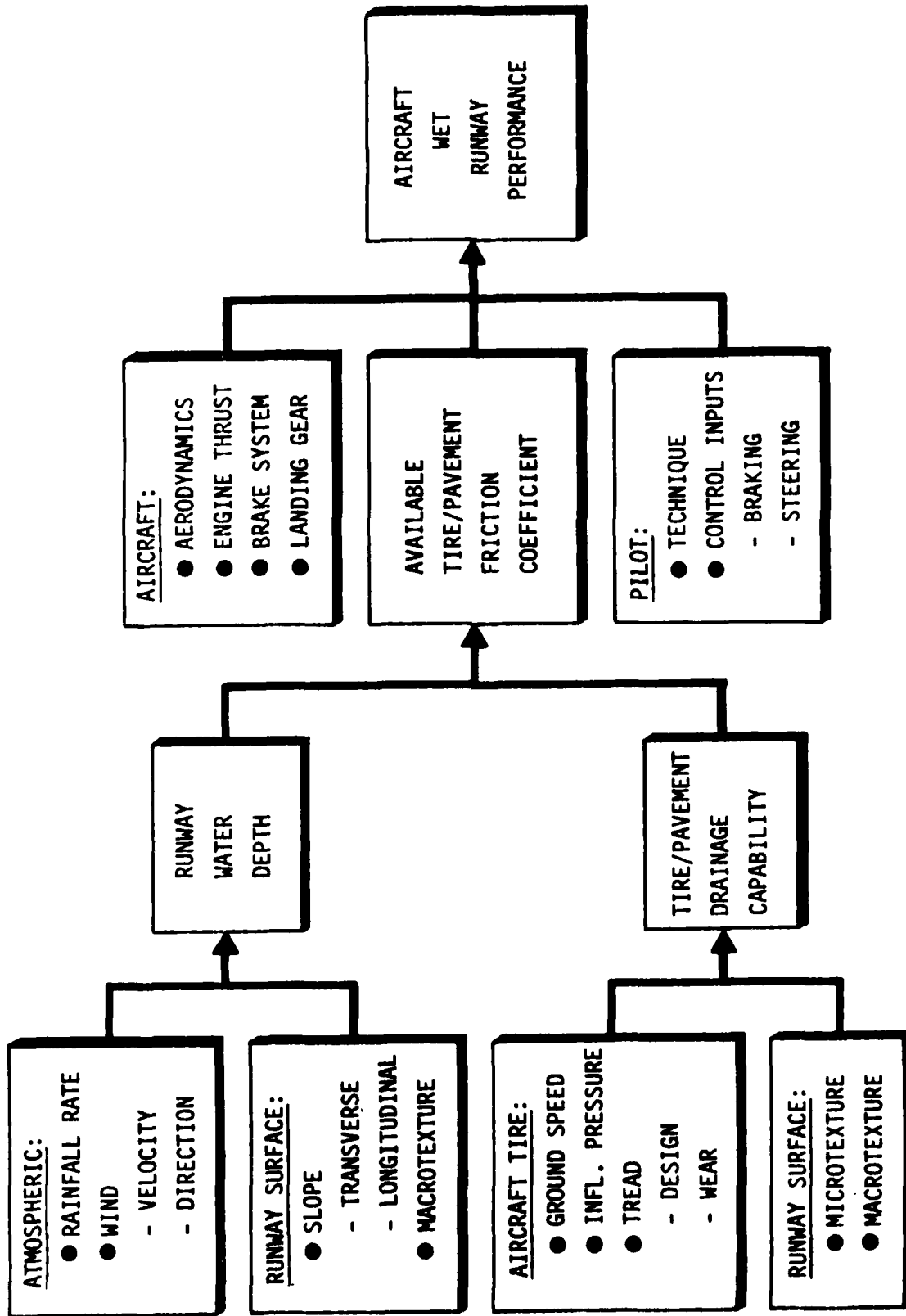
FIGURE 1. FACTORS AFFECTING AIRCRAFT WET RUNWAY PERFORMANCE (REFERENCE 5)

5

P

RUBBER ELEMENT

$F \approx F_A + F_H$

AGGREGATE

$\longrightarrow V \longrightarrow$

BINDER

$F_{Ai} = SA_i$

ADHESION COMPONENT $\quad F_A = S \sum_1^n A_i$

HYSTERESIS COMPONENT $\quad F_H = C \sum_1^n (E_c - E_e)_i$

$(E_c - E_e)_i$

E_{ci}

E_{ei}

$F_{Hi} = C(E_c - E_e)_i$
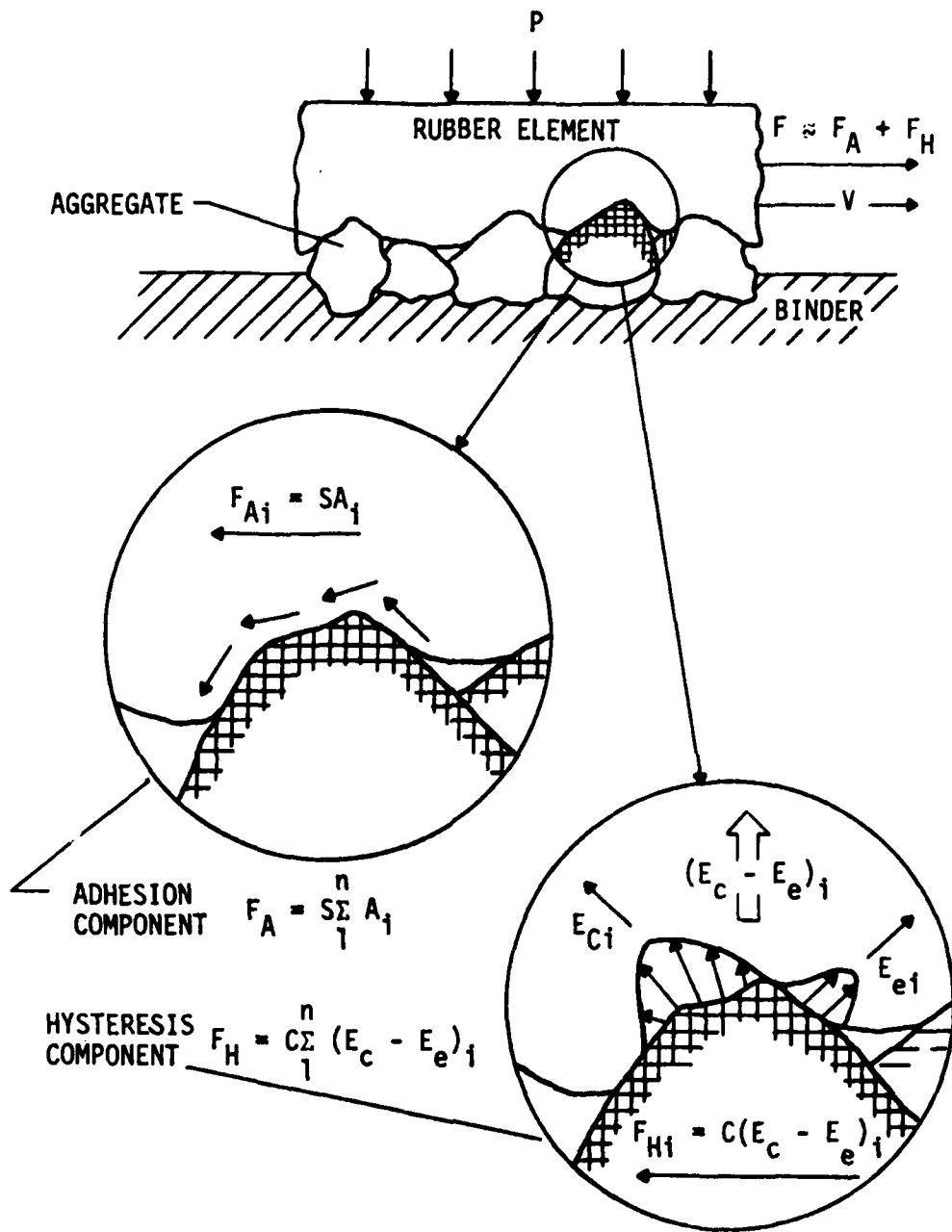
FIGURE 2. MECHANISM OF RUBBER FRICTION (REFERENCE 6)

6
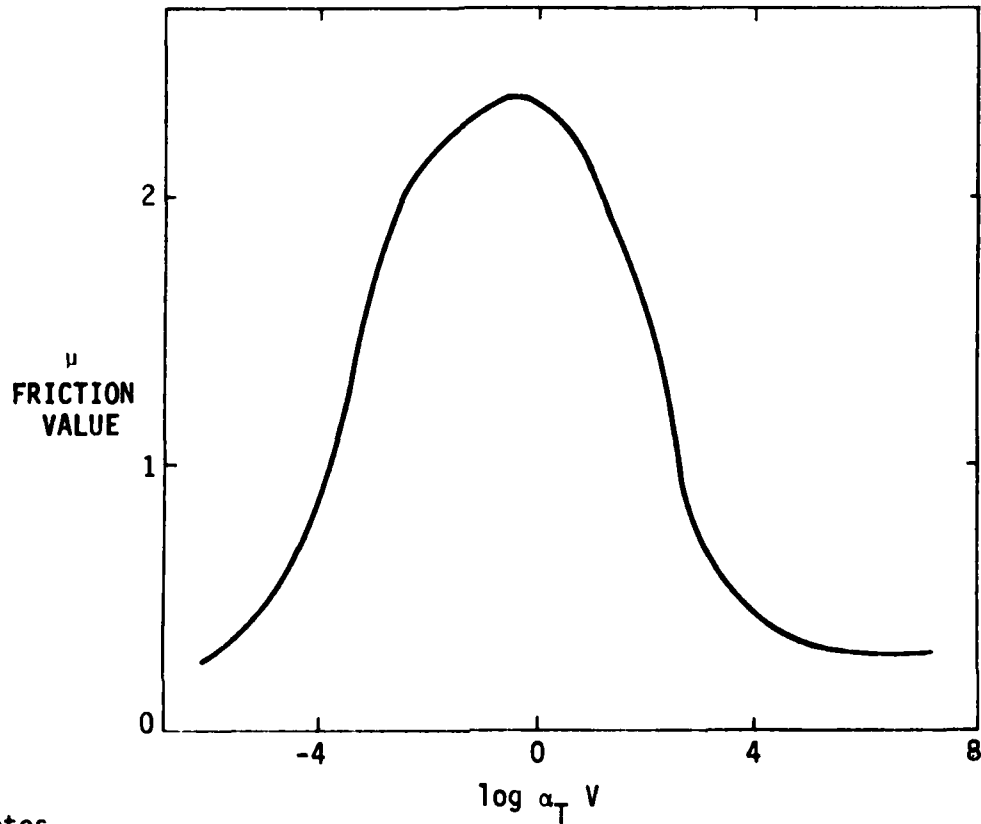
Notes

α_T = Temperature frequency shift as determined by the WFL equation

V = Rubber excitation frequency proportional to
   sliding velocity

FIGURE 3. FRICTION MASTER CURVE (REFERENCE 9)

Schallamach's proposed theory assumed independent bonding of the rubber molecules. This independence between bonds did not predict static friction, since independent bonds would break under the smallest force, just as a Newtonian liquid flows under the slightest shear stress. Hatfield and Rathman (Reference 11) suggested that a finite domain of bonding exists. This theory explained static friction as the result of an equilibrium forming between making and breaking of bonds, which could permit a small finite force to exist.

Savkoor's theory (Reference 12), which becomes quite involved, assumes these finite domains of bonding and Van der Waals bonding, yet uses energy criteria rather than force criteria for bond breakage. This theory was quite successful in predicting adhesional energy behavior; however, equality between stored and bonded energy is not a criterion for bond breakage, and a bonded asperity that is not strained should not support a force.

Kummer (Reference 6) describes adhesional friction by means of an equivalent electrical roughness and a concept of microhysteresis. He describes molecular forces as a series of equivalent sawtooth roughness, and describes the energy losses as microdeformation losses within the rubber. This derivation allows him to describe both adhesional and hysteretic friction as being two processes dependent upon the same rubber properties. However, this theory assumes that the rubber undergoes cyclic deformation due to the making and breaking of bonds, yet does not describe how these bonds are broken. Secondly, this theory is generalized from consideration of cleavage planes of ionic crystals, making it difficult to explain rubber friction on smooth metal surfaces.

Various others have attempted to explain this controversial process of adhesional friction, but detailed descriptions of their work are beyond the scope of this report.

Hysteretic Friction Theories

At this time attention will be turned to hysteretic friction. To make this phenomonen easier to understand, a brief history of analytical modeling follows.

In 1966, Kummer published the **Unified Theory of Rubber and Tire Friction** (Reference 6). In this classical work, he described the mechanism of hysteretic friction to be a function of asperity shape, height and density, and the draping and damping properties of the rubber. He modelled the bulk rubber as a Kelvin element, and used this model and elastic-draping theory to describe both the volume of rubber deformed and the energy dissipated within this volume. In 1969, Hegmon (Reference 13) used the concept of conservation of strain energy coupled with the viscoelastic relaxation times of rubber to describe deformation or hysteretic losses of rubber. He also theorized that a specific volume of rubber is deformed during loading and that losses are generated within this volume. This derivation agrees in general with Kummer's, with the major difference being that the rubber damping was modelled by a Maxwell rather than a Kelvin model. Both Kummer and Hegmon describe the energy losses in the area of the displaced rubber.

8

Yandell (Reference 14) determined hysteretic losses, using a mechano-lattic analogy to calculate the stresses and deflections in a rubber slider of infinite length, unit width, and finite thickness, fastened to a rigid backing plate. He modeled the losses within a rubber block as an arrangement of eight Kelvin elements. Using this model and simple triangular asperities, his mathematical derivation describes the hysteretic losses as a function of changes in the stress flux of the rubber. This analogy allows energy dissipation to occur in rubber volumes larger than that which is displaced by the surface asperity. He further describes a condition of stress saturation. This condition occurs when residual stresses remain in the rubber at locations of low-stress contours.

As neither component of tire-pavement friction is clearly understood, controversy arises as to the importance of adhesional versus hysteretic friction. Yandell (Reference 14) hypothesizes that hysteretic friction is the primary cause of wet tire-pavement friction. Conversely, Hegmon (Reference 13) believes that the majority of this friction is caused by a suppressed but not completely damped adhesive friction component. Moore (Reference 15) also believes that the adhesional component of friction is the dominating factor at low sliding speeds. He bases this opinion on the tire having an essentially dry contact zone where these adhesional forces are generated. His model of wet tire-pavement friction is discussed later in this report.

EFFECTS OF PAVEMENT TEXTURE ON TIRE-PAVEMENT FRICTION

Two important features of the pavement govern its characteristics with regard to tire-pavement friction. These are the pavement's adhesional bonding potential and its texture. Since the pavement's adhesional bonding potential has not yet been identified, pavement engineers concentrate on the pavement's textural characteristics.

Pavement texture has been found to govern many aspects of the tire-pavement interaction. Among these are: noise generation, tire wear, and tire-pavement friction. As the main focus of this report is the role of pavement texture in tire-pavement friction, emphasis will be given there.

Pavement texture is generally divided into two segments according to typical profile wavelengths; these are termed macrotexture and microtexture, respectively. Moore (Reference 15) differentiates the macrotexture from the microtexture as follows. The individual asperities or stones in a pavement surface constitute the macrotexture, while the finer asperities (or grit) on the larger asperities (macrotexture) constitute the microtexture. Figure 4 illustrates the difference between macro- and microtexture. According to Moore, typical wavelengths (λ) associated with macrotexture are 6 to 20 mm (0.25 to 0.80 inch), and for microtexture are 10 to 100 μm (0.0004 to 0.004 inch).

The pavement's macrotexture performs two functions, the first of which is to provide drainage channels for dissipation of bulk water. Removal of this bulk water prevents the occurrence of dynamic hydroplaning under the leading edge of the tire. Second, the shape of the major asperity determines both the hysteretic losses generated by the tire rubber sliding over this asperity (Reference 14) and the local contact pressures generated at the tip of this asperity (Reference 15). Highly angular asperities, generally represented as

9
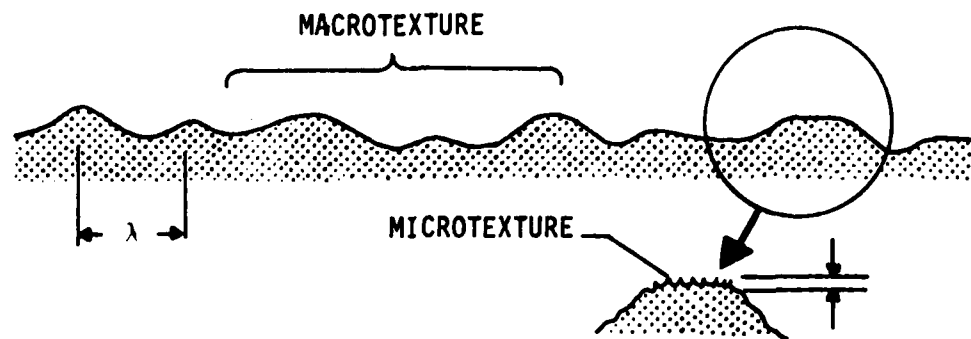
FIGURE 4. PAVEMENT ROUGHNESS INDICATING MACROTEXTURE AND MICROTEXTURE
(REFERENCE 15)

cones, cause local contact pressures greater than the viscous fluid pressures;
thereby, the bulk water is removed through the drainage channels and the vis-
cous film is broken, allowing the tip of the asperity to be in dry contact
with tread rubber. However, road aggregates do not retain this high angular-
ity because of wear and polish. Therefore the macrotexture predominantly
determines the frictional decline with speed on wet pavements. Its prime role
is to displace the bulk water so the microtexture can penetrate the thin films
remaining.

The pavement's microtexture on these larger protrusions must generate
these higher contact pressures necessary to penetrate the viscous film. Moore
(Reference 16), in his derivation of a viscous hydroplaning theory, estimates
the film thickness at the crest of a sinusoidal asperity to be approximately
that of average microtexture depth (see h* in Figure 5). Williams' study
(Reference 17) showed an optimum texture band of microtexture, from 10 to
100 μm average texture depth, at which wet friction was adequate yet tire
abrasive wear was not excessive. This texture band expressed in texture depth
confirmed Moore's estimated microtexture requirements. Therefore, micro-
texture determines the peak of a wet friction speed curve by determining a
percentage of the tire's footprint which remains in dry contact.

The importance of the pavement's microtexture cannot be overemphasized in
determining a peak friction value. However, this fraction of the pavement's
texture is both the hardest to quantify and the most variable, because of
seasonal variations and traffic polish.

10
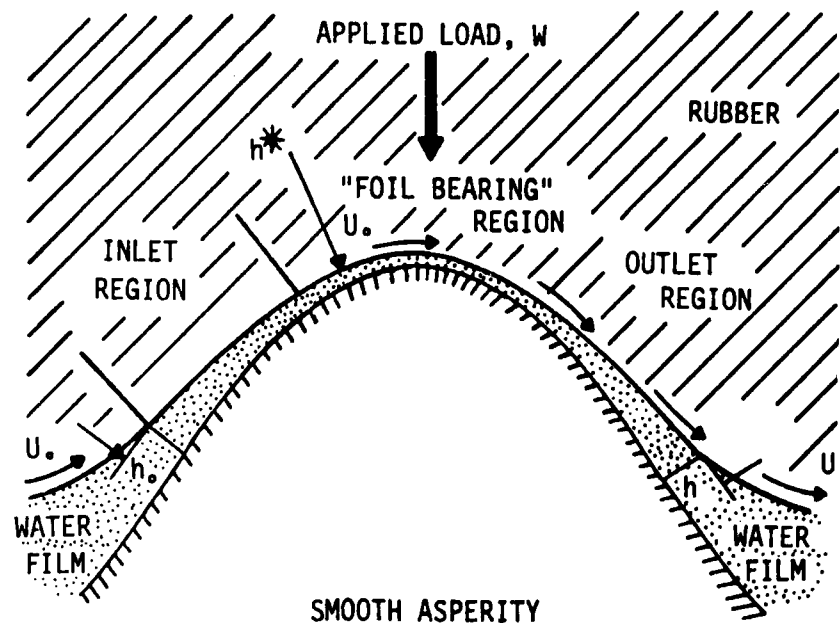
FIGURE 5. THE THREE CHARACTERISTIC REGIONS FOR THE CASE OF RUBBER
SLIDING ON A SMOOTH, SINUSOIDAL ASPERITY COVERED WITH A
THIN WATER FILM (REFERENCE 16)

HYDROPLANING

The loss of wet tire-pavement friction due to lubrication effects is
termed hydroplaning. Since tire-pavement traction becomes critical when the
pavement is wet, this case is of utmost importance. Hydroplaning manifests
itself in one or more of three forms: dynamic, viscous, and reverted rubber
hydroplaning.

Dynamic hydroplaning occurs when the fluid thickness between the tire and
the pavement is such that fluid inertial effects predominate in its removal.
Two conditions must be met for dynamic hydroplaning to occur. They are: (1)
fluid film thickness must be greater than some minimum (this can be as low as
0.05 inch for a Goodyear 29 by 16 aircraft tire placed on a Hawker Siddeley
Hunter F-6 Jet Fighter traveling at 1.47 times the critical hydroplaning speed
on very lightly brushed concrete [Reference 18]) and (2) a critical velocity
at which hydroplaning occurs must be reached. Horne and Joyner (Reference 19)
found that the critical velocity is proportional to the square root of the
tire inflation pressure. Namely, for aircraft tires $V_c = 1.8 \sqrt{P_{in}}$, where V_c
is the critical hydroplaning speed in m/s and P_{in} is the tire inflation
pressure in kilopascals.

Viscous hydroplaning, unlike dynamic hydroplaning, can occur at any speed
and requires only a thin film of water to be present. Moore (Reference 16)
describes the formation of a viscous film on an idealized surface and dis-
cusses the necessity of microtexture to penetrate this film. Full development

11

of a viscous film prevents the adhesional component of friction from forming, thereby drastically reducing the wet friction value. The film thicknesses encountered during viscous hydroplaning are slight; therefore, fluid viscous effects predominate. Thus, high localized stresses are required to penetrate these water films, making them much harder to remove than bulk water.

Reverted rubber hydroplaning is caused by heat generated at the tire-pavement interface during tire lockup on a damp pavement, causing the rubber to melt or revert back to its uncured state. Nybakken, Staples, and Clark (Reference 20) estimate interface temperatures to be of the order of 204°C to 315°C (400 to 600°F). Two possibilities seem to exist with reverted tire hydroplaning. The first possibility is the tire remains locked, and heat generation continues to occur at the interface between the tire and the damp pavement. This would cause steam generation beneath the tire as first proposed by Obertop (Reference 21). Horne and Joyner (Reference 19) expanded upon this concept and generalized that reverted rubber may form and possibly provide a seal around the periphery of the footprint, thus allowing a very thin film of water to be trapped in the footprint, which upon heating will cause steam. This steam pressure could lift the tire from contact with the pavement; as a result, the tire would slide upon molten rubber and a cushion of steam. The second possibility, suggested by Nybakken et al. (Reference 20), was that the reverted rubber, once formed, could not sustain the high localized stresses necessary to penetrate a viscous film of water, and a resultant process analogous to viscous hydroplaning would exist.

Yager (Reference 5) summarized the types of hydroplaning with the contributing and alleviating factors associated with them. Since wet tire-pavement friction is modelled as a combination of hydroplaning zones and dry contact zones interacting in a complex manner, tire and pavement engineers must rely heavily upon empirical modelling to determine optimum parameters for both the tire and the pavement.

EMPIRICAL MODELLING OF WET-TIRE TRACTION

Empirical modelling of wet tire traction evolves from Moore's generalization of the rolling tire friction zones (Reference 22). A pictorial representation of these zones is shown in Figure 6 and described below.

Sinkage, or Squeeze-Film Zone

Under wet conditions, the forward part of what under dry conditions would normally be considered the contact area floats on a thin film of water, the thickness of which decreases progressively as individual tread elements traverse the contact area. Since the tire, water-film, and road surface have virtually no relative motion in the contact area, the tread elements in effect attempt to squeeze out the water between rubber and pavement.

Draping, or Transition Zone

The draping zone begins when the tire elements, having penetrated the squeeze film, begin to drape over the major asperities of the surface and to make contact with the lesser asperities.

12
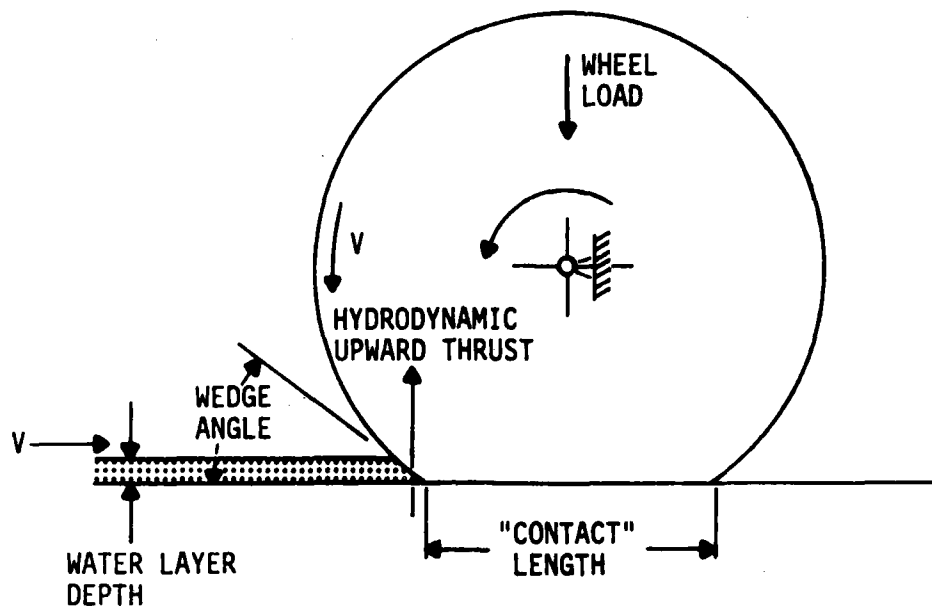
(a) GENERAL
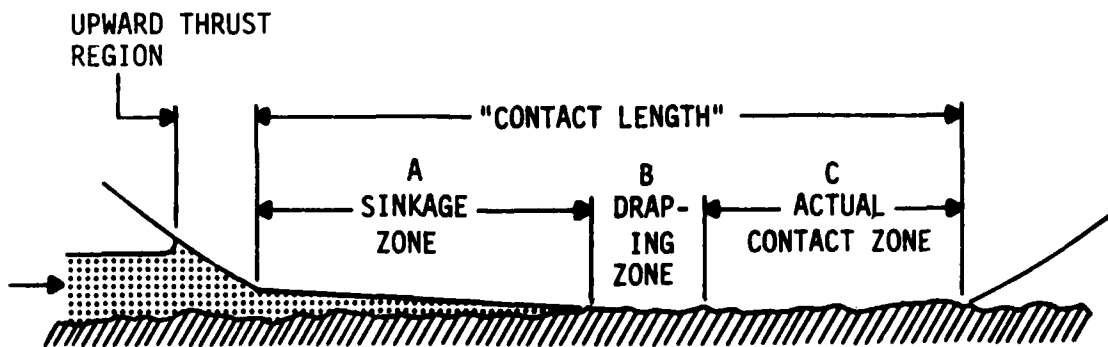
(b) THREE ZONES IN THE CONTACT AREA (ROUGH SURFACE)

FIGURE 6. WET-ROLLING BELOW THE HYDROPLANING LIMIT (REFERENCE 22)

13

Actual Contact, or Tractive Zone

This is the region where the tire elements, after draping, have attained an equilibrium position vertically on the surface. The length of this region depends on vehicle velocity; it occupies the rear portion of the overall contact area. Tractive effort is developed here.

The frictional forces generated in the tractive zone (Zone C) of the tire footprint depend on the tire's stiffness in the direction of slip and upon the slipping or sliding velocity of the tread elements. As very little slip occurs in an unyawed free-rolling tire, the tire's rolling resistance is not caused by a friction couple between the tread elements and the pavement, but by hysteretic energy losses in the tire structure caused by cyclic deformations and by drag forces. However, during acceleration, braking or cornering, the tread element slips in contact with the pavement. Empirical research has determined that the slip ratio, where wet pavement friction reaches a maximum, ranges from 6 to 12 percent. Both the peak friction value and the slip percent where it occurs is dependent upon many variables, including the tire's structural stiffness, aspect ratio, inflation pressure, operating mode (locked, yawed or transient slip), the tread pattern, physical and chemical characteristics of the tire, and textural and chemical characteristics of the pavement. Figure 7 demonstrates this general relationship between slip and friction.

Figure 7 shows three curves combined to explain the measured wet friction speed curves. The top curve or the theoretical friction curve is analogous to the friction master curves presented earlier. This curve depends on both the tread rubber and the pavement. The tire structural influence curve is dominated by structural properties of the tire and is substantially "slip distance dependent" and substantially independent of speed. These first two curves combine to form the experimentally derived wet friction speed curves (Reference 23).

The tire footprint hydroplaning model is not pictorically correct as to the geometry of the footprint. However, high-speed photos of tires passing over a glass plate have verified the existence of these three distinct zones (References 16, 24). This simplified model has been very useful in explaining the reduction of wet tire-pavement friction, and has enabled engineers to generalize about the role of pavement texture in this reduction of friction levels.

CURRENT SURFACE-CHARACTERIZATION TECHNIQUES

The pavement's surface texture governs its frictional response. An extensive literature search conducted by the authors reviewed current methods of both measuring surface texture and relationships between texture and friction (Reference 3). A review of methods used to characterize texture and applicable relationship will be reviewed.

The measurement techniques reviewed were divided into three categories according to how the textural property was measured. These three categories were

14
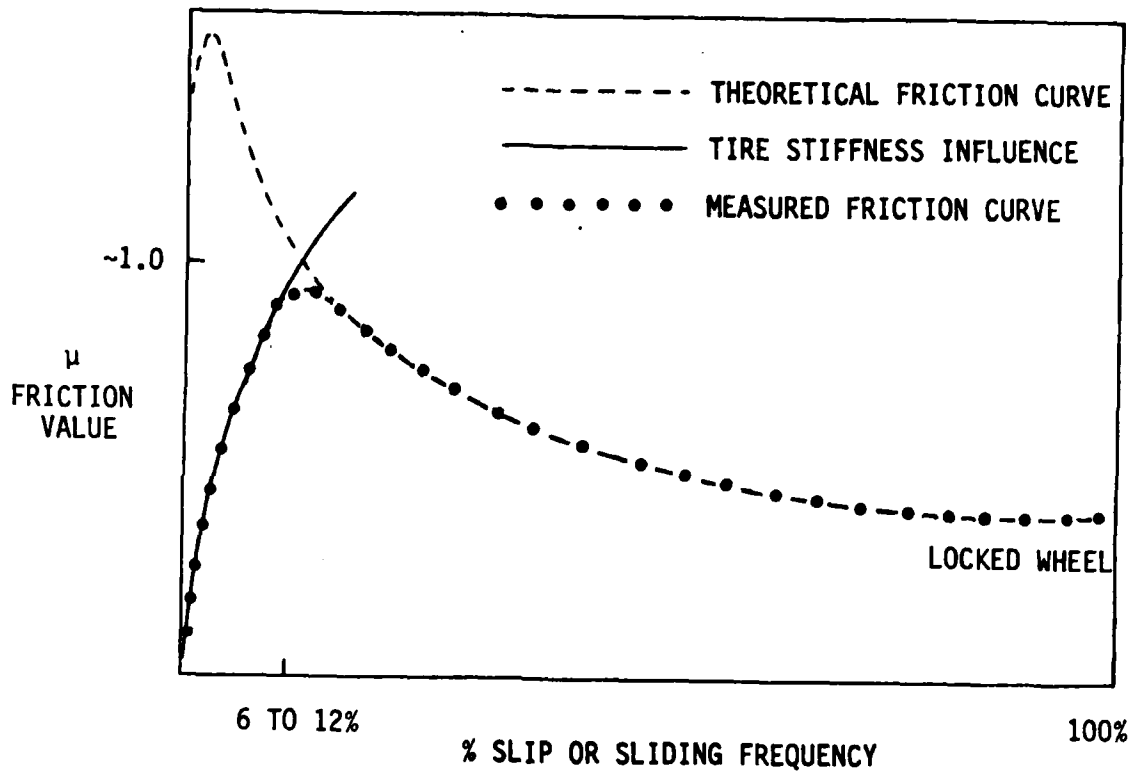
FIGURE 7. SLIP DEPENDENCY OF FRICTION (REFERENCE 23)

1. Direct profile measurement methods,

2. Direct measurements yielding average texture values, and

3. Indirect texture measurement techniques.

Since this study included two direct average texture depth techniques and two indirect texture measurement techniques, theories or relationships involv-ing profiles are excluded from this report. Emphasis is given to relation-ships involving measurements taken.

Recalling the shape of the wet-friction speed curves (see Figure 7), large differences in sliding speeds experienced by a locked wheel tester form an exponentially decaying curve, while smaller differences in sliding speed experienced by either limited slip or yawed test modes exhibit linearity in these plots. This difference in testing modes yields two distinct friction speed plots: exponential and linear curves.

Wambold et al. (Reference 25) cite the importance of the two components of texture (macro and micro) on surface friction. They found that the most conceptually satisfying model relating locked wheel friction and texture characteristics is that developed by Leu and Henry (Reference 26), namely

$$SN_V = C_0 \exp(C_1 V) \tag{1}$$

15

where SN is the skid number (friction number), V is the sliding velocity of the tire, and C_0 and C_1 are regression coefficients which define the skid number velocity curve. The coefficient C_0 defines the peak or intercept value and can be correlated with microtexture, while the coefficient C_1, which describes the frictional decay with speed, depends on macrotexture alone.

However, since the differences in sliding speed experienced by a yawed test trailer, such as Mu-Meter, produced wet friction speed plots that are linear, a conceptually satisfying model relating yawed or side force friction and texture should be

$$MuN_V = B - MV \qquad (2)$$

where MuN_V is the Mu-Meter number (friction number), V is the towing velocity, and B and M are the intercept and slope of the linear wet friction speed curves, which are dependent on micro- and macrotexture, respectively.

Horne and Buhlmann (Reference 27), using rolling and yawed aircraft tires, presented another conceptual model that involved the use of interfacial fluid pressures and pavement drainage coefficients to describe the wet frictional performance of the pavement. Using variations of fluid pressures measured under rolling aircraft tires at different speeds, they defined three zones of a tire footprint. Congruent with Moore's footprint model, these zones consisted of a bulk fluid zone, a thin film zone, and a dry contact region. However, unlike Leu and Henry, they modeled the wet friction speed curves as linear, and developed two pavement drainage coefficients, C_{mic}, and C_{mac}, which are related to microtexture and macrotexture, respectively. C_{mic} determines drainage rates through the microtexture, and C_{mac} determines drainage rates through the macrotexture. These pavement drainage coefficients are determined by transformation of the linear wet-friction speed curves by dividing both scales by a peak or critical value to obtain nondimensional parameters. Thus the measured friction is divided by a peak friction value and the velocity is divided by a critical hydroplaning velocity. From these curves a transformed slope, m, and intercept, b, are determined. This slope and intercept are used in regression equations to determine C_{mic} and C_{mac}, namely;

$$C_{mic} = 1.153 - 1.153b + 0.297|m| \qquad (3)$$

$$C_{mac} = -0.155 + 0.155b + 0.725|m| \qquad (4)$$

where

    b is the transformed intercept
    |m| is the absolute value of the transformed slope
    C_{mic} is the microtexture drainage coefficient
    C_{mac} is the macrotexture drainage coefficient

A more detailed description of this method is given in Section V, "Data Analysis."

EFFECTS OF RUBBER DEPOSITS

A certain amount of rubber is removed as a result of heat and abrasion as aircraft tires spin up during landings. This rubber is deposited on the pavement surface as thin layers that adhere to the pavement materials. Subsequent rubber deposits increase the buildup to significant thicknesses. Rubber affects tire-pavement friction by first coating the finer microtexture, then occluding the macrotexture as rubber buildup increases.

During dry operations this rubber buildup is not critical, yet during wet operations, friction levels can be dramatically reduced. The rubber coating the microtexture changes the sharp asperities to rounded spheres which cannot generate the hydraulic pressures necessary to penetrate the thin viscous films of water found on a wet runway. This reduces the efficiency of the pavement in removing viscous water films, thereby reducing both the area of dry contact and the adhesional friction developed. Once rubber buildup is excessive, the bulk water drainage capability of the runway is lost. This is caused by the rubber deposits occluding the macrotexture, whereby the bulk water no longer has flow path by which to drain. Thus the combined micro/macrotexture losses could cause high potential for hydroplaning to exist on rubber-contaminated runways.

SECTION III
DESIGN OF FIELD EXPERIMENT

Since the evaluation of runway friction by use of the Mu-Meter is impractical, an extensive literature search was conducted to develop field evaluation procedures (Reference 3). That investigation suggested the use of the pavement's textural characteristics to quantify runway friction levels. A thorough analysis of current textural measurement procedures was compiled in that earlier report. The selected candidate test procedures were subject to the following constraints: (1) economic: costing less than $10,000 to implement; (2) simple: tests and techniques must be readily understandable and usable by typical airport personnel; (3) reliable and sensitive: must be able to predict friction and differences in friction levels due to rubber removal; (4) readily accepted: tests that are currently available and do not require large amounts of research and development to substantiate.

The following test methods were selected for evaluation. Two volumetric techniques of determining average texture depth, the Sand Patch and Silicone Putty tests, were used to quantify the pavement's macrotexture. Two distinctive methods, a rubber slider device (the Penn State Drag Tester) and a chalk wear device (the Chalk Wear Tester developed by NMERI), were used to quantify the pavement's microtexture. The last method, which has yet to be analyzed, is stereophotography. This technique uses an automated system to analyze stereophoto pairs by a technique first proposed by Schonfeld (Reference 28) and further developed by Holt and Musgrove (Reference 29). The test procedures used in predicting friction are summarized in Table 1. Procedures for each of these tests were presented by Lenke et al. (Reference 3).

As the intent of this experiment was both to evaluate runway touchdown zone friction levels before and after rubber removal and to correlate the pavement's textural properties to friction levels as measured by the Mu-Meter, various theoretical concepts were considered. First, rubber removal is not always 100 percent effective in increasing friction levels of the pavement. Therefore, two control sections were included which would determine the effects of both weathering and traffic polish and indicate the maximum

TABLE 1. SELECTED FIELD PROCEDURES

Macrotexture	Sand Patch Volumetric Technique (ASTM E965)
	Silicone Putty Volumetric Procedure
Microtexture	Penn State Drag Tester
	Chalk Wear Test
Combined Micro/Macro	Stereophotography

obtainable friction levels on any particular pavement. This concept is further illustrated by Figure 8. On this figure are three theoretical friction curves. The lowest curve is the rubber-contaminated zone before removal. It has the smallest intercept and largest negative slope, due to the rubber deposits coating the microtexture and occluding the macrotexture. The middle curve is representative of the rubber zone after removal. The intercept has increased because of improvement of the pavement's microtexture, and the negative gradient is less because of increase in the macrotexture. The upper curve is indicative of the control sections. The clean pavement's microtexture allows large adhesional friction forces to form and, since the pavement's macrotexture provides good bulk water drainage, the frictional decline with speed is less.

The test matrix (Figure 9) collected both wet and dry Mu-Meter values at 32, 64, and 96 km/h (20, 40, and 60 mi/h), pavement temperatures corresponding to each Mu-Meter run, sand patch average texture depth, silicone putty average texture depth, both dry and wet Penn State Drag Test numbers (DTN) in both the longitudinal and transverse directions with corresponding pavement temperatures, chalk wear coefficients as measured by the chalk wear test in the longitudinal and transverse directions, and two sets of stereophoto pairs for each repetition. The various wet Mu-Meter test speeds (32, 64, 96 km/h [20, 40, 60 mi/h]) were used to develop friction speed curves as discussed previously. An unpublished data report by Burk (Reference 30) suggested that a combination of macrotexture and microtexture dictates the wet 64 km/h (40 mi/h) Mu-Meter values. In addition, dry Mu-Meter testing was performed. The dry Mu-Meter testing was also thought to be indicative of the maximum friction or intercept of the wet friction speed curves.

As the Mu-Meter provides an analog output of friction over a given test section, a point-by-point comparison of the Mu-Meter testing with the five candidates was performed. This comparison was performed by using a standard test section layout, as shown in Figure 10. Three distinct sections were analyzed. These included a centerline rubber section, tested before and after rubber removal, a centerline nonrubber section, and a pavement edge nonrubber section. Within each section, three locations, placed at the quarter points of the section approximately 120 feet apart, were tested in a random sequence with two repetitions per location. Since analysis of the effect of both rubber buildup and removal of this buildup on any specific pavement required control sections to gage, the two control sections were used. The centerline nonrubber control section was tested to judge the possible effects of traffic polish. The pavement edge nonrubber section was included to determine both the possible effects of weathering and the maximum friction level of any specific pavement texture. Each of these sections was tested on pavement of the same material and surface texture as the rubber buildup area, enabling comparisons to be valid.

This statistical approach described above was used in collecting a data base to find meaningful relationships between the Mu-Meter and texture measurements. Because runway access time for testing was limited, two replicative measurements were made at each location to analyze test variability.

19
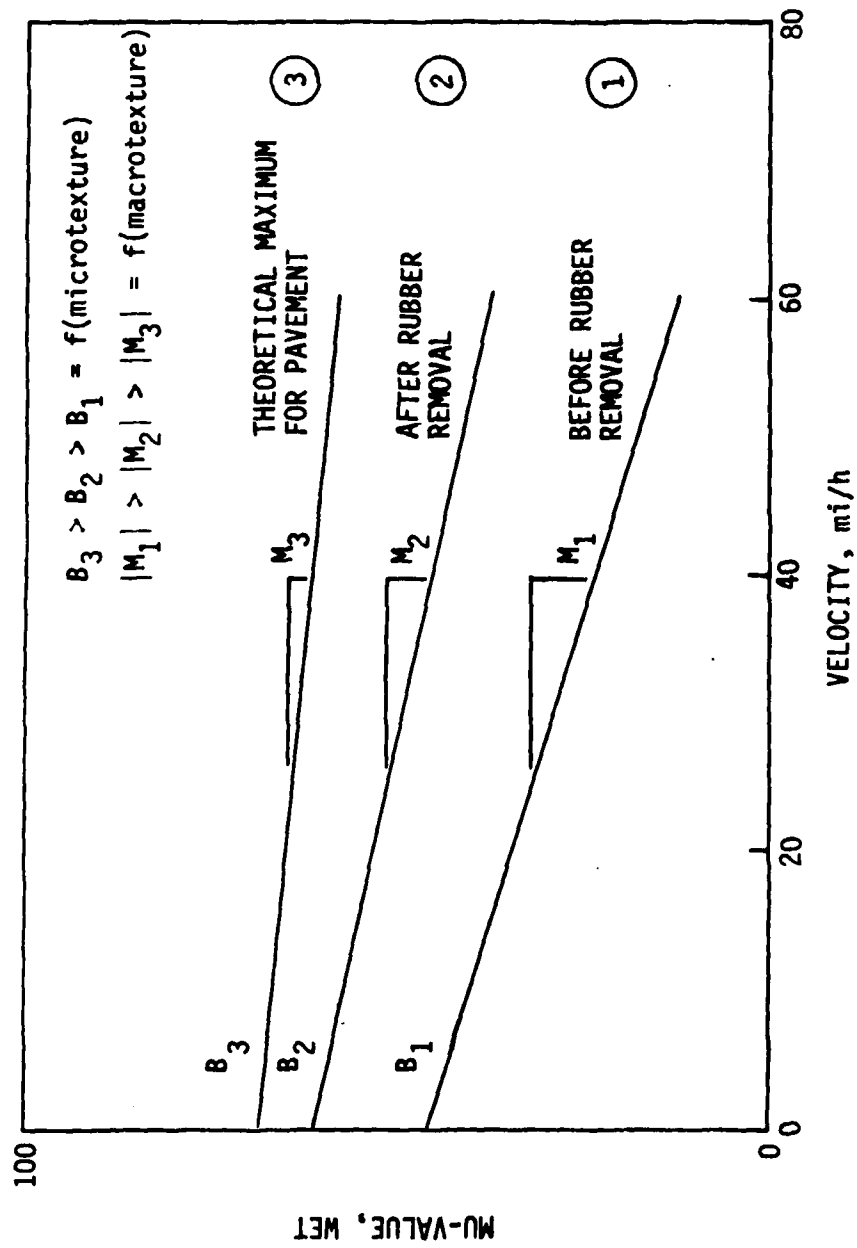
FIGURE 8. THEORETICAL FRICTION CURVES (REFERENCE 3)

20

FIGURE 9. FIELD EVALUATION TEST MATRIX (REFERENCE 3)

Notes: "Temp." is pavement temperature in degrees Fahrenheit.
Two repetitions per cell (four for stereophotography).
"Long." is longitudinal direction of runway.
"Trans." is transverse direction of runway.

21
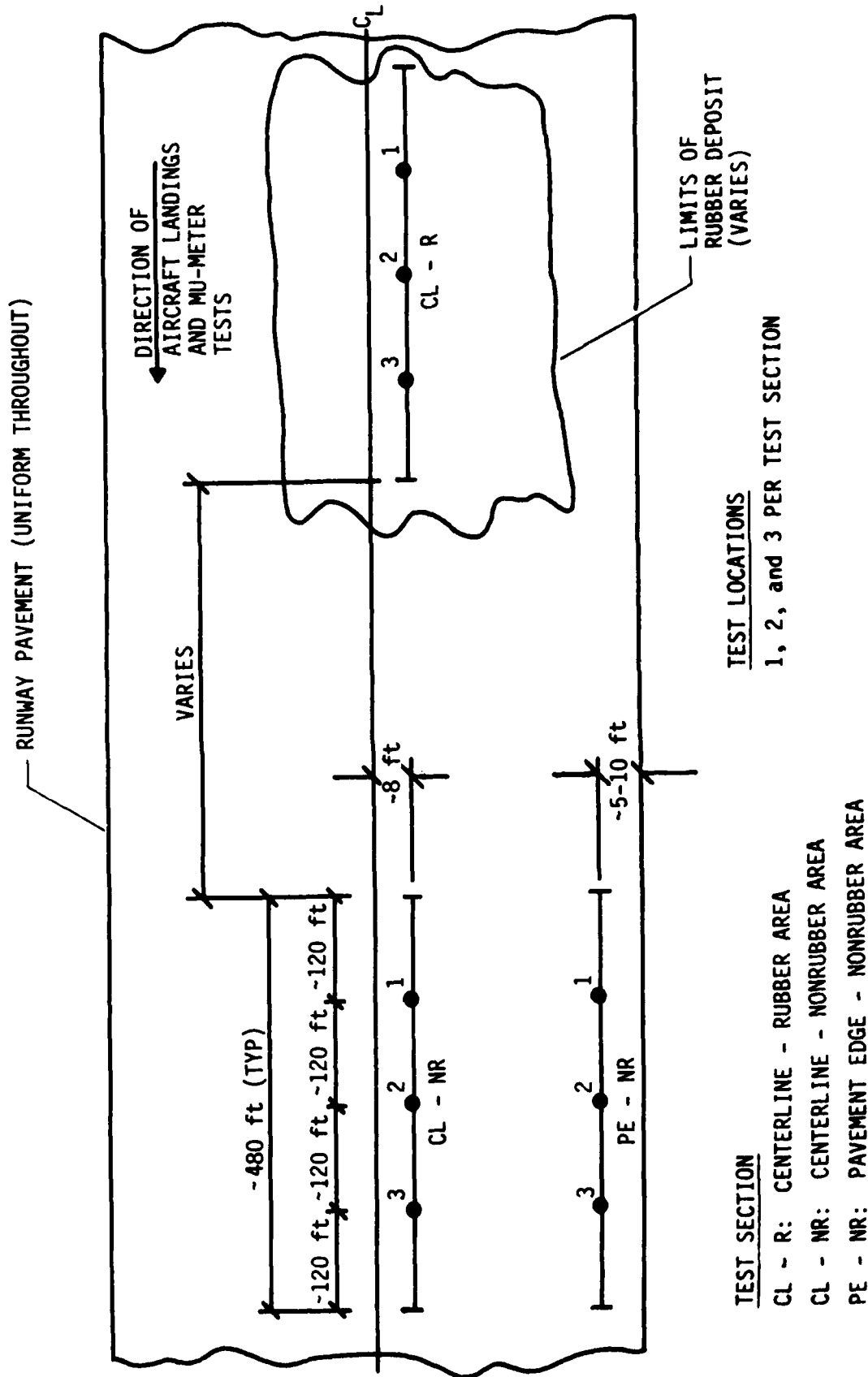
FIGURE 10. TYPICAL TEST SECTION LAYOUT (REFERENCE 3)

SECTION IV
TEST SITES EVALUATED

As this experimental design required testing of rubber-contaminated runways prior to and after rubber removal, arrangements for field testing were made in two ways. The first attempt was contacting the various rubber removal contractors. These contractors agreed to notify the NMERI Principal Investigator of pending rubber removal jobs. Upon notification, NMERI personnel would contact the airport or airbase and arrange for testing. This method proved to be unsuccessful after testing the fourth site, so an alternative means of identifying sites for field testing was found. This was accomplished through a massive canvassing of all airports and airbases where rubber removal projects might be conducted. The canvassing questionnaire and cover letter are shown in Appendix A.

PAVEMENT TYPES TESTED

During the field-testing phase of this program, 18 runways were investigated. These are designated A through R; they are discussed briefly later in this report and summarized here. They were located at seven Air Force Bases, nine commercial air facilities, and two Naval Air Stations. These pavements were classified into four basic pavement types discussed below. Photographs of these pavement types are shown in Appendix B.

Seven runways were grooved portland cement concrete (PCC). Five of these runways (C, E, G, P, and Q) were transversely saw-cut PCC with grooves of 6.4 mm by 6.4 mm and 38.1 mm (1/4 inch by 1/4 inch and 1-1/2 inch) center-to-center groove spacing. Figure B-1, which is a photograph of runway Q, typifies the saw-cut grooving. One runway (F) was a plastic-grooved or wire-tined concrete. This runway was textured by a stiff steel brush being swept across the runway while the concrete was still in its plastic state. Figure B-2 demonstrates this texturing. The last of the grooved PCCs (B) was a longitudinal wire-combed PCC. This texturing produced a multitude of small longitudinal channels, which is shown in Figure B-3.

Seven runways were ungrooved PCC pavements. Five of these runways (I, M, N, O, and R) were burlap dragged PCC. The surface texture of these pavements is shown in Figure B-4. Two of these runways (A, D) were worn PCC surfaces. On these surfaces, the original finish of the concrete was worn or weathered away, leaving the aggregate showing through the matrix (Figure B-5).

Three runways were porous friction surfaces (H, J, K). These runways consisted of a thin overlay (0.75 to 1 inch) of a uniform-graded asphaltic concrete mix. The overlay has a porosity of 20 to 45 percent, making it very pervious; thus water drains from both the top surface of the runway and within the thin overlay. Examples of this runway type are seen in Figures B-6 and B-7.

The last runway type (L) was a grooved dense graded asphalt concrete pavement which is seen in Figure B-8.

Table 2 displays a summary of the bases tested, the pavement type, and the type of facility.

TABLE 2. SUMMARY OF RUNWAYS TESTED

Base	Pavement Type	Facility Type
A	PCC	AFB
B	GPCC[a]	AFB
C	GPCC	CAF
D	PCC	AFB
E	GPCC	CAF
F	GPCC[b]	CAF
G	GPCC	CAF
H	PFS	AFB
I	PCC	AFB
J	PFS	CAF
K	PFS	CAF
L	GAC	CAF
M	PCC	AFB
N	PCC	NAS
O	PCC	NAS
P	GPCC	CAF
Q	GPCC	CAF
R	PCC	AFB

Pavement type describes the pavement's surface characteristics.

PCC   Portland cement concrete

GPCC Grooved portland cement concrete

PFS   Porous friction surface

GAC   Grooved asphalt concrete

Facility type describes major usage of runway.

AFB   Air Force Base

CAF   Commercial air facility

NAS   Naval Air Station

[a] wire-combed portland cement concrete

[b] wire-tined portland cement concrete

RUNWAYS INVESTIGATED

Runway A is a military runway comprised of old portland cement concrete. Primary usage of this runway is for heavy military aircraft. Rubber is removed once a year in conjunction with paint removal and repainting operations. As total operations are limited, the degree of rubber buildup was medium with the surface retaining a grittiness, indicating that the larger microtexture asperities were coated but not yet obliterated. Pavement slabs were old and polished yet structurally sound, with little differential settlement at the joints. Field notes indicate that friction levels after rubber removal may not be indicative of true friction improvement resulting from rubber removal, because of the presence of glass beads on the runway surface. These glass beads were used in the reflective paint markings, and during application of the reflective paint some of the beads scattered over the runway. These beads may have acted as a ball bearing lubricant.

Runway B is a military runway comprised of a wire combed portland cement concrete (PCC) touchdown zone and an asphalt interior. This runway is used primarily for light fighter aircraft; therefore, rubber buildup was not critical. Rubber is removed regularly once a year, as part of the maintenance program. Permanent slabs were fairly new with a wire combed concrete finish placed longitudinally down the runway. Pavement was structurally sound with good sideslope and a smooth ride. Field notes and visual examination suggested rubber buildup was not a problem. Field testing was performed in the opposite direction of aircraft landing because of limited runup distance.

Runway C is a commercial runway comprised of grooved portland cement concrete. The surface texture was formed by longitudinally wire combing and transversely saw cutting 6.4 by 6.4 by 38.1 mm (1/4 by 1/4 by 1-1/2-inch) grooves. This runway is a high-volume commercial hub with high rubber buildup rates. Although rubber was removed twice a year, rubber buildup was a problem. Pavement structure had been recently constructed and was in good condition in terms of both smoothness and soundness. Here again, measured friction levels after rubber removal may not have been as high as they actually were immediately following removal, since testing was performed 10 days after removal took place. This delay permitted rubber deposits to form on the lands between grooves and possibly reduced friction levels.

Runway D is a military runway comprised of low-texture, worn portland cement concrete. Low volumes of heavy military aircraft formed light rubber deposits. As with most military runways investigated, rubber is removed once a year in conjunction with paint removal and repainting operations. Pavement slabs were old, weathered, and polished. These slabs were structurally sound, yet pavement roughness caused the Mu-Meter to bounce up and down during 64 km/h (40 mi/h) test runs, making traces difficult to read. Thus the reliability of these readings on centerline is a potential source of error.

Runway E is a heavy commercial air cargo runway constructed of portland cement concrete. Surface texture was transversely wire combed and transverse 6.4 by 6.4 by 38.1 mm (1/4 by 1/4 by 1-1/2-inch) grooves were saw cut into the pavement. Rubber buildup was medium, with rubber coating many but not all of the lands. Rubber is removed from this runway twice a year. Pavement structure was sound and smooth. Some surface cracking was noted but considered nondetrimental to the pavement.

Runway F is a medium-density commercial runway constructed of a wire-tined or plastic grooved portland cement concrete. Rubber buildup on this runway was light, and was removed twice a year. Pavement structure was sound and smooth, showing few signs of weathering. Field notes indicate that the removal operation may not have been too effective because of silicone putty that remained on the runway after rubber removal. This indicates that little energy was imparted to that area of the pavement during the removal process, and as a result little rubber could be removed. Friction measurements were taken opposite to the direction of landing.

Runway G is the opposite end of runway E. Traffic density at this end is higher, as this is the preferred direction of landing. Rubber buildup was also higher at this end than the E end.

Runway H is a military Runway with a varied traffic pattern. The runway surface consisted of low textured portland cement concrete at both ends with a porous friction course overlay in the center portion of the runway. Typically rubber removal is performed on only the concrete touchdown zones; however, since many touchdowns occurred beyond the concrete touchdown zone, and inter-est was expressed in removing rubber from porous friction courses, a small test section was selected and rubber was removed from this section. Since the structural integrity of any asphalt friction overlay is dependent upon the strength of the base pavement, this particular runway was in the process of being replaced because of a faulty base. Rubber buildup was light to medium in this area, with much of the pavement texture still visible.

Runway I is a military runway with both varied traffic densities and an asphalt runway with concrete touchdown zones. The touchdown zone had an unu-sual pattern of rubber buildup. This pattern seemed to develop as a result of pilot technique. Since, at the beginning section of the touchdown zone, the concrete slabs were cracked, and settled and provided a rough landing surface, the pilots tended to touch down beyond this section, depositing rub-ber near the end of the landing zone. Crack patterns also affected the Mu-Meter readings since water ponding was noticed after multiple runs in areas of cracked slabs. This base did not have a nonrubber centerline section of the same material and the pavement edge nonrubber control section was not of the same texture as the rubber-contaminated zone. This change of texture, coloration and visible gradation indicates that the centerline sections were replaced at some time during the life of the pavement. Rubber buildup was medium, covering much of the pavement's texture. The rubber was removed once a year. All testing was performed opposite to direction of landing.

Runway J is a commercial runway with a porous friction surface which receives low usage due to its orientation (used only during high cross-wind conditions). This surface had minimal rubber buildup with good sideslope. Minor damage in the form of popouts was noticed at location 3 of the center-line nonrubber section. These popouts caused an extremely high average texture depth measurement.

Runway K is also a commercial runway with a porous friction surface. However, this surface serves large volumes of traffic, and had had substantial rubber buildup over a period of 12 years before cleaning operations began. Coating this runway was a hardened rubber which could not be cut by a knife as

on most runways, but could only be sampled by chiseling a piece off using a hammer and screwdriver. This coating covered approximately 25 percent of the total exposed area in the touchdown zones and was 6.4 mm (1/4 inch) thick in areas of heaviest deposits. Rubber removal is performed here once a year. The airport manager reported favorable visual impressions following removal. Each year more of the original pavement is cleaned. Effectiveness of rubber removal at this site is dependent upon the removal of recent deposits along with removing the previously deposited, hardened rubber deposits; therefore, this runway was not typical of most removal jobs.

Runway L is a grooved dense-mix, asphalt concrete surface which had been recently constructed with sulfur extenders. Since this runway is used for touch-and-go training of Boeing 747 crews, rubber buildup on the lands was of a medium thickness and grooves were mostly clogged with rubber debris. However, friction values as measured by the Mu-Meter did not show an appreciable reduction in friction levels. The reason for this is not known.

Runway M is a military runway with concrete touchdown zones and an asphalt concrete interior. Rubber buildup was heavy and channelized down the middle 7.62 meters (25 feet) of the runway. Beyond these limits very little rubber was deposited. This heavy buildup completely occluded the pavement's texture, yet the rubber layer had a fair amount of microtexture due to wind-blown sand embedded in the top rubber layers. The pavement was in good condition, although aged and having little texture. Since the center of the runway was asphalt, only two sections could be tested. The centerline nonrubber section of the same pavement type did not exist. Because of the runway configuration, testing was performed opposite to the direction of aircraft landing.

Runway N, a Naval Air Station runway, is of portland cement concrete. The rubber buildup zone tested was a simulated aircraft carrier deck. The deck was simulated by both painting and lighting the outline of an aircraft carrier's runway on the side of an existing runway. Carrier pilots practice their landings by continously doing touch and go operations in a controlled crash pattern. In other words, the pilot must land within a limited space at a high approach and drop into this zone to ensure grabbing the arresting gear. These landings cause extreme wear rates on the tires and heavy rubber buildup. Unlike most landings where minimal tread wear occurs, this style of landing causes sections of the tire to revert under the high-impact loads, depositing thick layers of rubber at a time. Rubber was being removed at this location once a year; however, because of damage occurring to pavement during removal operations, the contractor ceased removal operations early without removing much of the rubber, and negotiated returning twice a year to remove rubber. Friction testing was performed opposite to direction of travel.

Runway O is also a Naval Air Station runway of portland cement concrete. This runway is a parallel of Runway N, where various types of aircraft landed. The rubber buildup occluded most of the pavement's texture, yielding low friction values before rubber removal. The contractor also damaged this pavement during removal operations, and agreed to return twice a year to remove rubber at lower pressures.

Runway P is a grooved portland cement concrete runway that had been recently constructed and that had been open to traffic only about 9 months.

This runway was textured by a wire-combing technique that left the surface rough to the touch. The area tested as a centerline rubber zone was beyond the area of heavier rubber buildup due to the test matrix's requiring 2500 feet of runup distance to perform the 96 km/h (60 mi/h) wet Mu-Meter runs. As there was little rubber on this runway, no improvement in friction levels was seen. High pavement temperatures were recorded during the day, and their effect upon results could not be determined.

Runway Q is a grooved portland cement concrete commercial runway that showed little or no rubber buildup. No evidence of rubber deposits was seen in the grooves of this runway, indicating that rubber buildup was minimal. This runway showed a decay in friction after rubber removal.

Runway R is a portland cement concrete military runway. This particular runway was in a constant state of repair because of an expansive aggregate problem in the concrete used. Pavement slabs were replaced as they became structurally unsound, and little thought was given to texturing. Texture on this runway ranged from a weathered portland cement concrete to a recently replaced broomed portland cement concrete. Since this runway was used to train pilots of light jet aircraft, rubber buildup was not yet a problem. However, the high-pressure water blasts used in rubber removal may accelerate the existing expansive aggregate problem.

Data collected at each of these sites, in accordance with the designed field experiment discussed in Section III, is listed in Appendix C. The sites are designated "Base A" through "Base R," corresponding to "Runway A" through "Runway R," respectively.

SECTION V
DATA ANALYSIS

This section discusses test distributions, analysis of variance (ANOVA) techniques, correlations between variables and regression modeling of texture measurements to predict runway friction levels.

Since the primary goal of this experiment was to predict runway friction levels from texture measurements, background information on the test distributions and general trends of the data is given to provide supporting evidence for the conclusions reached.

TEST DISTRIBUTIONS

The validity of inferences from regression analysis and analysis of variance require certain assumptions concerning the variable populations; therefore, descriptions of the variable populations are presented here.

The first step in analyzing the test populations was checking for homogeneity of population variance. The Burr Foster Q test of homogeneity (Reference 31) was used to determine whether or not the hypothesis of equal population variances should be rejected. This test proved to be inconclusive because of the large number of degrees of freedom. However, with 210 cells within the matrix, it was felt that only large departures from homogeneity would affect the data analysis (Reference 32).

Next an estimate of variable variance was computed. Since the number of cells was large but replications within cells were limited to two, only an estimate of variance could be computed. A description of how variable variance was computed is described in Appendix D with the results being expressed as Table 3.

Further descriptive information on the test variables is included in Appendix E, which includes frequency histograms on each of the test variables. The pertinent points of each variable are the following.

The variable M20, or the MuN measured at 32 km/h (20 mi/h) on a dry pavement, has both a very low variance and coefficient of variation. This implies that measurement of this variable is highly repeatable and is fairly precise as to the measured value. The histogram in Figure E-1 of Appendix E shows a wide variation in measured levels. This variation indicates that, on a dry pavement testing at the same speed, tire inflation pressure, rubber compound, and testing mode, the pavement's type and composition play an important role in determining friction levels since, if the measured friction level were independent of the pavement, the range of values would have been smaller. This evidence disputes the concept of an ultimate tire-pavement friction level determined by tire inflation pressure proposed by Horne and Buhlmann (Reference 27).

M40 is the measured MuN at 64 km/h (40 mi/h) on dry pavement. This variable is also highly repeatable and has a range of 20 MuN. This high range of values would not be expected if the pavement did not have some influence in determining the friction levels.

29

TABLE 3. VARIATION OF FIELD MEASUREMENTS

Variable Name	Estimated Variance σ^2	Lower Limit Variance σ_L^2	Upper Limit Variance σ_u^2	Coefficient of Variation, %	Range of Measurement
M20	1.27	1.16	1.48	1.5	65-88
M40	1.06	0.97	1.24	1.3	68-88
M60	2.62	2.39	3.06	2.1	66-91
MW20	2.57	2.35	3.00	2.3	32-88
MW40	4.58	4.18	5.34	3.7	16-87
MW60	6.88	6.28	8.03	5.5	7-82
SAP	1700	1550	1990	13.0	87-1126
SIP	11960	10900	14000	17.6	148-2109
PTIL	9.15	8.35	10.68	3.5	52-112
PTIT	3.99	3.64	4.66	2.3	54-102
PTIWL	11.42	10.43	13.32	5.8	32-87
PTIWT	5.11	4.67	5.96	3.8	30-85
CTL	273.00	250.00	319.00	15.8	21-220
CTT	195.00	178.00	227.90	12.6	24-221

M20   20 mi/h dry Mu value

MW20   20 mi/h wet Mu value

M40   40 mi/h dry Mu value

MW40   40 mi/h wet Mu value

M60   60 mi/h dry Mu value

MW60   60 mi/h wet Mu value

SAP   Average texture depth as measured by sand patch measured in 10^{-4} inches

SIP   Average texture depth as measured by silicone putty measured in 10^{-4} inches

PTIL   Raw drag test number (DTN) measured dry in the longitudinal direction

PTIT   Raw DTN measured dry in the transverse direction

PTIWL   Raw DTN measured wet in the longitudinal direction

PTIWT   Raw DTN measured wet in the transverse direction

CTL   Chalk test measured in the longitudinal direction and recorded as a wear coefficient in 10^{-4} in/ft

CTT   Chalk test measured in the transverse direction and recorded as a wear coefficient in 10^{-4} in/ft

M60 is the measured MuN at 96 km/h (60 mi/h) on a dry pavement. This variable exhibits much the same characteristics as M20 and M40.

MW20 is the MuN measured at 32 km/h (20 mi/h) on a pavement with 1 mm (0.04 in) of water depth delivered to the pavement under the test tires. The water distribution was described in a previous report (Reference 3). Thus the presence of a lubricant is introduced into the testing. This lubrication of the pavement caused a much greater range of measured values while the variance increased only slightly. Thus the measured values are slightly less precise, yet the pavement characteristics caused an appreciably larger difference in range. Of particular note on the frequency histogram (Figure E-4) are the values in the thirties. These values occurred in an area of extremely heavy rubber buildup and their influence will continue throughout the wet testing.

MW40, the MuN measured at 64 km/h (40 mi/h) on a wet pavement, has higher variation than the MW20 which can be attributed with lubrication effects becoming more variable at higher speeds. On the histogram (Figure E-5) there is a slight tendency for two separate peaks to occur. These peaks are caused by the distinct differences in average texture depth or degree of drainage paths between the low textured portland cement concrete pavements and the high textured pavements such as grooved pavements or porous friction surfaces. These peaks will become more evident as the test speed increases to 96 km/h (60 mi/h).

MW60, the MuN measured at 96 km/h (60 mi/h) on a wet pavement, emphasizes the two separate peaks on the frequency histogram (Figure E-6). The lower peak occurs on pavements with an average texture depth of less than 0.8 mm (0.03 in), while the higher peak was on pavements where the average texture depth was greater than 0.8 mm (0.03 inch). This demonstrates the effect of texture depth on friction levels at higher speeds.

SAP, or the average texture depth as measured by the sand patch procedure and recorded in 10^{-4} inches, has high variability and its distribution is skewed towards the lower values. The skewed distribution is caused by both the large number of low texture surfaces and the lower texture measured in the rubber contaminated zones. Thus this variable has two distinctive problems, making its predictive worth suspect. First, its high variability is evidenced by a coefficient of variation of 13 percent. Secondly, the Mu-Meter friction data does not exhibit the same skewed frequency distribution. However, as seen later, this variable has the greatest influence and is most stable in the predictive modeling. Therefore, macrotexture is important in determining friction levels; yet average texture depth specifically as measured by the sand patch may not be informative enough to determine friction levels.

SIP is the average texture depth, as measured by the silicone putty procedure, and is also expressed in 10^{-4} inches. This test has a higher variability than the sand patch, which is probably a result of its averaging texture over a smaller area. Its distribution is not as badly skewed and the values recorded are higher than those obtained by the sand patch. This is due to the method of applying the putty to the pavement. This point is emphasized in an earlier report (Reference 3). However, this high variability (COV ~18%) causes this variable to be insensitive to all but very large changes in friction.

31

PTIL is the raw drag test number measured dry in the longitudinal direction. The variability of this number is low; however, the range of values is also low, making its measurement insensitive to changes in pavement characteristics.

PTIT is the raw drag test number measured dry in the transverse direction. Its characteristics are identical to those of PTIL.

PTIWL is the raw drag test number measured wet in the longitudinal direction. Its variability is greater than that of either of the dry values. However, since the measurement system is only slightly damped, the "bouncing" of the measurement needle of the pressure gage introduced a bias on grooved or highly textured pavements. This bounce may have been as great as 20 DTN in number and therefore the first recorded number biased the second recording number. This bouncing also demonstrated the strong influence of macrotexture on this instrument that was designed to measure microtexture independent of macrotexture. Another inherent problem with this device was the difficulty in testing rubber-contaminated zones. The rubber slider would adhere to the rubber-coated pavement momentarily, then slip quickly as this bond was broken. Thus the continuously changing friction, also known as slip-stick friction, was also not damped by the measuring system, making the recorded value a judgment measurement.

PTIWT is the raw drag test number measured wet in the transverse direction. Since this test was not influenced by pavement grooving, its variability was slightly lower than the longitudinal direction. However, the same problems existed here, especially where the rubber-to-rubber contact exhibited a pronounced slip stick friction.

CTL is the chalk wear coefficient measured by the chalk test in the longitudinal direction and recorded in 10^{-4} in/ft. This test method had high variability over the wide range of levels measured. Influence of macrotexture on this microtexture testing device could not be evaluated. Unlike the impact loading condition of the drag tester on grooved pavements, the 25.4-mm (1-inch) diameter chalk was able to bridge the 6.35-mm (1/4-inch) grooves without an adverse effect.

CTT is the chalk wear coefficient measured in the transverse direction. This test also had high variability, making its predictive capabilities suspect.

ANALYSIS OF VARIANCE (ANOVA)

Following is a discussion of the results obtained by using an analysis of variance computational package available from the SAS Institute (Reference 33). This statistical procedure was used to identify general trends in the data. This procedure examines differences between class means to determine whether a significant difference exists between the class variable means. Class variables investigated were the location, section, and base where the test was performed. Results of these ANOVA program runs follow.

The first class variable, location, is the building block of this experiment. No significant difference between means of the different locations was found. Thus, each section can be considered a homogeneous pavement with respect to the variables tested.

Next, the four section means were analyzed. The ranking of sections for the wet Mu-Meter tests, the intercept of a linear wet friction speed curve, and the two microtexture tests (the drag tester and the chalk wear tester) were the same. In order of increasing means, this ranking was centerline rubber before removal, centerline rubber after removal, centerline non rubber, and pavement edge nonrubber. Another group of tests ranked in similar order. These were the dry Mu-Meter tests, the slope of the wet friction speed curves, and both macrotexture tests (sand patch and silicone putty volumetric techniques). The ranking here was centerline rubber before removal, centerline rubber after removal, pavement edge nonrubber, and centerline nonrubber. These ranking inverted the relative positions of both the centerline nonrubber and the pavement edge nonrubber control sections. This reversal is caused by two bases not having a centerline nonrubber control section, which biased the pavement edge nonrubber section lower. However, this reversal does show that the macrotexture tests follow the same reversal as the slope of a linear wet friction speed curve.

The ANOVA of section groupings for the wet Mu-Meter tests showed little difference between the friction levels before and after removal. The four sections' centerline rubber before, centerline rubber after, centerline nonrubber, and pavement edge nonrubber had increasing means of 51.9, 54.9, 64.3 and 66.0 MuN, respectively. This ordering is consistent with aggregate polishing and rubber buildup mechanisms present upon a runway. However, the differences between the before and after values in the rubber-contaminated area are slight, and the overall friction level before removal is above the minimum of 50; therefore, rubber removal at some locations is being needlessly done. This confirms the need for a specification or guidelines or both to improve the cost effectiveness of the rubber removal program. Similarly the candidate procedures showed improvement between the conditions before and after rubber removal. However, with these tests, improvement was likewise insignificant. The differences between control sections is also slight. However, this can be attributed to the two bases (I, M) without a centerline nonrubber section and four bases (B, F, N, O) that were tested opposite the direction of travel, which produced an upward bias to the centerline nonrubber Mu Numbers (MuN).

The last group of ANOVA runs compared base means. Comparing base means of Mu-Meter runs to other tests by ranking was impracticable, as the individual candidate procedures were not sensitive enough to detect these differences. Yet, ranking of the pavement edge control section by order of increasing means reveals the importance of texturing. Table 4 highlights the importance of texturing on airfield pavements. As the friction levels increase, the general trend is for the average texture depth to increase. This table emphasizes the difference in average texture depth between the plain portland cement concrete and the grooved or porous friction pavements. The wire-tined portland cement concrete did not significantly improve either the average texture depth or the friction level over the ungrooved portland cement concrete pavements.

33

TABLE 4. MEANS OF PAVEMENT EDGE CONTROL SECTIONS

Runway Identification	64 km/h (40 mi/h) Wet Mu-Meter Number (MuN) Pavement Edge Control	Average Texture Depth SAP (10^{-4} in)	FACTYPE	PVMTYPE
I	[a]39.2	127	AFB	PCC
M	52.5	138	AFB	PCC
N	53.5	170	NAS	PCC
R	57.3	133	AFB	PCC
A	58.2	201	AFB	PCC
O	59.8	251	NAS	PCC
D	62.2	169	AFB	PCC
F	62.5	261	CAF	GPCC[b]
E	65.3	429	CAF	GPCC
G	69.3	362	CAF	GPCC
K	71.5	673	CAF	PFS
Q	72.3	408	CAF	GPCC
J	74.5	626	CAF	PFS
H	75.3	524	AFB	PFS
L	75.5	528	CAF	GAC
B	78.2	309	AFB	GPCC[c]
C	79.8	381	CAF	GPCC
P	83.5	626	CAF	GPCC

[a]Control section not representative of centerline pavement.

[b]Wire-tined portland cement concrete.

[c]Wire-combed portland cement concrete.

Notes:

FACTYPE	= facility type	PCC	= portland cement concrete
PVMTYPE	= pavement type	GPCC	= grooved portland cement concrete
AFB	= Air Force Base	PFS	= porous friction surfaces
NAS	= Naval Air Station	GAC	= grooved asphaltic concrete
CAF	= commercial air facility		

CORRELATIONS

Once general trends of the data were established by the ANOVA computa-
tions, efforts to model the friction level, measured by the Mu-Meter, through
use of texture measurements began. This was accomplished by use of correla-
tions matrixes.

The correlation matrix (Table 5) highlights some interesting relation-
ships. First there is a strong relationship between the various test speeds
for both wet and dry MuN. The correlation between MW60 (MuN measured wet at
96 km/h [60 mi/h]) and MW40 (MuN measured wet at 64 km/h [40 mi/h]) is the
strongest relationship. This may be due to the low pressure tire having a
sheoretical hydroplaning speed of 52.7 km/h (32.75 mi/h) or a measured hydro-
planing speed of 73 km/h (45 mi/h), thus the influence of pavement drainage
characteristics is more pronounced in preventing hydroplaning (Reference 34).
The lower correlation coefficients between MW20 (MuN measured wet at 32 km/hr
[20 mi/h]) and MW40 or MW60 might be caused by a different lubrication condi-
tion, since both the 64 km/h (40 mi/h) and the 96 km/h (60 mi/h) test runs are
near or above a critical hydroplaning speed. The high correlation coefficient
between M20 (MuN measured dry at 32 km/h [20 mi/h]) and M40 (MuN measured dry
at 64 km/h [40 mi/h]) may be due to slight differences in relative sliding
speed within the rising portion of the adhesion curve. Lower correlation
coefficients were noted between M60 (MuN measured dry at 96 km/h [60 mi/h])
and M20 or M40. These lower coefficients are not explainable at present.

The correlations between the various macrotexture candidate procedures
also indicate some interesting relationships. The low correlation (0.86)
between SIP and SAP (average texture depth measured by the silicone putty and
sand patch procedure, respectively) demonstrates either that the different
techniques measure different texture depths due to test technique, or that
sample variation is too high for accurate correlations. The different
techniques measuring different average texture depth was demonstrated earlier
by Lenke et al. (Reference 3), where texture measurements were performed on
controlled surfaces. The high sample variation is evidenced by Table 3.
Since both conditions exist simultaneously, determining which is the deciding
factor is impracticable.

The correlations between the microtexture candidate procedures demon-
strate the low correlations between the various procedures, indicating that
different mechanisms occur between wet and dry testing, and between rubber
slider devices versus chalk wear devices. The chalk test seemed to be less
influenced by direction than the PTI drag tester. This could probably be
attributed to the impact loading which occurred with the drag tester while
testing longitudinally on grooved pavements. The chalk wear tester did not
experience this impact loading because the 25.4-mm (1-inch) diameter chalk was
able to bridge the 6.35-mm (1/4-inch) grooves, and was thus less influenced by
direction.

The dry MuN values did not correlate well with any of the candidate
procedures. Thus, the techniques used did not address the controversial issue
of tire-pavement adhesion. The increasing influence of macrotexture with
speed during wet testing demonstrates the influence of bulk water dissipation
from the tire-pavement interface. Conversely, the decreasing influence of
microtexture indicates the reduced draping of the tread rubber allows thin
film lubrication to become more effective as speed increases.

35

TABLE 5. CORRELATION COEFFICIENT MATRIX

	M20	M40	M60	MW20	MW40	MW60	SAP	SIP	PTIL	PTIT	PTIWL	PTIWT	CTL	CTT
M20	1.00													
M40	0.93	1.00												
M60	0.85	0.87	1.00											
MW20	0.48	0.46	0.34	1.00										
MW40	0.31	0.28	0.17	0.84	1.00									
MW60	0.24	0.20	0.10	0.73	0.95	1.00								
SAP	-0.00	-0.05	-0.10	0.34	0.67	0.75	1.00							
SIP	-0.07	-0.14	-0.18	0.29	0.60	0.67	0.86	1.00						
PTIL	0.29	0.28	0.30	0.18	0.29	0.32	0.35	0.34	1.00					
PTIT	0.39	0.39	0.39	0.21	0.27	0.27	0.29	0.29	0.78	1.00				
PTIWL	-0.01	-0.02	-0.12	0.50	0.50	0.48	0.32	0.36	0.21	0.15	1.00			
PTIWT	0.14	0.13	0.00	0.60	0.53	0.50	0.30	0.32	0.14	0.25	0.79	1.00		
CTL	0.31	0.22	0.20	0.48	0.44	0.41	0.23	0.28	0.11	0.14	0.32	0.35	1.00	
CTT	0.35	0.26	0.23	0.53	0.47	0.43	0.20	0.28	0.11	0.15	0.35	0.42	0.84	1.00

36

REGRESSION ANALYSIS

Attempts were made to verify one of four possible models or methods for predicting the wet 64 km/h (40 mi/h) MuN. These four methods were:

1. Burk's concept of correlating 64 km/h (40 mi/h) wet MuN by a cross-product of macrotexture and microtexture (Reference 30).

2. Correlating microtexture with intercept and macrotexture with slope of linear wet friction speed curve.

3. Correlating the Horne and Buhlmann (Reference 27) method, C_{mic} and C_{mac}, to microtexture and macrotexture, respectively.

4. Correlating the 64 km/h (40 mi/h) wet MuN directly with micro- and macrotexture measurements.

Burk's Correlation Concept

Burk (Reference 30) suggested that the wet 40 mi/h MuN can be attributed to a cross-product of microtexture and macrotexture. Lenke et al. (Reference 35) described Burk's theory and analysis in a previous paper. This theory indicates that isofriction lines exist that are defined by the pavement's texture. Figure 11 demonstrates this concept. As either component of the pavement texture increases, the measured friction value should increase. This theory can be related to Moore's rolling tire hydroplaning model in the following manner. An increase in macrotexture reduces the sinkage zone of the tire footprint, enabling more of the tire to be in a traction zone. Also as macrotexture increases beyond a certain limit, the asperities become more conical in shape, thereby generating contact pressures necessary to penetrate the viscous film (Reference 20). Similarly, an increase in microtexture reduces the draping zone of the footprint, increasing both the tractive zone area and, correspondingly, the friction level.

Using a General Linear Models Procedure (SAS GLM) the 64 km/h (40 mi/h) wet MuN was modelled by a cross product of a macrotexture (average texture depth measured by the sand patch SAP), and a microtexture measurement (either a raw Drag Test Number [DT] from the PTI drag tester or a chalk wear coefficient [CT] measured by the chalk wear tester). Two combinations showed the most promise, namely:

$$Mu40 = 0.00080 \text{ SAP} \times DT + 43 \tag{5}$$
$$R = 0.72$$
$$\sqrt{MSE} = 9.4$$

and

$$Mu40 = 0.00035 \text{ SAP} \times CT + 46 \tag{6}$$
$$R = 0.70$$
$$\sqrt{MSE} = 9.6$$

where

R is the correlation coefficient
$\sqrt{MSE}$ is the root mean square error expressed in MuN
Mu40 is the 40 mi/h wet MuN predicted by texture measurements

37

INCREASING FRICTION

MuN = 60

MuN = 50

MuN = 40

TEST SPEED 40 m1/h

MICROTEXTURE
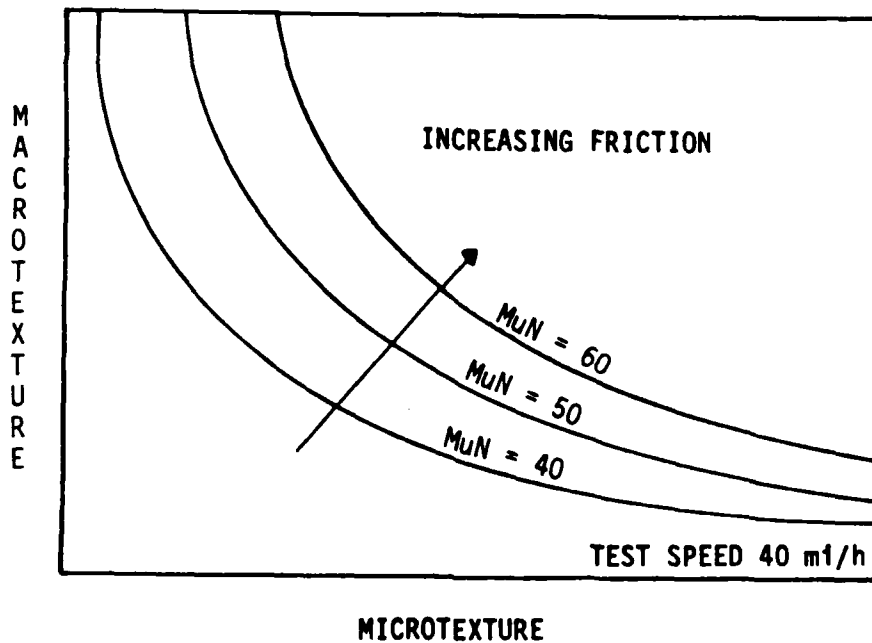
FIGURE 11. BURK'S THEORY OF ISOMETRIC FRICTION
(REFERENCE 30)

However, neither of these regression models, which determine friction levels within approximately 19 MuN, are able to predict friction to the close tolerances necessary to develop specifications for rubber removal. Also the fit of the regression equation, as determined by the correlation coefficient, did not improve much over predicting by macrotexture (SAP) alone. The Pearson correlation coefficients increased from 0.67 for predicting with sand patch alone to 0.70 and 0.72 for the cross-product regression Equations 5 and 6. This demonstrates the strong predictive value of the sand patch with little additional variation being explained by the microtexture parameters, drag tested number, or chalk wear coefficient. Comparison plots of values predicted by the regression models presented in this section and actual measured values are shown in Figures F-1 through F-16 in Appendix F.

Slope and Intercept Correlation

This method of regression modelling correlates the slope and intercept of a linear wet friction speed curve with macrotexture and microtexture parameters, respectively. Since the Mu-Meter measures side force friction, the differences in sliding speeds are limited by the experimental design. This places the measured friction values in the approximately linear range of the wet friction speed curves (see Figure 7). Therefore the developed friction speed curves are expressed as linear functions, unlike the exponential model developed by Leu and Henry (Reference 26). Two parameters are computed from these friction speed lines, namely slope (M) and intercept (B).

The slope (M) describes the frictional decay with speed similar to the exponential decay coefficient C_1 developed by Leu and Henry (Reference 26). This decay of friction with speed is predominantly a result of lubrication becoming more effective as speed increases. Using the tire footprint hydroplaning model, increasing the test speed increases the fluid pressures in the tire-pavement interface which causes both fluid zones of Figure 6, sinkage (Zone A), and draping (Zone B) to encroach upon the dry tractive zone (C), thus resulting in lower friction levels. Measurement of the pavement's drainage capacity, obtained by measuring the average texture depth, can be related to this decay since this relates to pavement drainage times.

Conversely, the intercept is conceptually the highest obtainable friction on any given pavement surface. Relating microtexture to optimum friction is based on Kummer's work of adhesional friction (Reference 6). In his derivation he models adhesional friction as a combination of electrical roughness and microhysteresis. Therefore, microtexture, as measured by a rubber slider device, should simulate both the microhysteresis created by the pavement's microtexture and equivalent electrical roughness.

Using linear regression techniques, both the slope and intercept of each set of data were computed. Using these values the slope (M), expressed in MuN/(mi/h), was modeled against the average texture depth measured by the sand patch (SAP). The regression equation

$$M = -1.0 + 0.0014 \text{ SAP} \tag{7}$$
$$R = 0.81$$
$$\sqrt{MSE} = 0.18$$

shows a relationship between slope and average texture depth; however, much data scatter exists. Including a microtexture term (CT, for the chalkwear coefficient, or DT, the raw drag test number), equivalent to a roughness term in the Manning equation for open channel flow, does little to explain further variance as evidenced by the following equations:

$$M = 1.0 + 0.00048 \text{ CT} + 0.0014 \text{ SAP} \tag{8}$$
$$R = 0.82$$
$$\sqrt{MSE} = 0.18$$

and

$$M = 1.11 + 0.0022 \text{ DT} + 0.0014 \text{ SAP} \tag{9}$$
$$R = 0.82$$
$$\sqrt{MSE} = 0.18$$

Next, the intercept (B), expressed in MuN, was modeled with the microtexture test values, Drag Test Number (DT) and chalk wear coefficient (CT). Correlations on this order were very poor. For example:

$$B = 0.45 \text{ DT} + 54 \tag{10}$$
$$R = 0.41$$
$$\sqrt{MSE} = 8.1$$

of

$$B = 0.084 \text{ CT} + 72 \tag{11}$$
$$R = 0.38$$
$$\sqrt{MSE} = 8.3$$

39

Inclusion of a macrotexture term, sand patch average texture depth (SAP), improved this model slightly; however, the correlation was still poor, namely

$$B = 0.56 \ DT - 0.017 \ SAP + 53 \qquad (12)$$
$$R = 0.52$$
$$\sqrt{MSE} = 7.6$$

Therefore, the intercept or optimum friction of a given pavement cannot be related to the simple microtexture devices used. Two major reasons for this lack of fit are probably the small range of both the computed intercepts and the Drag Tester values (DTN) and the high variability of the chalk test (CT).

Equations 7, 8, and 9 emphasize the importance of macrotexture in retaining tire-pavement friction levels at higher speeds. These equations reinforce the trend shown by the ANOVA computations (Table 4) that greater macrotexture yields higher friction levels at high speeds.

Another technique employed in analyzing the importance of texture on the slope M is computing a normalized slope, that is, dividing the value of the slope by the central friction number (Reference 25); namely,

$$PNS = M/MW40 \qquad (13)$$

where PNS is the percent normalized slope expressed in $(mi/h)^{-1}$, M is the calculated slope and MW40 is the MuN measured wet at 64 km/h (40 mph). Normalizing the slope eliminates the influence of various levels of friction; however, friction values are no longer independent of pavement characteristics. The following relationship was statistically shown between PNS and average texture depth:

$$PNS = 0.000035 \ SAP - 0.022 \qquad (14)$$
$$R = 0.75$$
$$\sqrt{MSE} = 0.0054$$

This technique did not improve the modeling effort.

Horne and Buhlmann Model

This method of modelling pavement friction levels from texture measurements is a conceptual model developed by Horne and Buhlmann (Reference 27). This method was derived from measurements of fluid pressures beneath an unyawed rolling tire. From these pressure measurements, they defined three zones of a rolling tire: a bulk fluid drainage zone, a thin film drainage zone and a dry contact zone. This model parallels the analytical model developed by Moore (Reference 22). The bulk fluid drainage zone is essentially the sinkage zone of Figure 6. Similarly, the thin film drainage zone describes the draping zone of the previous model, with the dry contact zone remaining the same with both models.

Since water films cannot generate appreciable shear forces, Horne and Buhlmann (Reference 27) theorized that tractive forces were generated in only the dry contact patch of the tire footprint. The magnitude of this force was thought to be a function of the percent of dry contact zone and the dry tire pavement traction. Namely

40

$$\mu_{wet} = \mu_{dry}\left(\frac{A_3}{A}\right) = \mu_{dry}\left(1 - \frac{A_1 + A_2}{A}\right) \tag{15}$$

where μ_{wet} is the wet friction coefficient
μ_{dry} is the dry friction coefficient
A_3 is dry contact zone area
A_2 is viscous water film zone area
A_1 is dynamic water layer zone area
A is total footprint area or the summation of A_1, A_2, and A_3

To relate the relative magnitudes of the fluid areas, they proposed two pavement drainage coefficients C_{mac} (macrotexture drainage coefficient) and C_{mic}. These are nondimensional drainage coefficients that correlate decreases in interfacial fluid pressures with increased drainage capacity. This is analogous to Darcy's law, where head loss across a sample decreases as permeability increases when all other variables remain constant. Combining this concept of reduced pressures with the concept of the tire as an elastic membrane (contact pressures remain equal to the tire inflation pressure), they hypothesize that a known portion of the tire is supported by these reduced fluid presures; namely,

$$C_{mac}\left(\frac{p_1}{p}\right)_u = \frac{A_1}{A} \tag{16}$$

and

$$C_{mic}\left(\frac{p_2}{p}\right)_u = \frac{A_2}{A} \tag{17}$$

where

C_{mac} = macrotexture drainage coefficient
C_{mic} = microtexture drainage coefficient
p_1 = dynamic fluid pressure
p_2 = viscous fluid pressure
u = a subscript detonating an ultimate pressure ratio
p = tire inflation pressure
A_1 = area of tire footprint supported by dynamic pressures
A_2 = area of tire footprint supported by viscous pressures
A = total tire footprint contact area

From Equations 16 and 17, the wet friction coefficient can now be expressed as a function of the fluid pressures and the pavement drainage coefficients.

$$\mu_{wet} = \mu_{ult}\left\{1 - \left[C_{mac}\left(\frac{p_1}{p}\right)_u + C_{mic}\left(\frac{p_2}{p}\right)_u\right]\right\} \tag{18}$$

Horne and Buhlmann (Reference 27) postulate that the ultimate tire-pavement friction coefficients are dependent upon tire inflation pressure, tread, rubber compound, tread design, vehicle speed, and tire operating mode utilized. They state that earlier research determined the ultimate friction coefficient could be determined from the tire inflation pressure, namely

$$\mu_{ult} = 0.93 - k_1 p \tag{19}$$

41

where $k_1 = 0.00016$ when p is expressed in kPa or
$k_1 = 0.0011$ when p is expressed in lb/in^2

Using this concept he redefines the functional function as follows

$$Y_r = 1 - \left[C_{mac} \left(\frac{p_1}{p} \right) u + C_{mic} \left(\frac{p_2}{p} \right) u \right] \tag{20}$$

where Y_r is the ratio of $\frac{\mu_{wet}}{\mu_{ult}}$

Next, Horne and Buhlmann derive the pavement draining coefficient (C_{mac} and C_{mic}) from a linear regression analysis of theoretical generalized friction speed curves. From this analysis they equate C_{mic} and C_{mac} to the transformed slope and intercept of linear friction speed curves.

$$C_{mic} = 1.153 - 1.153b + 0.297|m| \tag{3}$$

$$C_{mac} = -0.155 + 0.155b + 0.725|m| \tag{4}$$

where b and m are the intercept and slope of the transformed friction speed plots, respectively.

Analysis of this section began with transforming the friction speed plots to the format of the theoretical generalized curves. This was accomplished by dividing the measured friction coefficients by an ultimate value of 91.9 MuN, as determined by Equation 19, and dividing the velocity by 32.73 mi/h. The critical hydroplaning speed was determined by $V = 10.35 \sqrt{P_{in}}$, where P_{in} is the Mu-Meter tire pressure during testing (10 lb/in^2). Transformed slopes and intercepts were calculated from these transformed plots and values of C_{mic} and C_{mac} were computed in accordance with Equations 3 and 4.

Correlating these values with texture measurements yielded the following results

$$C_{mac} = 0.242 - 0.00037 \ SAP \tag{21}$$

$$R = 0.78$$

$$\sqrt{MSE} = 0.052$$

and

$$C_{mic} = 0.333 - 0.0012 \ CTT \tag{22}$$

$$R = 0.47$$

$$\sqrt{MSE} = 0.093$$

Little confidence was placed in either of these relationships. First, the correlation coefficients were low, showing little dependence of the calculated drainage coefficients on texture measurements. Second, values of the intercept coefficients were extremely low. Since a surface with no macrotexture and no microtexture should have values of $C_{mac} = 1$ and $C_{mic} = 1$, respectively, the low intercept values of 0.243 and 0.333 seemed unrealistic,

42

since they should be approximately unity. The third and most important reason for rejection is that the standard errors are as high as 20 percent of the estimated value at their best case. Therefore this method was eliminated from further analysis.

MuN Predictive Modelling, 40 mi/h

This last method relates texture measurements to friction measurements using multilinear regression modelling of the 64 km/h (40 mi/h) wet MuN to the best possible set of texture parameters. Since a macrotexture measurement, average texture depth as measured by a volumetric technique, is indicative of bulk water dissipation and a microtexture measurement is indicative of viscous water dissipation, a regression model including at least one parameter of each texture band was included in developing the model.

Table 6 describes the best models determined from a detailed regression analysis. The data scatter for the Equation 23, using all the data, is comparable to the previously discussed techniques; therefore, refinements by separating data into various sections were investigated.

First the data were separated into test sections and the multilinear regression equations were computed. This resulted in a reduction of some other data scatter, evidenced by the lower root mean square values. This subdivision of the data also demonstrated the strong relationship of SAP to friction levels and the unstable predictive value of the microtexture parameters. Thus, if a method were available to measure the average texture depth with less variability the predictive models might have been of more use.

The measurement of microtexture seems to have eluded this experimental design. Research has indicated the transient nature of microtexture determines the seasonal effects on friction levels. From this research, it has been proposed that the variances in microtexture may be indicative of changing levels of friction. However, much development work is still being done in this area and its influences are not fully understood.

Further analysis of the section models was conducted to ascertain the effects of pavement temperature, chronological order of testing, runway type, and higher order regression models, including more of the measured texture variables. None of these techniques were able to improve significantly the predictive qualities of these models. Therefore, any further refinements due to other variables were either hidden in the inherent variability of the texture techniques employed or they were not measured by the experimental design employed here.

TABLE 6. FRICTION MODELS USING TEXTURE MEASUREMENTS

Section[a]	Equation[b]	R[c]	$\sqrt{MSE}$[d]	Eqn. No.
All	Mu_p = 16.0 LSAP + 0.096 CTT + 0.016 CTL - 43	0.80	8.13	23
C_L-R+PE-NR	Mu_p = 17.0 LSAP + 0.10 CTT + 0.018 CTL - 50	0.82	8.20	24
C_L-R-B	Mu_p = 16.0 LSAP + 0.12 CTT + 0.080 CTL - 53	0.88	6.43	25
C_L-R-A	Mu_p = 14.1 LSAP + 0.091 CTT + 0.044 CTL - 36	0.82	6.76	26
C_L-NR	Mu_p = 10.9 LSAP + 0.041 CTT - 0.051 CTL + 2	0.66	6.49	27
PE-NR	Mu_p = 16.8 LSAP + 0.056 CTT - 0.049 CTL - 31	0.84	6.24	28

Notes

[a] Section descriptions are as follows:

All   All data collected during experiment

C_L-R   Centerline rubber area both before and after removal

C_L-R-B   Centerline rubber area before removal

C_L-R-A   Centerline rubber area after removal

C_L-NR   Centerline nonrubber control area

PE-NR   Pavement edge nonrubber control area

[b] Variables descriptions:

Mu_p Mu Number predicted by texture measurements

LSAP   Natural log of average texture depth measured by the Sand Patch Procedure and expressed in 10^{-4} in

CTT   Chalk wear coefficient measured in the transverse direction expressed in 10^{-4} in/ft

CTL   Chalk wear coefficient measured in the longitudinal direction expressed in 10^{-4} in/ft

[c] R is the Correlation Coefficient

[d] $\sqrt{MSE}$ is the root mean square error, essentially the standard deviation about the regression line (MuN).

SECTION VI
CONCLUSIONS

The following conclusions can be reached as a result of this field experiment.

The influence of average texture depth on higher friction levels is strongly evident. This is based upon the strong correlations between average texture depth and the wet 64 km/h (40 mi/h) Mu-Meter testing. MacLennan et al. (Reference 36) reached this same conclusion in the National Runway Friction Program. However, they state that measurement of friction rather than texture is a preferable basis for planning routine runway maintenance. The results of this experiment verify this conclusion for the following reasons:

(1) The measurement of macrotexture by either the sand patch or the silicone putty volumetric procedures is an inexpensive method of quantifying macrotexture. However, important parameters of macrotexture are not measured by these procedures. Average texture depths do not determine the general shape of the pavement's asperities; in addition, nonconnected voids measured by these methods do not help in the removal of bulk water. Each of these parameters is deemed important in friction literature, yet their influence has not been empirically validated. Furthermore, the techniques necessary to measure these parameters are more expensive and require highly trained personnel, thus defeating the purpose of this experiment.

(2) The measurement of microtexture has an elusive quality. The correlations of microtexture measurements to either the intercept of a friction speed curve or to the dry Mu-Meter tests with which it is generally believed to correlate is evidence that microtexture could not be measured by the simple methods employed in this experiment. Current technology has not developed an alternate method of measuring this textural band.

(3) The Mu-Meter was designed to determine averages in friction over an extended length, usually of a 152.4-meter (500-foot) test section. Being designed for such use, the system damping caused by both the test tires and the hydraulics of the load cell make this device insensitive to all but extreme localized texture variations. A friction test device using tires is not sensitive to localized texture variations, since such devices are designed to average friction values over an extended section. Therefore, the pavement's localized textural variability will not affect its readings, making the measurement of texture more variable than that which it is predicting.

(4) Therefore, the measurement of texture to determine friction levels of a pavement will only give an indication or an approximation of values measured by a friction test device. For this reason, if need arises to measure friction closely for performance specifications, one should use a friction measuring device on which acceptance levels were previously established.

45

SECTION VII
RECOMMENDATIONS

The following recommendations are offered as a result of this experiment.

First, the use of highly textured pavements or use of grooving systems is essential in obtaining high friction levels. Therefore, widespread usage of these pavements is encouraged.

Second, the use of texture measurements to determine accurately the friction levels of a pavement cannot be accomplished with present technology. Therefore, the use of texture measurements should only be used as a guide in determining friction levels, with a friction test device being used for accurately defining friction characteristics of a pavement.

Third, alternate methods of measuring or quantifying the microtexture of the pavement are required for the prediction of friction from texture measurements. These methods must be researched to determine empirically the role of microtexture in pavement friction.

Fourth, alternate methods of measuring the pavement's macrotexture should be investigated. Emphasis should be given to nonconnected voids, asperity density, asperity shape, and profiles of the pavement's macrotexture.

Fifth, investigations into the analysis of stereophoto pairs in determining the microtexture and the shape, density, and nonconnected voids of the macrotexture should be conducted. This concept arises often in friction literature, yet detailed analysis of such procedures has not been reported. This method, if analyzed by appropriate computer algorithms, would be insensitive to operator error; therefore, it would be able to determine true pavement textural variability. Furthermore, if the resolution of the photo pairs is fine enough, the role of microtexture in determining pavement friction may be better defined. Therefore, the stereophoto pairs collected in the designed field experiment should be analyzed in an effort to improve upon the friction predictive models developed in this report. This test may be used to improve the accuracy of methods employed in determining the relationship between texture and friction, enabling friction to be predicted from texture with greater certainty.

REFERENCES

1. McKeen, R. G., and Lenke, L. R., **Alternatives for Rubber Removal from Porous Friction Surfaces**, DOT/FAA/PM-84/28, U. S. Department of Transportation, Federal Aviation Administration, Washington, DC, 1984.

2. Burk, D. O., **Effectiveness of Rubber Removal Processes at Six Air Force Bases**, AFCEC Memorandum 4-77, Air Force Civil Engineering Center, Tyndall Air Force Base, FL, 1977.

3. Lenke, L. R., McKeen, R. G., and Graul, R. A., **Runway Rubber Removal Specification Development: Field Evaluation Procedures Development**, Interim Report No. DOT/FAA/PM-84/27, U.S. Department of Transportation, Federal Aviation Administration, Washington, DC, July 1984.

4. Standiford, D. L., Graul, R. A., and Lenke, L. R., **Permeability Equipment for Porous Friction Surfaces**, Interim Report, DOT/FAA/PM-85/xx, U.S. Department of Transportation, Federal Aviation Administration, Washington, DC, April 1985.

5. Yager, T. J., **Factors Influencing Aircraft Ground-Handling Performance**, NASA TM-85652, National Aeronautics and Space Administration, Hampton, VA, 1983.

6. Kummer, H. W., **Unified Theory of Rubber and Tire Friction**, Engineering Research Bulletin B-94, Pennsylvania State University, College of Engineering, University Park, PA, 1966.

7. Schallamach, A., **Rubber Chemistry and Technology**, Vol. 41, Part 1, pp. 209-244, 1968.

8. Williams, M. L., Landel, R. F., and Ferry, J.D., **Journal of American Chemical Society**, Vol. 77, p. 3701, 1955.

9. Grosch, K. A., in **Proceedings**, Royal Society, A274.21, 1963.

10. Schallamach, A., **Rubber Chemistry and Technology**, Vol. 39, Part 1, p. 320, 1966.

11. Hatfield, M. R., and Rathman, G. B., **Journal of Physics and Chemistry**, Vol. 60, 1956, p. 957.

12. Savkoor, A. R., **Rubber Chemistry and Technology**, Vol. 39, p. 306, 1966.

13. Hegmon, R. R., **Rubber Chemistry and Technology**, Vol. 42, p. 1122, 1969.

14. Yandell, W. O., **Wear**, Vol. 17, pp. 229-244, 1971.

15. Moore, D. F., **The Friction of Pneumatic Tyres**, Elsevier Scientific Publishing Company, New York, NY, 1975.

16. Moore, D. F., "A Theory of Viscous Hydroplaning," International Journal of Mechanical Sciences, Vol. 9, pp. 797-810, 1967.

17. Williams, A. R., "Tire Design," ChemTech, pp. 756-764, December 1984.

18. Williams, J. R., "Aquaplaning," Pavement Grooving and Traction Studies, NASA TP 5073, National Aeronautics and Space Administration, 1974.

19. Horne, W. B., and Joyner, U. T., Pneumatic Tire Hydroplaning and Some Effects on Vehicle Performance, International Automotive Engineering Congress, Society of Automotive Engineers, Detroit, MI, January 1965.

20. Nybakken, G. H., Staples, R. V., and Clark, S. K., "Laboratory Experiments on Reverted Rubber Friction," NASA CR-1398, National Aeronautics and Space Administration, August 1969.

21. Obertop, D.H.F., "Decrease of Skid-Resisting Properties of Wet Road Surfaces at High Speeds," ASTM Special Technical Publication No. 326, June 1962.

22. Moore, D. F., Prediction of Skid-Resistance Gradient and Drainage Characteristics for Pavements, Highway Research Record 131, Highway Research Board, Washington, DC, 1966, pp. 181-203.

23. Gough, V. E., "A Tyre Engineer Looks Critically at Current Traction Physics," The Physics of Tire Traction Theory and Experiment, Plenum Press, NY, 1974.

24. Yeager, R. W., "Tire Hydroplaning: Testing, Analysis, and Design," The Physics of Tire Traction, pp. 25-63, Plenum Press, 1974.

25. Wambold, J. C., Henry, J. J., and Hegmon, R. R., "Evaluation of Pavement Surface Texture Significance and Measurement Techniques," Wear, Vol. 83, No. 2, pp. 351-368, 1982.

26. Leu, M. C., and Henry, J. J., Prediction of Skid Resistance as a Function of Speed From Pavement Texture Measurements, Transportation Research Record 666, Transportation Research Board, Washington, DC, pp. 7-13, 1978.

27. Horne, W. B., and Buhlmann, F., "A Method for Rating the Skid Resistance and Micro/Macrotexture Characteristics, of Wet Pavements," Frictional Interaction of Tire and Pavement, ASTM STP 793, W. E. Meyer and J.D. Walter, Eds., pp. 191-218, American Society for Testing and Materials, 1983.

28. Schonfeld, R., Photo-Interpretation of Pavement Skid Resistance in Practice, Transportation Research Record 523, Transportation Research Board, Washington, DC, pp. 65-75, 1974.

29. Holt, F. B., and Musgrove, G. R., "Surface Texture Classification: A Guide to Pavement Skid Resistance," ASTM STP-763, **Pavement Surface Characteristics and Materials**, pp. 31-44, American Society for Testing and Materials, Philadelphia, PA, 1982.

30. Burk, D. O., **Simplified Quantifiable Determination of Rubber Removal Requirements**, unpublished U.S. Air Force document, Air Force Engineering and Services Center, Tyndall Air Force Base, FL, August 1979.

31. Anderson, V. L., and McLean, R. A., **Design of Experiments: A Realistic Approach**, Marcel Dekker, Inc., New York, NY, 1974.

32. Bedrick, Edward J., Assistant Professor of Mathematics and Statistics, University of New Mexico, Albuquerque, NM, personal communication, April 1985.

33. **SAS User's Guide**, SAS Institute, Inc., Cary, NC, 1982.

34. Yager, Thomas, National Aeronautics and Space Administration, personal communication, March 1985.

35. Lenke, L. R., Graul, R. A., and Standiford, D. L., "The Influence of Pavement Surface Texture on Runway Friction," **Proceedings**, 22nd Paving and Transportation Conference, Department of Civil Engineering, University of New Mexico, Albuquerque, NM, January 1985.

36. MacLennan, J. R., Wenck, N. C., Josephson, P. D., and Erdmann, J. B., **National Runway Friction Measurement Program**, FAA-AAS-80-1, U. S. Department of Transportation, Federal Aviation Administration, Washington, DC, 1980.

(The reverse of this page is blank.)

APPENDIX A

RUBBER REMOVAL QUESTIONNAIRE AND NMERI COVER LETTER

July 18, 1984

Return to:

Lary Lenke, Research Engineer
New Mexico Engineering Research Institute
Campus P. O. Box 25
Albuquerque, NM 87131

RUBBER REMOVAL QUESTIONNAIRE

Does your base or airport regularly perform runway rubber removal? _____

If so, how often (times per year)? _____

What technique(s) is (are) used to remove rubber at your base or airport?

_____

Does your base of airport use a specification for rubber removal? _____

If so, please send a copy of your specification for our files. (Your
specification will aid NMERI's specification development effort.)

How many runways does your facility have? _____

What are their designations (R/W No.)? _____

What type pavement surface does each of your runways have (PCC, AC, PFS,
etc.)? _____

_____(Please be
specific).

Is your base or airport planning rubber removal operations during the
remainder of 1984? _____

If so, when (approximate dates)? _____

Is it possible for the NMERI to perform field testing during your rubber
removal operations? _____

Please provide a point of contact for further correspondence and for arranging
possible field testing.

NAME: _____

_____

_____

_____

Telephone:_____ Autovon: _____
                                    (If applicable)

THE UNIVERSITY OF NEW MEXICO | ALBUQUERQUE, NEW MEXICO 87131

NEW MEXICO ENGINEERING RESEARCH INSTITUTE
CAMPUS POST OFFICE BOX 25
TELEPHONE (505) 844-4644

July 18, 1984

Dear Sir:

The New Mexico Engineering Research Institute (NMERI) has been contracted by the Air Force Engineering Services Center (AFESC) [Tyndall AFB, FL] and the Federal Aviation Administration (FAA) to conduct research and development concerned with runway rubber build-up. The NMERI has been tasked with developing contractor specifications for rubber removal and measurement techniques for evaluating rubber build-up.

The developed specifications will include this measurement technique as a quantifiable method of ascertaining rubber build-up and its effect on decreased wet friction value. This measurement technique will also aid the base or airport engineer in determining when the contractor has satisfied the rubber removal specification.

The NMERI has developed a field test experiment to aid in the development of the field test procedures and resultant specifications. This field experiment includes friction measurements (with a Mu Meter) and various texture measurement techniques performed before and after rubber removal.

It is highly desirable to obtain experimental data from as many bases or airports as possible during the remainder of 1984. Therefore, notification of anticipated rubber removal operations at your facility during this time frame is requested. The enclosed questionnaire is provided for your convenience and quick response to this query.

The NMERI pavement friction evaluation team has recently worked at Hill AFB (UT), Stapleton International (Denver) Airport, Ontario (California) Airport, Tulsa Airport, Holloman AFB, Fairchild AFB, Moses Lake (Wash.) Airport, and Mountain Home AFB. At all test sites, the experiment has been successfully conducted without incident. Our evaluation team is equipped for night operations (if required) and has communication equipment for safe operation. Normal operation of our experiment requires uninterrupted access of 12 hours before (two six-hour sessions are acceptable) and six hours after rubber removal. However, in emergency situations, the team can clear the runway within three minutes.

We appreciate your cooperation in this work, which will provide base and airport engineers and inspectors the simple test procedures necessary to quickly and objectively evaluate runway rubber build-up. The field test proceudres and specifications will be available from the FAA in October, 1985.

Inquiry letter
July 18, 1984
Page two

If your organization is not responsible for runway pavements at your facility,
please forward to the responsible party. Should your facility not have run-
ways, please return questionnaire stating such. For additional information,
please feel free to contact the undersigned.

Sincerely,

Lary R. Lenke, P.E.
Research Engineer
(505) 846-0430
Autovon: 246-0430

P.S. Please return questionnaire and specifications (if any), even if rubber
removal is not planned for your facility during 1984.

Enclosure
LRL:lt

APPENDIX B
PHOTOGRAPHS OF PAVEMENT TYPES EVALUATED

55

FIGURE B-1. RUNWAY Q, A GROOVED PORTLAND CEMENT CONCRETE
(RUNWAYS C, E, G, AND P SIMILAR)
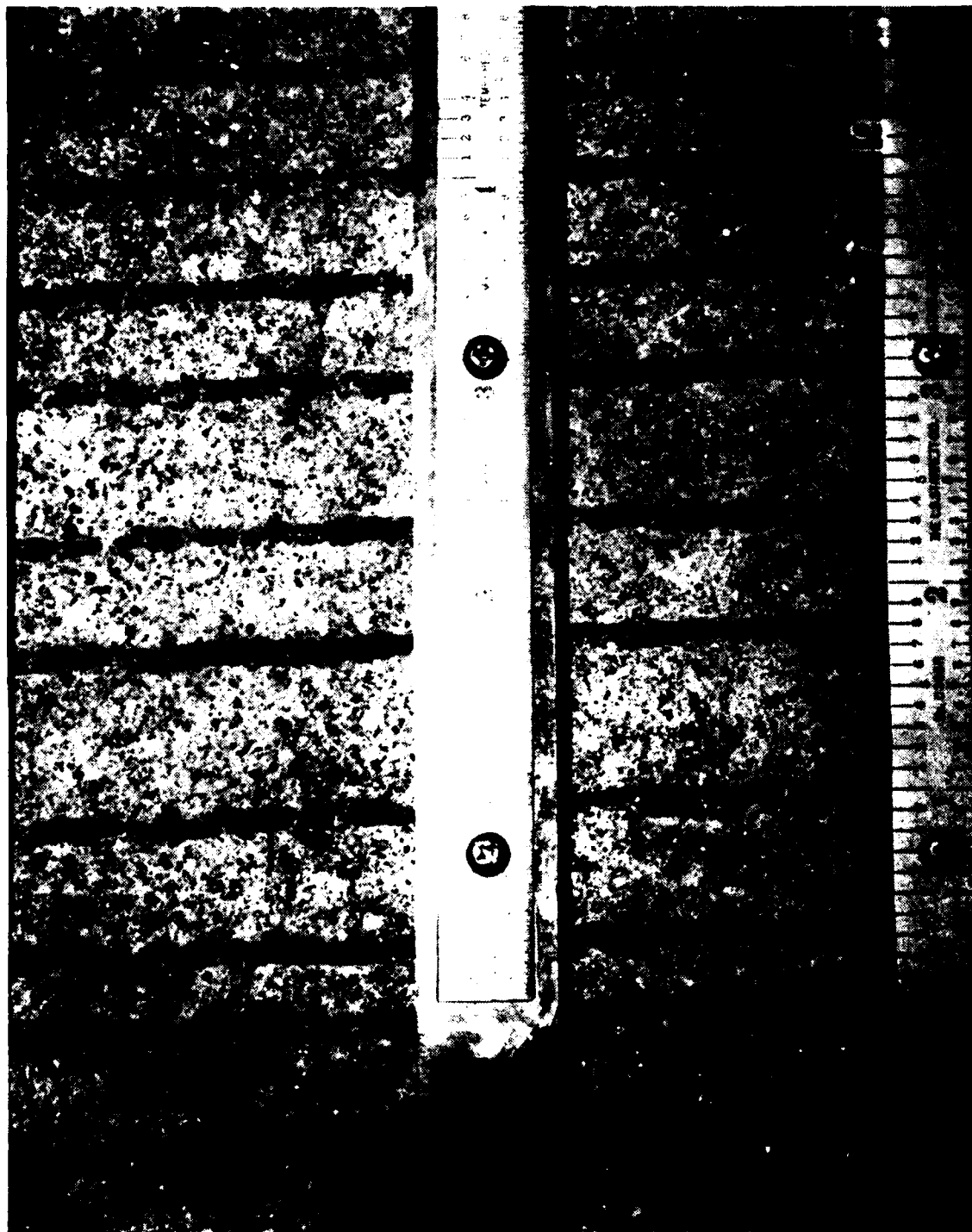
FIGURE B-2. RUNWAY F, A WIRE-TINED PORTLAND CEMENT CONCRETE
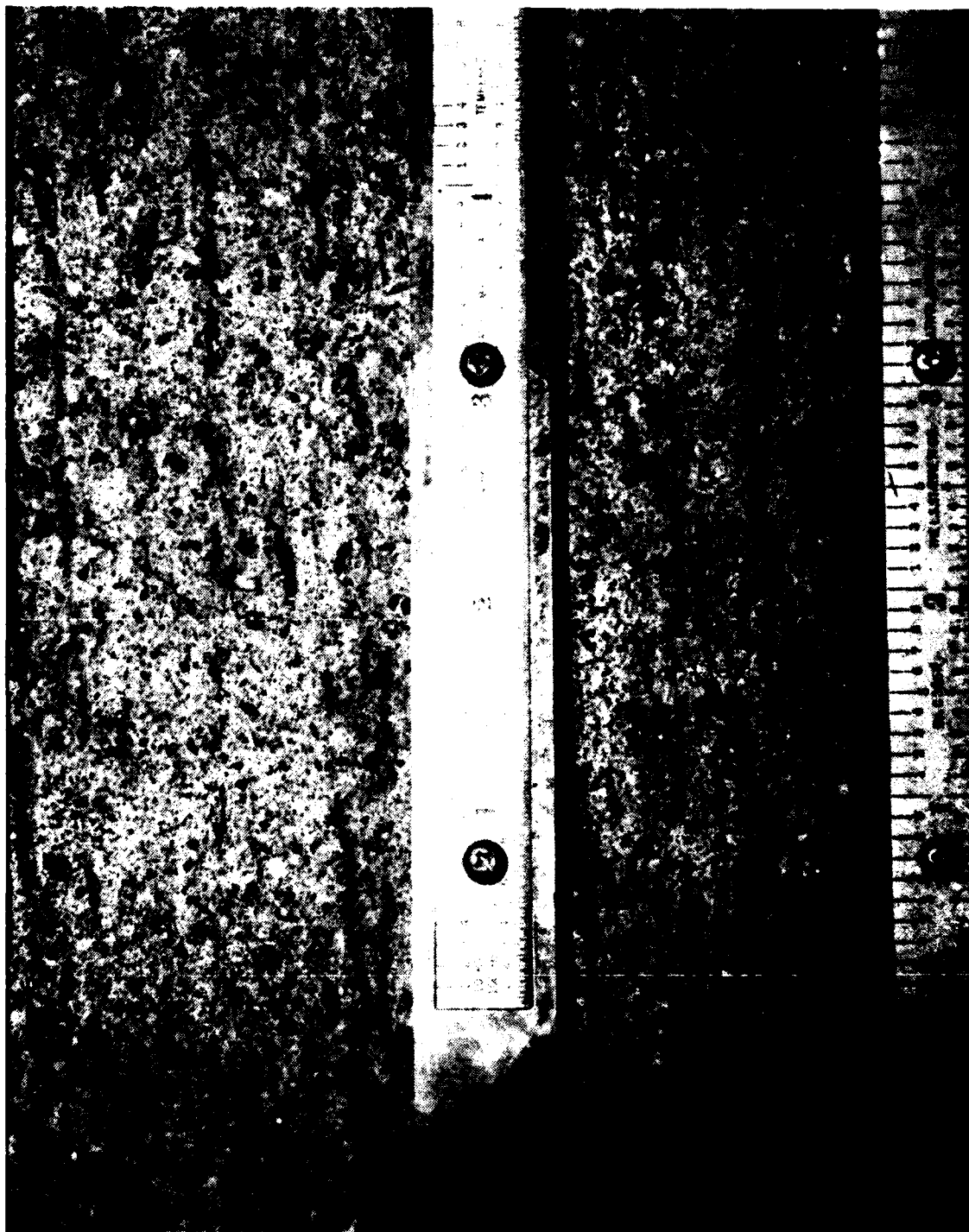
FIGURE B-3. RUNWAY B, A WIRE-COMBED PORTLAND CEMENT CONCRETE
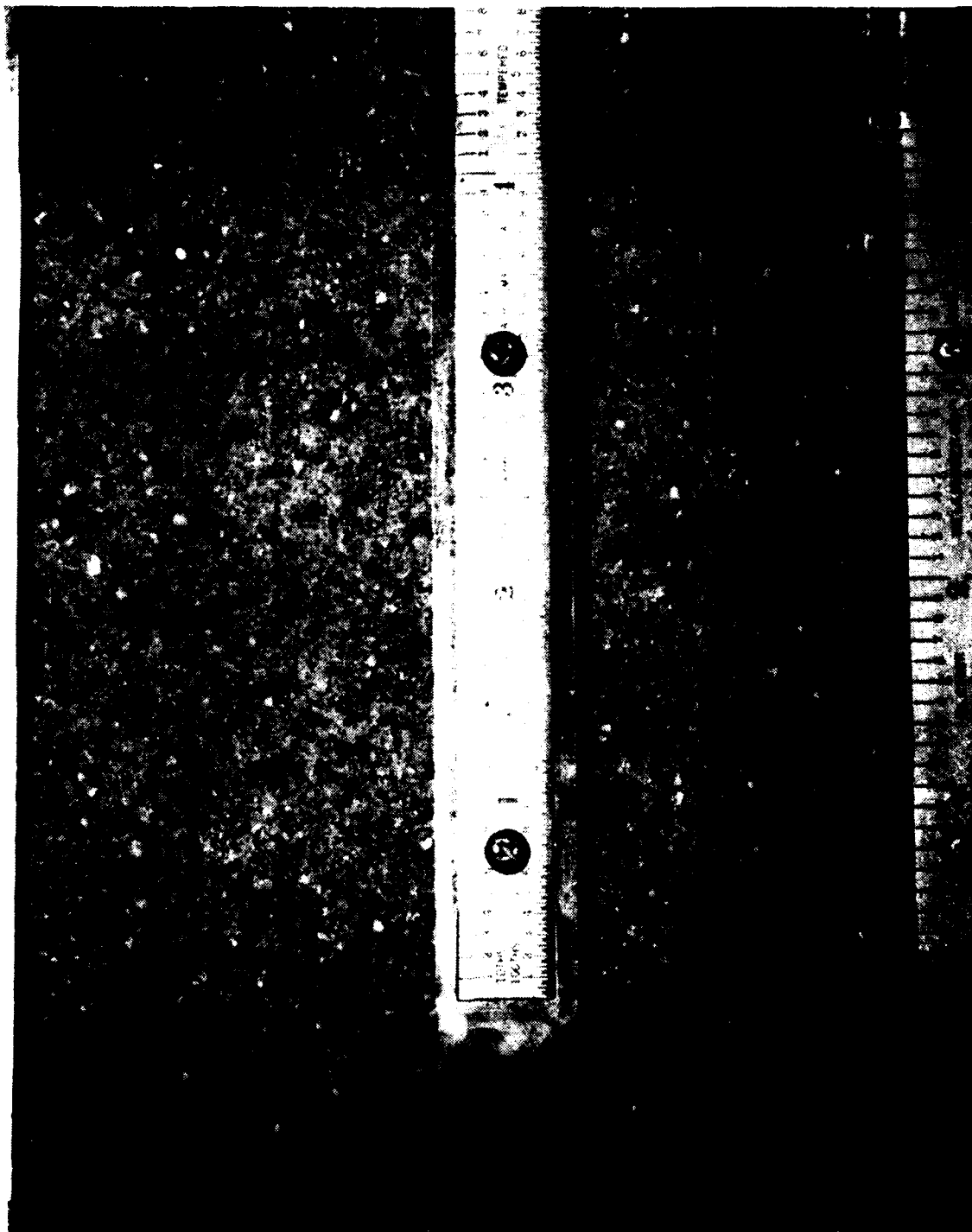
FIGURE B-4. RUNWAY O, A BURLAP DRAGGED PORTLAND CEMENT CONCRETE
(RUNWAYS I, M, N AND R SIMILAR)
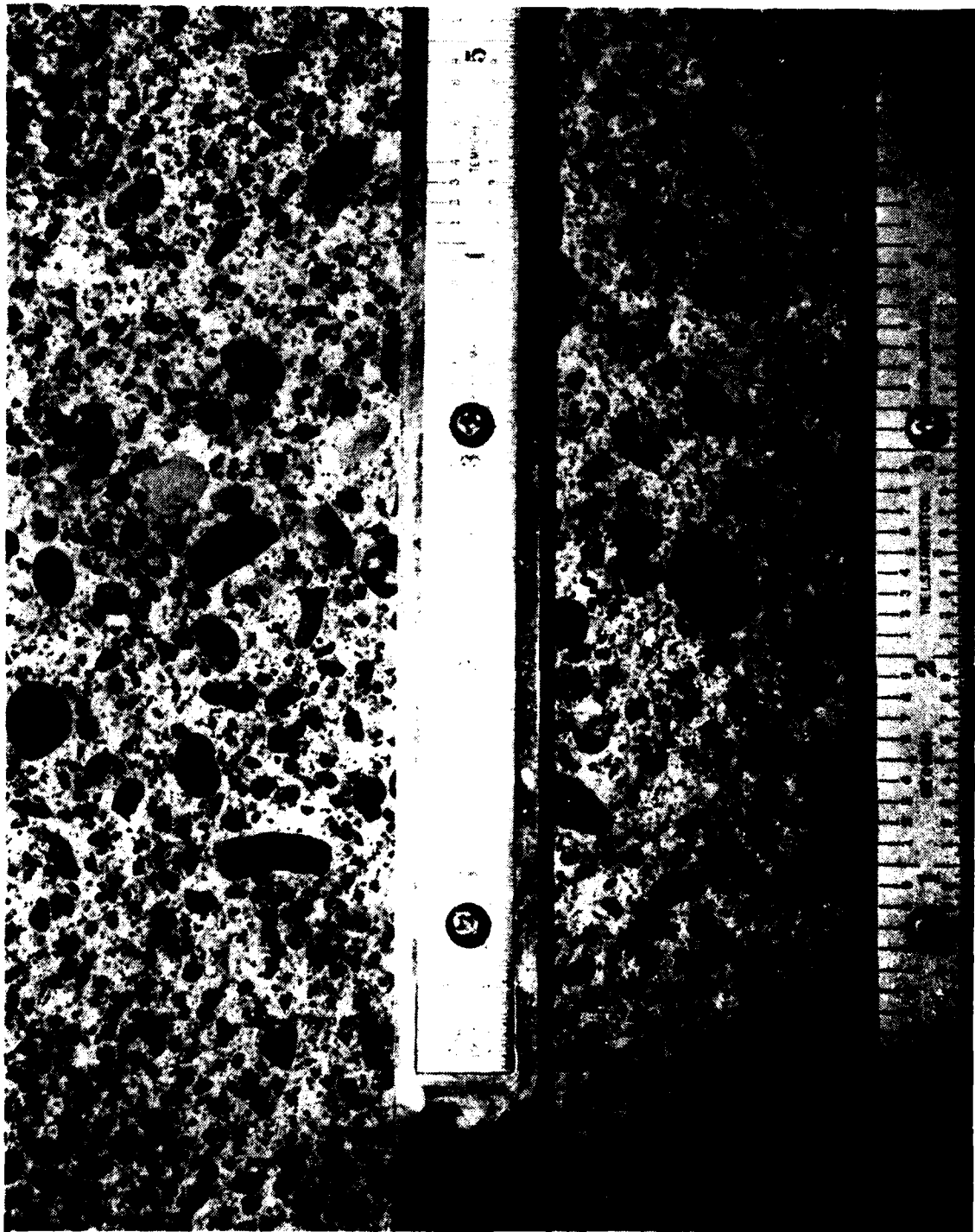
FIGURE B-5. RUNWAY D, A WORN PORTLAND CEMENT CONCRETE (RUNWAY A SIMILAR)
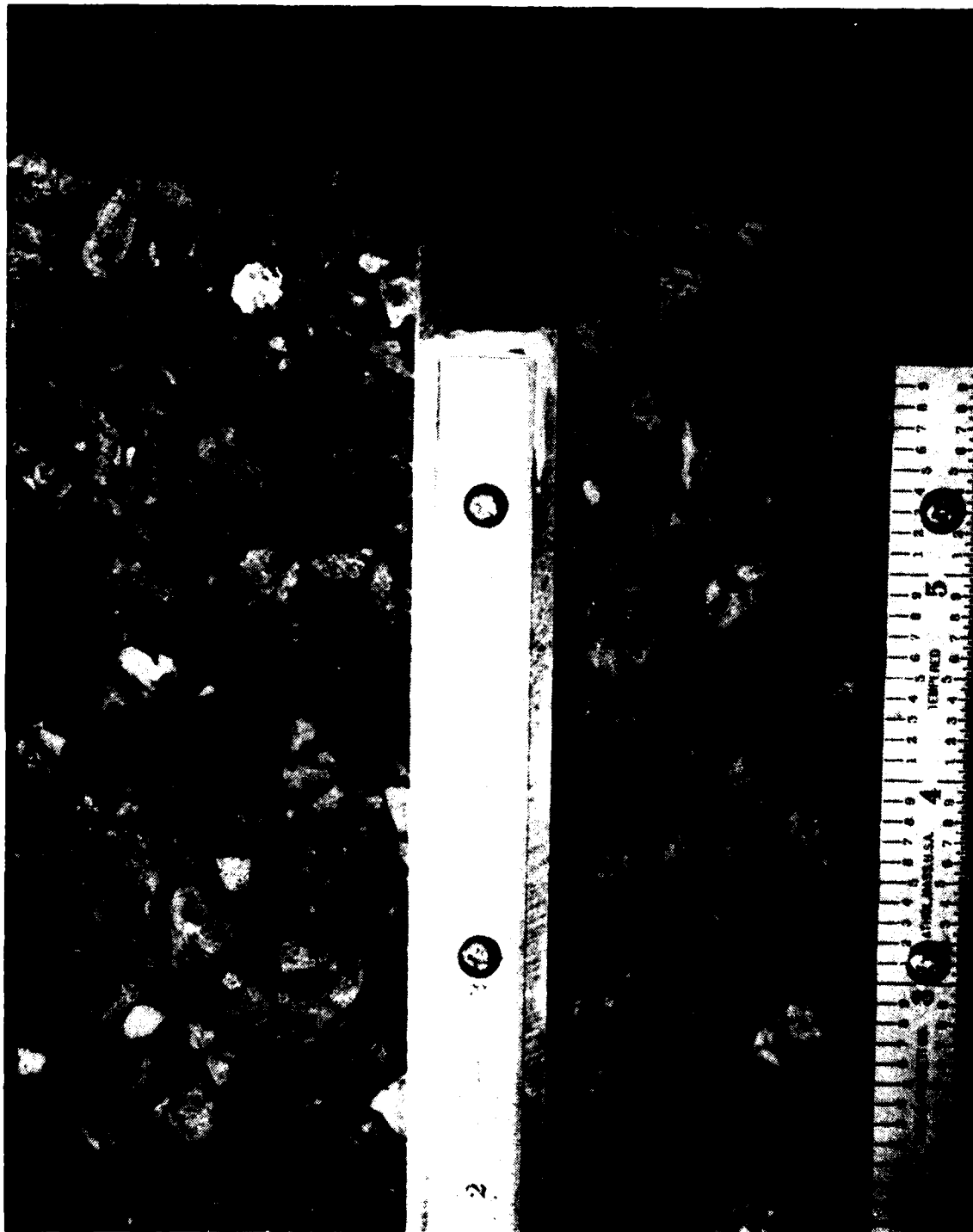
FIGURE B-6. RUNWAY H, A POROUS FRICTION SURFACE
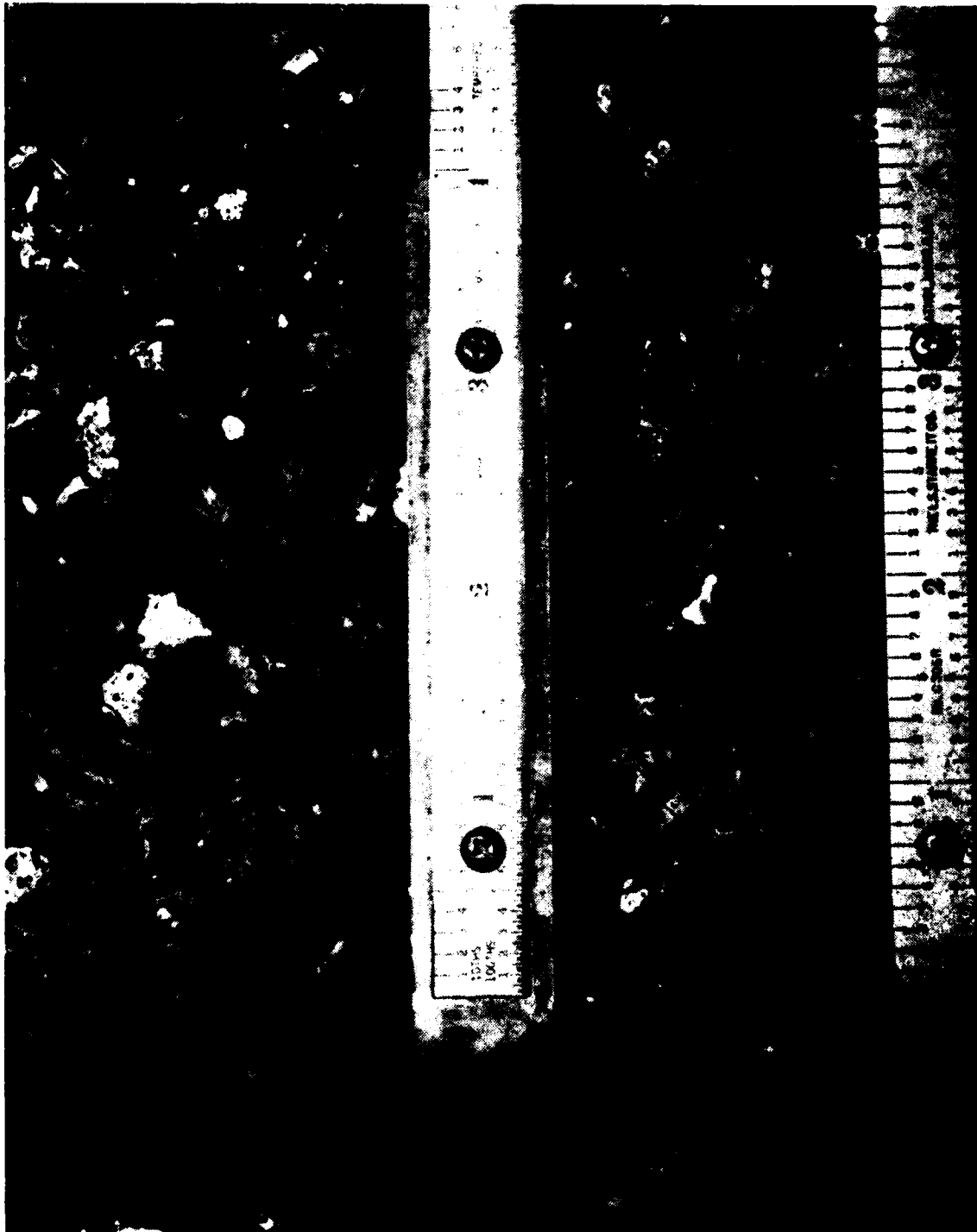
FIGURE B-7. RUNWAY K, A POROUS FRICTION SURFACE (RUNWAY J SIMILAR)
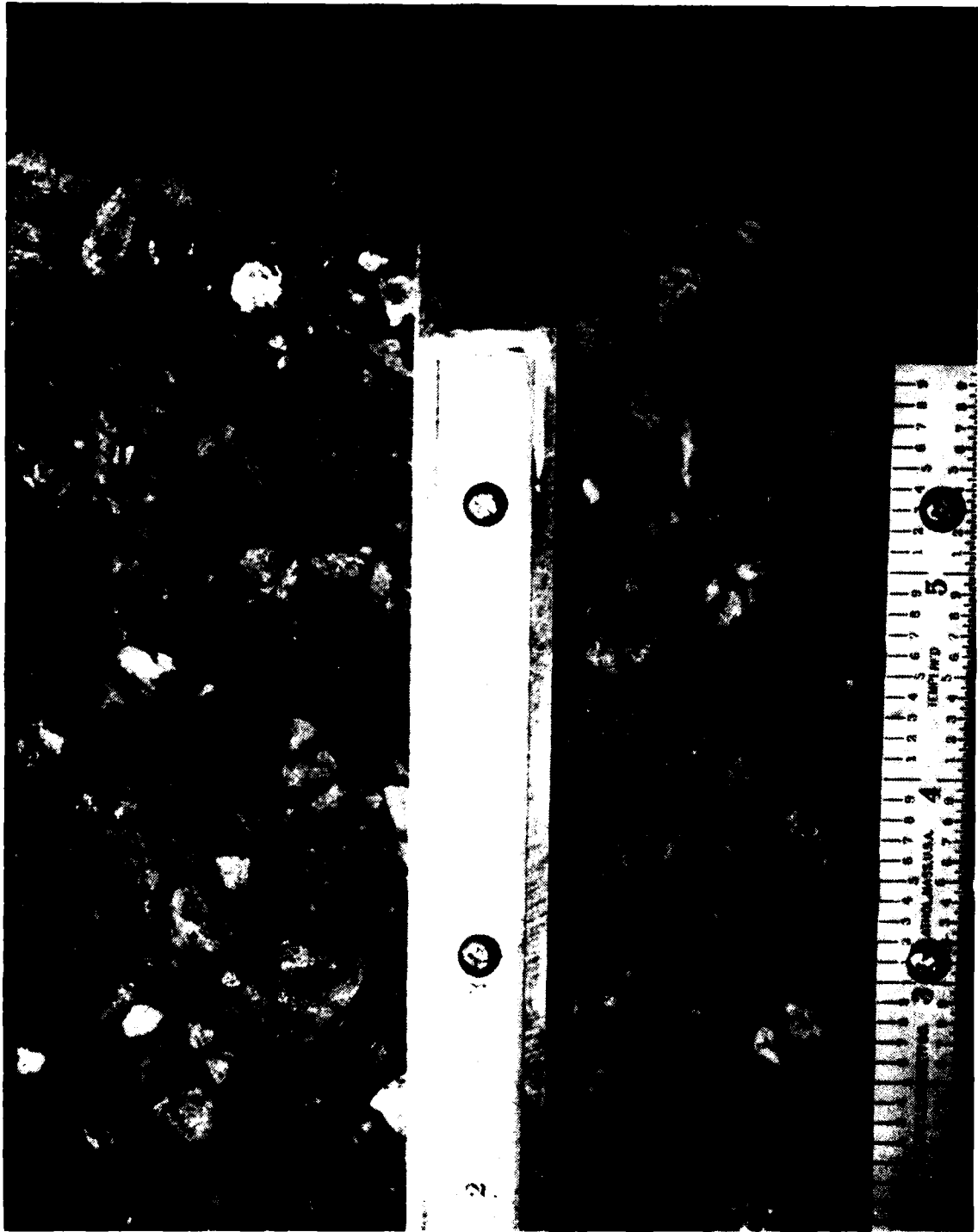
FIGURE B-6. RUNWAY H, A POROUS FRICTION SURFACE
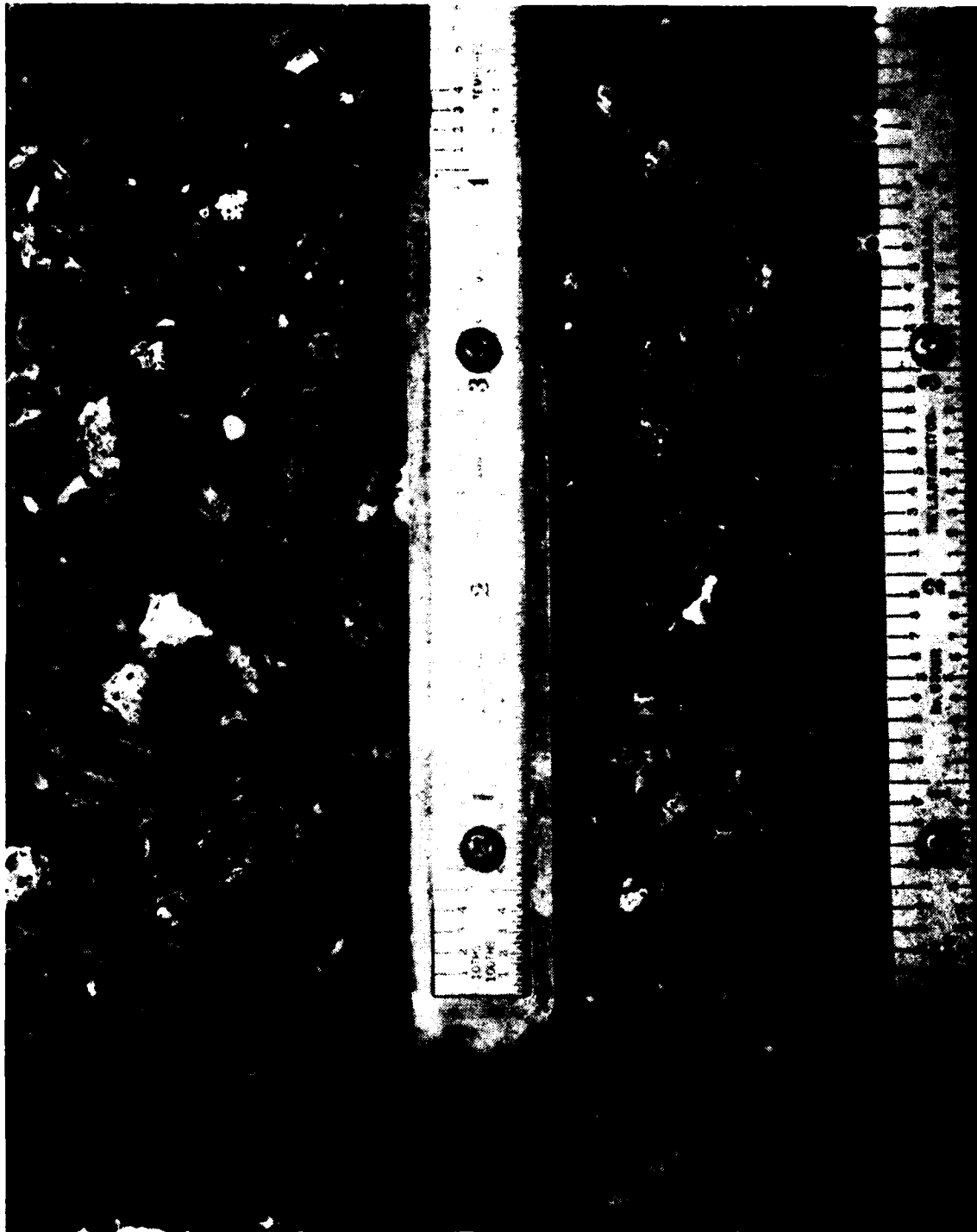
FIGURE B-7. RUNWAY K, A POROUS FRICTION SURFACE (RUNWAY J SIMILAR)
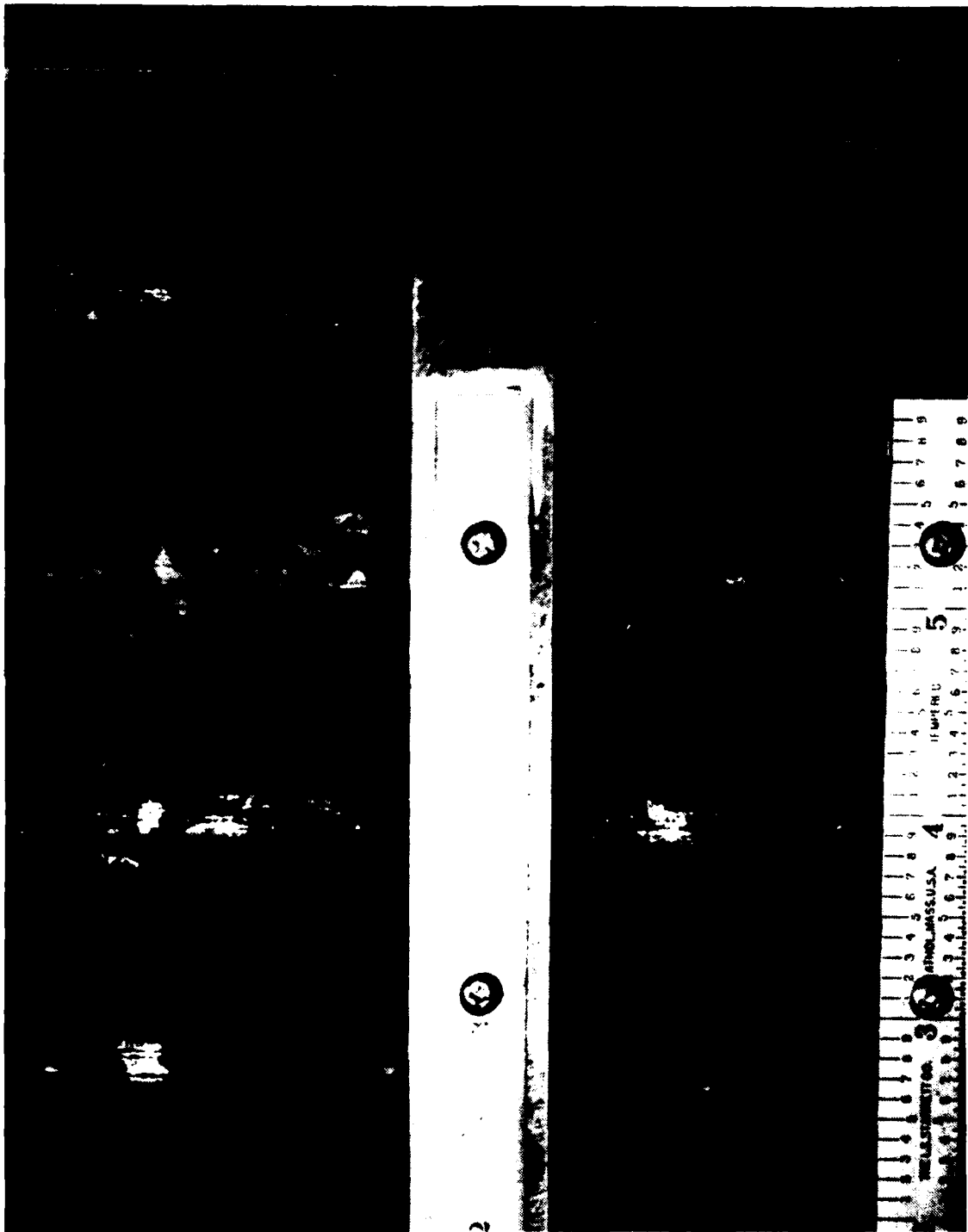
FIGURE B-8. RUNWAY L, A GROOVED ASPHALT CONCRETE

63

(The reverse of this page is blank.)

APPENDIX C
COLLECTED DATA BASE

The following is an explanation of variables that appear in the data base.

Base   is runway identification code (A through R).

Date   is approximate date of field testing.

Sec   is test section.

    1. 1 being centerline rubber before.

    2. 2 being centerline rubber after.

    3. 3 being centerline nonrubber.

    4. 4 being pavement edge nonrubber.

Loc   is test sites.

    1. 1 is 120 ft from start of test section.

    2. 2 is 240 ft from start of test section.

    3. 3 is 360 ft from start of test section.

Rep   is repetitions of tests.

M20   is 20 mi/h dry Mu value.

T20   is pavement temperature for 20 mi/h dry Mu value.

MW20   is 20 mi/h wet Mu value.

TW20   is pavement temperature for 20 mi/h wet Mu value.

M40   is 40 mi/h dry Mu value.

T40   is pavement temperature for 40 mi/h dry Mu value.

MW40   is 40 mi/h wet Mu value.

TW40   is pavement temperature for 40 mi/h wet Mu value.

M60   is 60 mi/h dry Mu value.

T60   is pavement temperature for 60 mi/h dry Mu value.

MW60   is 60 mi/h wet Mu value.

TW60   is pavement temperature for 60 mi/h wet Mu value.

SAP   is average texture depth as measured by sand patch measured in 10^{-4} in.

SIP   is average texture depth as measured by silicone putty measured in 10^{-4} in.

PTIL   is raw drag test number (DTN) measured dry in the longitudinal direction.

PTIT is raw DTN measured dry in the transverse direction.

TP is pavement temperature corresponding to the dry DTN.

PTIWL is raw DTN measured wet in the longitudinal direction.

PTIWT is raw DTN measured wet in the transverse direction.

TPW is pavement corresponding to wet DTNs.

CTL is chalk test measured in the longitudinal direction and recorded as a wear coefficient in 10^{-4} in/ft.

CTT is chalk test measured in the transverse direction and recorded as a wear coefficient in 10^{-4} in/ft.

OBS	DATE	SEC	LOC	REP	M20	T20	MM20	TH20	M40	T40	MM40	TH40	M60	T60	MM60	TH60	SAP	SIP	PTIL	PTIT	TP	PTIWL	PTIWT	TPW	CTL	CTT
1	840710	1	1	1	75	88	52	82	78	88	36	82	82	88	16	82	93	197	97	80	88	40	45	88	90	60
2	840710	1	1	2	76	88	52	82	76	88	33	82	82	88	20	82	97	170	85	85	88	40	45	88	47	70
3	840710	1	2	1	75	88	59	82	78	88	36	82	84	88	24	82	180	319	88	98	88	42	45	88	77	71
4	840710	1	2	2	80	88	52	82	78	88	32	82	88	88	26	82	118	344	90	96	88	46	50	88	75	47
5	840710	1	3	1	76	88	56	82	79	88	38	82	84	88	23	82	112	229	101	95	88	40	43	86	76	78
6	840710	1	3	2	80	88	50	90	80	88	34	82	84	88	27	82	143	214	95	97	88	42	41	86	84	52
7	840710	2	1	1	72	88	66	82	72	88	40	90	76	88	34	90	119	225	70	70	92	48	52	92	110	125
8	840710	2	1	2	74	88	61	90	74	88	44	90	76	88	32	90	116	189	68	71	92	49	53	92	80	105
9	840710	2	2	1	70	88	62	90	74	88	48	90	78	88	34	90	179	361	75	69	90	48	50	90	124	115
10	840710	2	2	2	77	88	62	90	72	88	44	90	76	88	29	90	116	344	71	70	90	47	52	90	133	155
11	840710	2	3	1	74	88	63	90	74	88	44	90	80	88	32	90	159	455	67	69	90	41	46	90	97	101
12	840710	2	3	2	82	88	61	82	83	88	44	82	86	88	28	82	133	215	70	65	90	40	48	82	125	131
13	840710	3	1	1	84	88	63	90	84	88	52	82	86	88	38	82	196	446	101	100	82	40	40	80	129	110
14	840710	3	1	2	82	88	62	82	83	88	54	82	87	88	34	82	235	464	93	98	82	40	40	80	147	163
15	840710	3	2	1	82	88	64	82	82	88	50	82	86	88	32	82	210	471	94	96	80	45	42	80	174	167
16	840710	3	2	2	82	88	64	82	82	88	50	82	86	88	38	82	226	356	91	92	80	40	40	80	175	168
17	840710	3	3	1	84	88	65	82	84	88	54	82	90	83	40	82	165	345	90	85	80	46	46	82	172	160
18	840710	3	3	2	84	87	68	84	84	87	60	82	80	87	43	80	191	471	85	83	82	50	50	82	204	179
19	840710	4	1	1	78	83	69	79	79	83	57	82	80	83	38	80	198	384	84	82	80	55	52	80	197	204
20	840710	4	1	2	78	87	70	80	78	87	56	82	79	87	38	80	197	386	84	80	80	55	52	80	155	186
21	840710	4	2	1	80	83	70	80	80	83	58	82	80	87	44	80	190	473	81	81	80	52	55	80	179	188
22	840710	4	3	2	78	83	68	80	80	83	60	80	76	83	42	80	227	532	80	80	80	55	56	80	192	203

OBS	DATE	SEC	LOC	REP	M20	T20	MM20	TH20	M40	T40	MM40	TH40	M60	T60	MM60	TH60	SAP	SIP	PTIL	PTIT	TP	PTIWL	PTIWT	TPW	CTL	CTT
25	840925	1	1	1	78	72	71	72	80	72	61	72	81	72	54	72	290	744	85	95	70	63	68	72	90	142
26	840925	1	1	2	78	110	72	110	79	110	67	72	83	72	48	72	296	655	85	96	72	63	65	72	119	163
27	840925	1	2	1	79	72	72	72	80	72	65	72	80	72	48	72	288	655	83	92	72	55	65	72	155	139
28	840925	1	2	2	80	72	74	72	80	72	65	72	82	72	54	72	303	657	88	86	72	60	63	72	127	137
29	840925	1	3	1	79	72	73	72	79	72	64	72	81	72	54	72	238	835	80	90	72	57	63	72	134	140
30	840925	1	3	2	79	72	76	72	79	72	61	72	81	72	56	72	231	486	84	91	72	57	70	72	144	124
31	840925	2	1	1	80	110	76	110	84	110	68	110	83	110	56	110	310	589	80	85	92	59	68	92	131	130
32	840925	2	1	2	82	110	82	110	82	110	68	110	82	110	52	110	312	632	72	86	92	64	70	92	129	127
33	840925	2	2	1	82	110	80	110	82	110	72	110	83	110	55	110	315	773	82	85	100	61	65	100	119	166
34	840925	2	2	2	82	110	79	110	82	110	72	110	84	110	50	110	327	707	75	85	108	61	65	108	119	163
35	840925	2	3	1	82	110	80	110	81	110	65	110	82	110	58	110	219	722	81	83	108	59	70	108	134	150
36	840925	2	3	2	83	72	84	110	83	110	72	110	85	110	57	110	234	477	74	82	108	70	75	108	150	143
37	840925	3	1	1	82	72	80	72	81	72	72	72	84	72	56	72	344	734	85	90	72	66	70	72	134	181
38	840925	3	1	2	82	72	81	72	83	72	69	72	82	72	59	72	409	667	84	91	72	65	72	72	148	155
39	840925	3	2	1	82	102	82	72	83	102	72	72	85	102	52	72	234	641	85	90	73	66	75	73	140	142
40	840925	3	2	2	82	102	80	72	81	102	72	72	84	102	59	72	639	1065	85	95	72	65	70	72	147	126
41	840925	3	3	1	84	102	78	72	83	102	73	72	82	102	72	72	441	854	80	86	72	70	72	110	140	149
42	840925	3	3	2	86	72	85	72	81	72	78	72	85	72	72	72	230	655	80	87	72	65	75	110	140	164
43	840925	4	1	1	87	102	84	110	83	102	80	110	87	102	72	110	260	522	83	86	72	64	70	110	155	175
44	840925	4	1	2	85	102	85	110	83	102	76	110	86	102	73	110	269	566	85	87	72	64	68	110	158	197
45	840925	4	2	1	85	102	85	110	83	102	77	110	88	102	72	110	491	892	83	97	70	68	75	70	147	174
46	840925	4	3	2	85	102	84	72	86	102	80	72	83	102	72	72	374	943	85	95	70	65	75	70	156	168

OBS	DATE	SEC	LOC	REP	M20	T20	MW20	TW20	M40	T40	MW40	TW40	M60	T60	MW60	TW60	SAP	SIP	PTIL	PTIT	TP	PTIWL	PTIWT	TPW	CTL	CTT
49	840423	1	1	1	78	49	60	49	80	49	44	52	84	39	36	49	312	439	92	97	44	37	37	49	43	45
50	840423	1	1	2	77	50	60	52	78	50	46	52	82	52	36	52	300	538	98	96	44	44	36	44	48	64
51	840423	1	1	1	78	49	54	49	79	49	39	52	82	39	25	49	325	538	78	80	44	45	30	44	71	70
52	840423	1	2	2	75	50	56	52	78	50	44	52	75	49	30	52	371	579	78	79	44	47	36	44	82	43
53	840423	1	2	1	77	49	61	49	78	50	44	52	80	39	26	49	308	497	85	81	44	45	41	44	57	79
54	840423	1	2	2	76	50	68	52	78	50	46	52	84	49	34	52	325	558	82	82	44	46	41	42	42	42
55	840423	2	1	1	84	44	70	45	85	44	58	39	84	43	43	44	313	610	85	85	42	53	55	42	69	107
56	840423	2	1	2	82	44	60	40	84	44	48	44	82	43	42	39	350	815	85	80	40	58	58	42	51	115
57	840423	2	1	1	83	44	60	45	84	44	54	39	84	43	34	44	253	660	91	85	40	48	50	40	21	64
58	840423	2	2	2	83	44	60	40	84	44	48	44	82	43	38	39	346	662	95	87	39	50	57	39	66	76
59	840423	2	2	1	83	44	70	45	76	44	60	44	84	43	36	44	335	648	90	92	39	51	55	44	66	55
60	840423	2	2	2	76	49	70	49	76	50	56	52	82	39	40	39	355	602	95	83	44	61	57	44	148	43
61	840423	3	1	1	76	49	76	52	76	50	73	52	78	49	62	49	357	628	91	82	44	51	55	44	143	134
62	840423	3	1	2	75	49	78	52	76	49	70	52	80	49	55	52	326	607	90	85	42	55	56	44	92	96
63	840423	3	1	1	76	50	76	52	76	50	73	52	78	39	64	49	316	581	86	86	44	52	54	44	61	101
64	840423	3	2	2	75	49	74	41	75	49	72	52	79	49	64	52	383	799	86	86	42	60	57	42	145	116
65	840423	3	2	1	76	50	76	52	76	52	73	52	72	48	64	52	412	919	76	75	42	58	54	42	124	130
66	840423	3	2	2	76	49	84	41	76	41	80	41	74	48	74	41	385	754	75	75	42	63	65	42	92	162
67	840423	4	1	1	76	50	82	40	76	50	80	41	76	48	70	40	306	709	82	75	43	63	65	43	183	104
69	840423	4	1	2	75	50	84	41	76	41	80	41	78	50	70	41	351	705	75	75	43	62	64	43	175	188
70	840423	4	2	1	76	50	83	40	76	50	80	40	78	48	71	40	456	688	75	73	43	63	63	43	159	151
71	840423	4	2	1	75	50	84	41	76	50	79	40	78	48	71	41	384	794	75	75	44	54	55	44	128	176
72	840423	4	2	3	76	51	84	40	76	50	80	40	76	50	71	40	403	778	75	75	44	55	55	44	131	153

OBS	DATE	SEC	LOC	REP	M20	T20	MW20	TW20	M40	T40	MW40	TW40	M60	T60	MW60	TW60	SAP	SIP	PTIL	PTIT	TP	PTIWL	PTIWT	TPW	CTL	CTT
73	840630	1	1	1	76	50	47	50	77	50	35	50	80	50	22	50	100	160	75	75	62	52	49	62	32	30
74	840630	1	1	2	76	50	50	49	80	50	36	49	80	50	20	50	102	381	74	75	62	62	50	63	48	32
75	840630	1	1	1	74	50	62	50	78	50	34	50	83	50	16	50	113	209	83	90	63	45	47	63	29	30
76	840630	1	2	2	74	50	54	50	80	50	37	50	80	50	14	50	135	284	86	90	63	46	46	61	40	24
77	840630	1	2	1	77	50	54	50	79	50	36	50	82	50	21	50	162	235	98	91	62	50	60	61	44	51
78	840630	1	2	2	76	50	48	49	80	49	30	49	82	50	17	50	164	326	90	94	62	52	55	53	57	38
79	840630	2	1	1	72	76	53	70	80	70	35	70	75	70	20	70	105	241	65	60	53	49	52	51	51	55
80	840630	2	1	2	70	76	56	70	75	70	35	70	70	75	18	70	104	270	60	67	68	53	47	59	59	41
81	840630	2	1	1	72	76	62	70	73	70	44	70	72	75	20	70	146	344	64	61	68	51	54	68	88	77
82	840630	2	2	2	74	76	64	70	71	70	34	70	74	75	22	70	146	352	55	65	70	56	63	70	83	96
83	840630	2	2	1	72	76	58	70	73	70	59	70	75	75	19	70	128	448	67	73	70	55	63	56	56	116
84	840630	2	2	2	81	50	74	50	82	50	64	50	86	50	52	50	209	475	95	70	53	67	59	55	111	75
85	840630	3	1	1	82	50	78	49	83	50	64	49	88	50	53	50	183	404	101	97	71	60	66	53	83	81
86	840630	3	1	2	80	50	78	50	86	50	64	49	87	50	54	50	169	422	97	98	60	59	63	72	70	79
87	840630	3	1	1	82	50	80	50	82	50	62	48	88	48	52	48	180	243	95	97	71	60	69	71	66	87
88	840630	3	2	2	82	50	80	48	84	50	64	48	81	48	55	48	233	419	96	93	70	59	60	67	99	101
90	840630	3	2	1	80	50	76	50	83	48	64	48	80	48	52	50	183	340	94	92	67	56	65	70	103	44
91	840630	4	1	2	78	48	80	48	79	50	65	48	79	48	46	48	186	273	92	96	56	58	63	67	48	52
92	840630	4	1	1	80	50	78	48	83	48	64	48	80	48	52	48	151	367	96	92	58	64	65	67	41	40
93	840630	4	2	2	80	48	80	48	84	50	64	48	79	48	54	48	169	450	94	96	64	64	63	70	45	58
95	840630	4	2	1	80	50	78	48	84	48	61	48	84	48	54	48	164	383	92	95	70	61	64	70	50	92
96	840630	4	2	2	77	48	78	48	79	50	58	48	82	48	50	48	150	336	86	92	70	60	64	70	59	104

---- BASE=E ----

OBS	DATE	SEC	LOC	REP	M20	T20	MW20	TH20	M40	T40	MW40	TH40	M60	T60	MW60	TH60	SAP	SIP	PTIL	PTIT	TP	PTIWL	PTIWT	TPW	CTL	CTT
97	841120	1	1	1	74	48	64	48	48	58	48	48	72	48	50	48	248	604	97	97	50	80	67	50	83	95
98	841120	1	1	2	73	48	66	48	48	52	48	48	74	48	50	48	309	499	100	96	50	70	65	50	82	83
99	841120	1	2	1	72	48	66	48	48	58	48	48	71	48	50	48	391	655	97	91	50	72	65	50	92	84
100	841120	1	2	2	72	48	64	48	48	58	48	48	72	48	48	48	281	810	105	90	50	75	65	48	93	97
101	841120	1	3	1	73	48	65	48	48	54	48	48	72	48	48	48	373	660	95	95	48	70	60	48	73	70
102	841120	2	1	1	74	48	59	48	48	52	50	48	75	48	48	48	297	702	96	93	48	70	55	48	92	85
103	841120	2	1	2	65	35	59	34	34	50	34	34	68	35	36	34	207	807	85	72	35	60	55	35	55	60
104	841120	2	2	1	66	35	62	34	34	48	34	34	66	35	34	34	306	606	76	76	35	65	55	34	75	70
105	841120	2	2	2	66	35	61	34	34	55	34	34	68	35	35	34	323	747	86	78	34	65	55	34	78	76
106	841120	2	3	1	67	35	60	34	34	46	34	34	68	35	35	34	384	869	85	76	34	65	58	34	80	76
107	841120	2	3	2	67	35	61	34	34	53	34	34	69	35	34	34	308	709	80	74	34	63	53	34	57	65
108	841120	3	1	1	68	48	60	48	48	61	48	48	74	48	34	48	326	846	95	86	40	61	56	40	79	60
109	841120	3	1	2	74	48	66	48	48	62	48	48	74	48	48	48	523	953	94	88	40	62	55	38	91	96
110	841120	3	2	1	74	48	66	48	48	62	48	48	74	48	48	48	435	1205	95	86	38	60	50	38	98	81
111	841120	3	2	2	74	48	66	48	48	65	35	48	74	48	48	48	421	1129	105	92	38	58	55	38	90	99
112	841120	3	3	1	74	48	66	48	48	66	35	48	74	48	48	48	424	685	94	83	36	55	50	36	98	103
113	841120	3	3	2	71	48	69	48	48	64	35	48	70	36	48	36	391	940	92	82	36	77	64	36	139	139
114	841120	3	3	3	70	36	70	36	36	66	35	36	74	36	36	36	444	874	94	82	36	80	65	38	144	137
116	841120	4	1	1	71	36	68	36	36	64	35	36	72	36	35	35	591	579	90	82	35	70	68	36	122	144
117	841120	4	2	1	72	36	69	36	36	66	35	36	72	36	35	35	345	1205	82	79	35	75	70	35	113	144
118	841120	4	3	1	72	36	68	36	36	64	35	36	72	36	35	35	639	760	87	80	35	76	71	35	143	152
119	841120	4	3	2	71	36	70	36	36	66	35	36	72	36	35	35	460	898	89	81	35	82	72	35	151	160
120	841120	4	4	3	70	36	70	36	36	67	35	36	70	36	35	35	403	1111	89	81	35	78	70	35	126	137

---- BASE=F ----

OBS	DATE	SEC	LOC	REP	M20	T20	MW20	TH20	M40	T40	MW40	TH40	M60	T60	MW60	TH60	SAP	SIP	PTIL	PTIT	TP	PTIWL	PTIWT	TPW	CTL	CTT
121	841123	1	1	1	70	40	60	38	38	42	38	38	72	40	30	38	203	674	87	88	42	71	68	42	66	93
122	841123	1	1	2	70	40	58	38	38	44	38	38	74	40	28	38	174	509	86	88	42	71	65	42	78	86
123	841123	1	2	1	69	40	61	38	38	47	38	38	72	40	38	38	302	883	85	87	42	55	60	42	83	94
124	841123	1	2	2	70	40	59	38	38	44	38	38	73	40	36	38	207	606	82	87	42	58	58	42	93	110
125	841123	1	3	1	69	40	62	38	38	50	38	38	69	40	38	38	360	639	80	83	42	70	69	42	66	74
126	841123	2	1	1	71	40	57	38	38	41	50	38	72	40	38	38	250	799	84	85	54	70	62	54	73	70
127	841123	2	1	2	76	52	58	50	50	40	50	50	78	52	30	50	162	544	86	87	54	58	59	54	57	75
128	841123	2	2	1	73	52	60	50	50	40	50	50	74	52	28	50	261	773	83	87	54	60	59	54	103	76
129	841123	2	2	2	73	52	62	50	50	48	50	50	75	52	32	50	279	840	88	86	54	61	60	54	104	116
130	841123	2	3	1	72	52	60	50	50	40	50	50	74	52	30	50	185	644	87	92	54	62	61	54	96	97
131	841123	3	1	1	72	52	62	50	50	48	48	50	76	52	31	50	244	857	85	88	42	66	65	42	88	103
132	841123	3	2	2	74	40	70	38	38	58	48	38	75	40	49	38	298	581	105	88	42	61	61	42	98	111
133	841123	3	3	1	74	40	69	38	38	60	56	38	77	40	55	38	256	648	103	88	42	75	70	42	95	115
134	841123	3	3	2	74	40	69	38	38	62	49	38	78	40	54	38	390	685	100	90	42	73	65	42	121	109
135	841123	3	3	3	76	40	77	38	38	58	54	38	79	40	49	38	279	835	100	93	42	68	68	42	110	124
136	841123	4	1	1	75	42	78	42	42	63	56	38	80	42	54	42	236	560	95	91	42	65	63	42	108	115
137	841123	4	2	1	74	42	76	42	42	65	52	38	84	42	58	42	278	617	93	85	38	60	60	38	129	128
138	841123	4	2	2	80	42	77	42	42	66	58	42	83	42	44	42	237	628	93	85	40	85	72	42	127	144
139	841123	4	3	1	80	42	78	42	42	62	44	42	84	42	58	42	272	697	91	83	40	75	70	38	153	148
140	841123	4	3	2	80	42	76	42	42	61	42	42	84	42	44	42	260	593	93	90	40	76	65	40	159	169
141	841123	4	4	1	79	42	76	42	42	58	42	42	84	42	44	42	271	709	92	88	40	80	64	40	156	167
143	841123	4	4	2	79	42	76	42	42	58	42	42	84	42	44	42	250	799	92	88	40	77	64	40	190	178
144	841123	4	4	3	79	42	76	42	42	58	42	42	84	42	44	42	250	799	92	88	40	77	64	40	189	155

69

OBS	DATE	SEC	LOC	REP	M20	T20	MW20	TH20	M40	T40	MW40	TH40	M60	T60	MW60	TH60	SAP	SIP	PTIL	PTIT	TP	PTIML	PTIMT	TPW	CTL	CTT
145	841117	1	1	1	74	52	58	50	74	52	48	50	78	52	35	50	313	615	96	95	54	71	60	54	44	47
146	841117	1	1	2	75	52	60	50	76	52	46	50	78	52	34	50	235	397	98	98	54	66	61	54	40	43
147	841117	1	2	1	74	52	63	50	75	52	47	50	80	52	36	50	306	574	96	97	52	70	64	52	46	54
148	841117	1	2	2	75	52	64	50	76	52	49	50	79	52	33	50	253	495	100	95	52	55	60	52	51	64
149	841117	1	3	1	75	52	65	50	75	52	52	50	76	52	40	50	279	655	95	94	52	65	60	52	68	71
150	841117	1	3	2	73	52	58	50	72	52	44	50	79	52	36	50	271	534	94	64	52	55	45	52	61	68
151	841117	2	1	1	72	44	60	42	76	44	44	42	74	44	33	42	230	854	75	65	46	53	50	46	45	49
152	841117	2	1	2	71	44	62	42	75	44	44	42	80	44	34	42	339	697	75	65	45	56	52	45	55	60
153	841117	2	2	1	74	44	66	42	76	44	46	42	72	44	36	42	325	662	80	75	45	61	52	45	49	47
154	841117	2	2	2	72	44	68	42	75	44	56	42	74	44	34	42	439	832	75	70	48	58	52	48	62	49
155	841117	2	3	1	74	44	72	42	76	44	57	42	80	44	43	42	296	697	78	97	48	60	56	48	60	71
156	841117	2	3	2	74	44	72	42	77	44	64	42	82	44	56	42	313	635	97	91	52	65	58	48	66	114
157	841117	3	1	1	79	44	71	42	80	44	65	42	81	44	52	42	391	857	96	88	52	62	60	48	105	122
158	841117	3	1	2	80	44	75	42	80	44	66	42	82	44	55	42	371	1075	93	86	52	73	61	48	112	133
159	841117	3	2	1	79	44	76	42	80	44	68	42	80	41	56	41	371	928	94	90	52	63	62	48	140	152
160	841117	3	2	2	78	44	76	40	80	44	69	40	82	41	60	41	427	943	89	82	52	75	63	48	135	127
161	841117	3	3	1	80	41	75	40	78	41	70	40	80	41	60	41	460	898	94	82	52	63	61	44	113	124
162	841117	3	3	2	80	41	77	40	78	41	68	40	80	41	62	41	363	734	90	83	44	68	65	44	117	151
163	841117	4	1	1	78	41	76	40	78	41	70	40	80	41	62	41	292	765	92	82	44	70	63	44	138	141
164	841117	4	1	2	78	41	78	40	78	41	69	40	80	41	60	41	306	904	88	83	44	74	65	44	162	183
165	841117	4	2	1	78	41	76	40	78	41	70	40	80	41	62	41	414	910	90	83	44	70	64	44	149	124
166	841117	4	2	2	78	41	74	40	78	41	69	40	80	41	62	41	372	1024	88	82	44	74	64	47	186	197
167	841117	4	3	1	78	41	76	40	78	41	70	40	80	41	60	41	377	734	90	83	44	68	64	47	197	197
168	841117	4	3	2	78	41	74	40	78	41	70	40	80	41	60	41	412	734	88	82	44	68	64	47	201	187

OBS	DATE	SEC	LOC	REP	M20	T20	MW20	TH20	M40	T40	MW40	TH40	M60	T60	MW60	TH60	SAP	SIP	PTIL	PTIT	TP	PTIML	PTIMT	TPW	CTL	CTT
169	840420	1	1	1	79	42	68	66	78	42	58	72	80	44	56	72	288	479	83	87	63	50	53	97	71	69
170	840420	1	1	2	79	42	64	64	78	50	60	67	79	44	58	67	260	414	85	87	63	51	56	97	45	57
171	840420	1	2	1	78	42	69	66	80	42	58	72	81	44	54	72	306	459	84	88	63	48	60	96	61	60
172	840420	1	2	2	78	42	66	66	80	50	61	67	80	44	52	67	303	490	92	87	63	51	57	96	78	84
173	840420	1	3	1	78	42	68	64	81	50	61	67	80	40	52	72	316	619	88	87	68	54	55	94	90	83
174	840420	1	3	2	75	42	70	75	78	50	64	73	77	61	56	67	312	587	91	87	68	53	55	94	70	70
175	840420	2	1	1	74	57	70	90	78	70	64	92	76	64	55	88	304	564	86	84	85	55	58	86	86	68
176	840420	2	1	2	75	62	69	75	78	64	68	73	76	61	56	85	264	564	84	83	85	59	60	86	65	72
177	840420	2	2	1	78	57	70	90	80	70	70	92	78	64	61	88	321	628	86	86	85	58	61	80	80	91
178	840420	2	2	2	74	57	71	75	80	64	70	73	76	61	62	85	286	574	86	85	85	54	62	80	76	66
179	840420	2	3	1	79	62	70	66	80	64	66	73	78	64	60	72	358	600	85	85	68	58	55	80	62	72
180	840420	2	3	2	74	57	67	64	80	50	66	92	82	64	61	85	371	595	89	86	68	53	55	80	88	115
181	840420	3	1	1	74	42	68	66	78	64	64	67	81	40	63	72	412	583	87	85	68	51	58	93	70	85
182	840420	3	1	2	75	57	70	66	80	50	66	72	78	44	60	67	396	550	92	92	68	58	55	86	52	86
183	840420	3	2	1	78	42	68	64	78	50	64	72	80	40	62	67	459	639	96	96	61	51	59	89	48	89
184	840420	3	2	2	75	57	70	64	80	50	64	72	80	40	62	67	439	705	95	95	61	48	54	88	78	89
185	840420	3	3	1	74	57	74	54	80	42	74	56	80	38	66	58	437	624	93	94	61	62	56	89	84	102
186	840420	3	3	2	83	46	74	54	84	42	76	56	80	46	66	58	422	576	87	86	60	61	57	72	83	93
187	840420	4	1	1	82	46	74	63	83	44	75	68	79	38	67	58	496	804	85	86	59	58	60	72	65	75
188	840420	4	1	2	84	46	76	63	82	42	75	56	80	46	70	58	523	775	87	86	59	59	57	72	77	67
189	840420	4	2	1	82	46	73	54	81	44	75	68	79	38	70	58	512	678	85	87	59	61	57	72	77	83
190	840420	4	2	2	82	46	76	63	81	42	76	56	81	46	69	58	515	762	85	87	59	66	58	72	84	93
191	840420	4	3	1	82	46		63	81			68	80	46		58	548	818	87	87	59	58	57	72	84	95
192	840420	4	3	2	82	46	76	63	81	44	76	68	80	46	69	58	548	872	88	87	59	58	60	72	83	97

------- BASE=I -------

OBS	DATE	SEC	LOC	REP	M20	T20	MW20	TW20	M40	T40	MW40	TW40	M60	T60	MW60	TW60	SAP	SIP	PTIL	PTIT	TP	PTIWL	PTIWT	TPW	CTL	CTT
193	840623	1	1	1	74	92	52	84	80	92	32	84	81	94	26	84	143	179	84	87	78	61	62	78	80	69
194	840623	1	1	2	77	94	52	84	78	94	32	84	80	94	16	84	171	317	83	87	78	55	61	78	66	52
195	840623	1	2	1	78	92	64	84	80	92	48	84	82	94	30	84	164	190	84	87	78	68	64	78	88	78
196	840623	1	2	2	76	92	60	84	80	94	34	84	81	94	21	84	183	289	82	87	78	58	62	78	68	71
197	840623	1	3	1	78	92	67	84	80	92	51	84	81	94	32	84	156	249	78	87	78	60	68	78	79	89
198	840623	1	3	2	78	94	64	84	80	94	36	84	78	94	11	84	186	273	84	87	78	57	68	78	62	86
199	840623	2	1	1	79	99	68	120	81	99	41	123	82	99	24	125	135	325	85	90	83	60	61	92	84	78
200	840623	2	1	2	80	99	70	120	82	99	42	120	84	99	24	121	131	244	85	90	83	60	60	92	73	100
201	840623	2	2	1	82	99	72	120	84	99	52	123	82	99	32	121	169	300	86	90	83	65	66	100	80	98
202	840623	2	2	2	80	99	70	120	83	99	49	120	80	99	39	125	171	274	85	90	83	64	67	100	76	92
203	840623	2	3	1	80	99	72	120	80	99	57	123	81	99	40	125	154	302	87	88	83	65	66	90	108	74
204	840623	2	3	2	78	87	68	90	80	87	52	90	80	91	22	90	186	344	83	85	78	60	67	90	85	114
205	840623	3	1	1	90	90	72	90	80	91	40	78	80	91	22	78	132	183	82	80	78	63	65	90	112	127
206	840623	3	1	2	78	90	63	90	80	87	37	78	80	91	20	90	128	156	83	81	78	61	61	78	127	115
207	840632	3	2	1	78	90	68	90	80	91	40	78	80	91	20	78	105	148	80	80	78	65	65	78	127	130
208	840623	3	2	2	78	90	68	90	80	80	36	90	80	91	20	90	156	182	83	82	78	60	65	78	123	133
209	840623	3	3	1	87	87	65	90	80	87	36	90	80	78	20	90	156	182	83	82	78	61	65	78	144	116
210	840623	3	3	2	78	90	67	90	80	91	40	78	80	91	20	78	132	197	80	82	78	63	64	78	91	123

------- BASE=J -------

OBS	DATE	SEC	LOC	REP	M20	T20	MW20	TW20	M40	T40	MW40	TW40	M60	T60	MW60	TW60	SAP	SIP	PTIL	PTIT	TP	PTIWL	PTIWT	TPW	CTL	CTT
211	841025	1	1	1	78	72	69	60	78	72	65	60	80	72	54	60	432	925	95	90	68	48	56	60	101	86
212	841025	1	1	2	78	72	68	60	78	72	65	60	78	72	59	60	427	796	87	90	68	50	55	60	131	75
213	841025	1	2	1	78	72	69	60	78	72	67	60	80	72	64	60	532	1329	91	91	70	50	60	60	69	81
214	841025	1	2	2	78	72	70	60	78	72	66	60	78	72	64	60	566	821	90	89	70	45	56	60	77	91
215	841025	1	3	1	78	72	68	60	78	72	66	60	80	72	66	60	628	1031	88	93	70	50	56	60	101	118
216	841025	1	3	2	78	51	69	51	76	51	66	51	77	51	64	51	462	975	89	91	70	55	53	60	171	120
217	841025	2	1	1	75	51	69	51	76	51	70	51	78	51	68	51	596	799	92	94	70	62	53	53	166	125
218	841025	2	1	2	75	51	72	51	75	51	66	51	78	51	66	51	522	1075	90	96	53	60	63	53	132	153
219	841025	2	2	1	74	51	70	51	76	51	69	51	78	51	66	51	596	775	88	89	53	60	62	53	82	120
220	841025	2	2	2	74	51	71	51	73	51	64	51	76	51	64	51	611	818	90	90	90	61	62	52	134	110
221	841025	2	3	1	74	72	69	51	76	51	68	51	78	51	66	51	680	988	89	93	52	61	61	52	106	111
222	841025	2	3	2	78	72	71	51	79	51	71	60	78	51	67	51	611	1093	89	94	52	56	56	52	98	133
223	841025	3	1	1	78	72	69	60	78	60	70	60	78	60	67	60	881	1286	100	98	64	54	56	56	149	132
224	841025	3	1	2	78	72	69	60	78	60	71	60	78	60	70	60	995	1237	98	98	64	55	59	60	153	109
225	841025	3	2	1	78	72	68	60	77	60	70	60	78	60	66	60	1126	1409	97	100	62	65	60	60	85	142
226	841025	3	2	2	77	72	68	60	78	60	70	60	77	60	68	60	1026	1643	98	100	62	63	70	60	148	136
227	841025	3	3	1	76	70	74	60	77	70	75	60	77	70	70	60	786	2109	97	98	64	63	66	60	172	178
228	841025	3	3	2	77	70	75	60	77	70	75	60	77	70	74	60	1074	823	100	100	70	70	65	60	135	140
230	841025	4	1	1	77	70	75	60	76	70	75	60	77	70	70	60	465	818	83	82	70	70	70	60	86	101
231	841025	4	1	2	76	70	74	60	77	70	64	60	77	70	74	60	551	1111	82	80	66	68	65	60	115	120
232	841025	4	2	1	77	70	74	60	77	70	68	60	77	70	74	60	639	823	82	85	66	67	68	60	98	112
233	841025	4	2	2	77	70	74	60	77	70	70	60	77	70	72	60	793	1007	85	92	66	65	66	60	220	84
234	841025	4	3	2	77	70	74	60	76	70	74	60	78	70	73	60	695	972	93	95	64	64	60	60	162	99

BASE=K

OBS	DATE	SEC	LOC	REP	M20	T20	MW20	TH20	M40	T40	MW40	TH40	M60	T60	MW60	TH60	SAP	SIP	PTIL	PTIT	TP	PTIWL	PTIWT	TPW	CTL	CTT
235	841027	1	1	1	77	63	63	59	78	63	48	59	79	63	34	59	381	910	92	98	60	45	40	60	104	102
236	841027	1	1	2	78	63	62	57	79	63	46	57	82	63	35	57	445	919	96	98	60	32	55	60	117	128
237	841027	1	2	1	76	63	62	59	78	63	46	59	79	63	33	59	376	928	87	97	59	54	53	59	128	98
238	841027	1	2	2	78	63	60	57	78	63	46	57	81	63	37	57	368	956	90	83	59	38	58	59	96	81
239	841027	1	2	3	78	63	63	59	79	63	50	59	80	63	33	59	376	840	91	92	59	55	54	59	77	65
240	841027	2	3	1	72	55	61	57	74	55	52	57	76	55	30	57	371	767	93	90	66	38	60	66	88	88
241	841027	2	1	1	73	55	62	54	74	55	58	54	78	55	44	54	513	925	88	92	66	56	52	66	77	59
242	841027	2	1	2	74	55	63	54	74	55	52	54	76	55	45	54	527	821	86	90	68	48	52	68	72	65
243	841027	2	2	1	73	55	61	54	74	55	58	54	80	55	45	54	409	821	86	88	68	50	52	68	93	82
244	841027	2	2	2	74	55	62	54	74	55	56	54	80	55	46	54	505	913	84	92	64	42	50	64	77	76
245	841027	2	2	3	72	55	58	54	74	55	57	54	78	55	38	54	453	883	88	90	64	54	52	64	102	79
246	841027	3	3	1	81	61	63	57	81	61	68	60	80	61	60	54	424	892	87	92	58	48	53	58	68	82
247	841027	3	1	1	80	61	70	57	80	61	67	57	81	61	64	60	600	1038	95	95	58	55	55	58	149	149
248	841027	3	1	2	80	61	70	57	80	61	66	60	82	61	66	60	673	1065	97	97	59	55	55	59	167	154
249	841027	3	1	3	81	61	70	57	81	61	66	57	83	61	62	60	626	1111	83	96	59	55	60	59	118	148
250	841027	3	2	1	81	61	70	57	80	61	66	60	78	59	64	60	479	840	88	98	59	56	65	59	140	116
251	841027	3	2	2	80	61	72	57	81	61	73	57	77	59	73	57	642	1079	100	85	58	56	62	58	121	129
252	841027	3	2	3	81	61	72	56	75	59	72	56	78	59	72	56	546	889	95	83	58	56	70	58	94	119
253	841027	4	3	1	76	59	72	59	76	59	70	59	77	59	70	59	557	962	85	83	55	72	68	55	129	135
254	841027	4	1	1	76	59	72	59	75	59	72	59	75	59	72	59	765	796	82	81	55	70	68	55	123	131
255	841027	4	1	2	76	59	72	56	76	59	73	56	78	59	73	56	658	874	82	80	55	70	70	55	136	132
256	841027	4	2	1	76	59	72	59	75	59	73	59	78	59	72	59	668	840	82	81	55	68	68	55	120	105
257	841027	4	2	2	76	59	72	59	76	59	73	59	77	59	73	59	701	913	82	80	55	68	70	55	139	105
258	841027	4	2	3	76	59	72	56	75	59	71	56	77	59	73	56	690	956	79	80	55	69	68	55	91	94

BASE=L

OBS	DATE	SEC	LOC	REP	M20	T20	MW20	TH20	M40	T40	MW40	TH40	M60	T60	MW60	TH60	SAP	SIP	PTIL	PTIT	TP	PTIWL	PTIWT	TPW	CTL	CTT
259	840704	1	1	1	82	74	80	71	84	74	66	70	89	74	51	71	398	1126	110	99	67	59	50	67	81	69
260	840704	1	1	2	84	72	75	71	84	72	66	70	88	72	46	71	452	509	107	96	67	58	55	67	81	70
261	840704	1	2	1	83	72	77	71	84	72	72	70	86	72	53	71	364	509	105	96	65	62	55	65	78	80
262	840704	1	2	2	84	72	76	70	84	72	72	70	86	72	53	71	387	660	96	98	65	60	54	65	86	68
263	840704	1	2	3	84	72	80	71	85	72	64	70	86	71	54	71	359	835	108	95	65	64	60	65	92	94
264	840704	2	3	1	84	72	72	70	80	72	65	68	83	70	53	64	332	657	100	93	75	64	55	74	78	94
265	840704	2	1	1	78	72	72	68	85	72	69	68	87	70	55	64	326	568	100	91	75	71	60	74	90	68
266	840704	2	1	2	79	70	75	64	79	72	72	68	82	70	56	64	424	595	97	95	68	50	60	68	96	83
267	840704	2	2	1	77	72	75	68	81	72	68	68	82	70	56	64	380	595	82	95	68	65	64	68	89	82
268	840704	2	2	2	78	72	75	64	80	72	68	68	84	70	58	64	405	737	90	95	68	60	60	68	78	89
269	840704	2	2	3	79	72	74	68	81	72	68	68	86	72	56	71	396	709	86	96	63	56	64	63	97	91
270	840704	3	3	1	85	74	79	71	85	72	68	70	84	72	58	71	458	889	102	94	63	71	63	63	95	114
271	840704	3	1	1	84	72	78	71	86	72	64	70	87	71	64	71	508	956	105	92	63	50	51	63	97	107
272	840704	3	1	2	84	74	74	70	86	74	71	70	88	71	62	71	606	1359	112	94	63	58	52	63	104	116
273	840704	3	1	3	84	72	75	71	85	72	73	68	87	71	68	71	546	788	108	94	63	51	62	63	103	139
274	840704	3	2	1	85	71	78	70	86	72	77	68	86	71	69	71	535	883	106	93	63	56	60	63	107	120
275	840704	3	2	2	85	71	78	68	85	70	73	70	90	71	70	71	508	697	105	94	63	51	64	63	148	128
276	840704	3	2	3	84	71	80	71	75	70	77	68	76	71	66	71	592	655	75	92	63	56	65	63	66	43
277	840704	4	3	1	77	71	78	68	73	72	75	68	72	71	62	71	502	851	78	94	60	50	65	60	49	55
278	840704	4	1	1	71	71	68	71	75	70	78	68	73	71	65	71	517	1359	68	68	63	54	60	60	47	52
279	840704	4	1	2	70	71	80	68	75	70	78	68	81	71	70	71	445	813	68	70	57	65	60	57	37	52
280	840704	4	2	1	72	71	78	80	73	71	78	68	79	71	70	71	551	835	70	67	57	68	65	57	51	52
281	840704	4	2	2	77	71	79	79	73	71	79	68	76	71	72	71	508	770	76	65	57	66	65	57	50	65
282	840704	4	2	3	77	71	79	71	73	71	79	68	76	71	72	71	508	770	76	65	57	66	65	57	50	65

72

OBS	DATE	SEC	LOC	REP	M20	T20	MW20	TH20	M40	T40	MW40	TH40	M60	T60	MW60	TH60	SAP	SIP	PTIL	PTIT	TP	PTIWL	PTIWT	TPW	CTL	CTT
283	840706	1	1	1	83	107	62	80	82	107	38	85	82	107	15	80	120	224	98	102	91	50	55	91	88	66
284	840706	1	1	2	84	103	52	80	82	107	32	80	84	107	16	80	134	196	110	80	91	50	56	91	52	74
285	840706	1	2	1	81	107	52	80	81	107	32	85	80	107	17	80	123	208	98	98	93	65	58	93	73	63
286	840706	1	2	2	81	103	50	80	82	107	32	80	86	107	17	80	103	189	102	100	93	45	50	93	27	72
287	840706	1	3	1	82	107	54	80	82	107	36	80	80	107	16	80	112	224	90	95	90	52	55	90	59	76
288	840706	1	3	2	83	103	50	90	82	107	34	80	84	107	18	80	138	219	92	98	98	45	55	90	62	71
289	840706	2	1	1	81	89	73	90	82	94	56	91	86	88	24	91	120	189	83	75	98	65	58	100	118	194
290	840706	2	1	2	82	96	72	90	86	94	50	87	84	94	24	89	139	253	70	80	98	60	55	100	77	76
291	840706	2	2	1	81	89	73	90	83	94	45	91	81	94	26	91	144	201	67	79	99	60	64	99	71	85
292	840706	2	2	2	81	96	72	90	85	94	45	91	84	88	25	89	118	209	81	75	92	58	60	99	55	97
293	840706	2	3	1	82	89	73	90	83	90	44	87	87	94	23	91	137	239	70	73	80	62	60	100	97	89
294	840706	4	3	2	84	95	73	78	84	90	50	78	87	94	28	89	151	248	75	71	80	59	55	100	75	79
295	840706	4	4	1	83	92	77	78	83	90	54	78	87	88	34	78	127	254	85	84	83	61	63	80	129	134
296	840706	4	4	2	84	95	73	78	84	90	48	78	81	88	39	78	115	355	87	83	83	62	61	80	140	141
297	840706	4	1	1	82	92	75	78	82	90	53	78	86	94	36	78	132	292	82	80	82	60	65	83	119	138
298	840706	4	2	2	99	95	74	78	84	90	57	78	83	94	40	94	182	271	84	81	85	62	61	83	151	95
299	840706	4	3	1	83	95	75	78	81	90	53	78	82	94	40	78	182	271	85	81	81	60	60	81	151	136
300	840706	4	3	2	82	92	74	78	84	90	57	78	83	88	38	78	133	356	85	85	81	64	61	81	146	140

OBS	DATE	SEC	LOC	REP	M20	T20	MW20	TH20	M40	T40	MW40	TH40	M60	T60	MW60	TH60	SAP	SIP	PTIL	PTIT	TP	PTIWL	PTIWT	TPW	CTL	CTT
301	841023	1	1	1	77	48	73	45	78	48	58	45	81	48	36	45	193	471	86	95	41	63	71	41	91	89
302	841023	1	1	2	76	48	74	45	78	48	54	45	82	48	38	45	179	516	89	95	41	65	72	41	93	104
303	841023	1	2	1	74	48	64	45	76	48	48	45	78	48	23	45	164	396	88	94	41	63	57	41	47	63
304	841023	1	2	2	74	48	63	45	77	48	16	45	78	48	26	45	184	693	86	95	41	65	60	41	61	78
305	841023	1	3	1	75	48	34	45	74	48	18	45	79	48	7	45	113	378	81	84	41	46	45	41	97	83
306	841023	1	3	2	77	48	32	45	79	48	56	51	82	48	9	45	89	299	80	82	58	48	43	58	97	104
307	841023	2	1	1	77	63	72	51	79	63	56	51	81	63	37	51	175	486	78	86	58	62	61	58	102	104
308	841023	2	1	2	77	62	71	51	78	62	60	51	80	62	36	51	185	505	72	84	58	59	63	58	108	71
309	841023	2	2	1	76	63	65	51	78	63	48	51	76	63	33	51	185	411	75	80	58	55	58	58	93	96
310	841023	2	2	2	77	62	66	51	78	62	50	51	80	62	34	51	176	388	70	80	58	54	60	58	100	89
311	841023	2	3	1	76	63	38	45	76	63	16	45	80	63	10	45	99	424	52	54	45	42	48	58	32	30
312	841023	3	3	2	80	48	73	45	80	48	20	45	82	48	32	45	114	396	54	56	45	45	46	45	41	36
313	841023	3	4	1	80	48	72	45	82	48	53	45	84	48	38	45	195	497	88	90	45	60	63	45	132	140
314	841023	3	4	2	80	48	74	45	80	48	52	45	84	48	33	45	218	466	88	92	45	59	64	45	132	140
315	841023	3	1	1	80	48	74	45	82	48	55	45	84	48	39	45	161	522	90	93	45	57	59	44	119	128
316	841023	3	2	2	80	48	74	45	82	48	53	45	83	48	36	45	174	598	87	89	44	58	62	44	120	123
317	841023	3	3	1	80	48	75	45	82	48	53	45	83	48	40	45	201	505	90	90	44	60	61	44	119	131
318	841023	3	4	2	81	51	76	48	82	49	54	48	82	50	38	48	197	518	85	88	44	59	65	44	139	152
319	841023	4	1	1	80	49	76	48	81	49	57	48	82	49	44	48	207	511	86	87	44	58	62	43	164	170
320	841023	4	2	2	80	51	75	48	80	50	54	48	81	50	41	48	101	332	85	89	43	60	60	43	170	156
321	841023	4	3	1	80	49	72	48	80	49	56	48	82	49	41	48	147	503	88	89	43	58	63	43	157	156
322	841023	4	3	2	80	51	74	48	81	50	50	48	80	50	36	48	179	391	86	88	41	58	65	41	162	167
323	841023	4	4	3	80	49	74	48	81	49	50	48	81	49	37	48	193	459	86	92	41	59	65	41	173	180

OBS	DATE	SEC	LOC	REP	M20	T20	MW20	TW20	M40	T40	MW40	TW40	M60	T60	MW60	TW60	SAP	SIP	PTIL	PTIT	TP	PTIWL	PTIWT	TPW	CTL	CTT
325	841024	1	1	1	78	67	73	65	78	67	54	67	81	67	44	65	114	335	82	86	58	61	65	58	112	120
326	841024	1	1	2	78	67	74	65	78	67	50	67	82	67	32	65	171	372	79	87	58	61	63	58	105	163
327	841024	1	2	1	76	67	72	65	75	67	51	67	74	67	30	65	160	648	82	85	56	56	60	56	58	98
328	841024	2	2	2	74	67	47	65	76	67	48	67	78	67	32	65	155	445	83	82	53	53	64	56	95	123
329	841024	2	1	1	74	67	52	65	76	67	32	67	78	67	16	65	117	436	80	87	57	43	55	57	32	72
330	841024	1	2	1	76	52	52	52	78	52	30	52	81	52	18	52	129	329	80	91	57	58	55	57	83	86
331	841024	2	1	2	78	52	74	52	76	52	58	52	80	52	36	52	125	450	85	88	56	65	50	56	62	107
332	841024	2	2	1	76	52	72	52	72	52	60	52	82	52	31	52	172	495	85	91	57	65	68	56	96	112
333	841024	2	3	2	77	52	74	52	72	52	55	52	78	52	34	52	218	495	81	83	56	62	70	57	78	121
334	841024	2	3	1	72	52	54	52	72	52	32	52	76	52	38	52	125	662	70	81	57	55	66	56	124	67
335	841024	3	1	2	74	67	72	65	67	67	55	67	83	67	19	65	143	505	78	82	54	54	56	55	81	70
336	841024	3	2	1	80	67	71	65	80	67	32	67	82	67	26	65	213	416	82	88	55	61	58	55	42	137
337	841024	3	2	2	80	67	72	65	80	67	54	67	84	67	38	65	251	690	85	90	58	62	65	55	127	142
338	841024	3	3	1	79	67	74	65	80	67	48	67	82	67	30	65	188	662	79	85	55	60	65	55	149	151
339	841024	3	1	2	82	67	72	65	80	67	52	67	82	67	43	65	194	495	86	85	55	58	65	55	135	140
340	841024	3	3	1	80	67	72	65	78	67	50	67	82	67	42	65	281	655	78	84	52	58	61	55	136	163
341	841024	4	1	2	80	67	70	65	76	67	56	52	79	67	40	65	199	481	83	86	55	55	60	52	156	167
342	841024	4	2	1	76	53	72	52	72	53	54	52	80	53	44	52	265	486	84	85	52	58	63	52	142	148
343	841024	4	2	2	75	52	72	52	76	52	58	52	78	53	42	52	224	505	74	80	52	60	65	52	167	171
344	841024	4	3	1	76	53	76	52	77	52	66	52	78	53	53	52	284	667	77	79	52	59	66	52	159	152
345	841024	4	3	2	76	52	78	52	78	52	68	52	80	53	52	52	253	773	80	84	52	60	68	52	153	181

OBS	DATE	SEC	LOC	REP	M20	T20	MW20	TW20	M40	T40	MW40	TW40	M60	T60	MW60	TW60	SAP	SIP	PTIL	PTIT	TP	PTIWL	PTIWT	TPW	CTL	CTT
349	840528	1	1	1	84	99	79	138	84	104	75	130	83	99	68	138	434	849	85	91	84	65	72	84	114	124
350	840528	1	1	2	83	116	78	144	84	112	79	132	84	106	66	132	523	1093	90	95	84	65	73	84	113	128
351	840528	1	2	1	83	99	80	138	83	104	78	130	83	99	71	138	644	1148	93	96	88	68	71	84	126	138
352	840528	2	2	2	88	116	80	144	84	112	76	132	82	106	67	132	508	1137	90	95	88	67	73	84	154	132
353	840528	2	1	1	82	99	80	138	84	104	74	130	83	99	70	138	523	799	94	95	89	65	71	89	141	132
354	840528	2	2	1	83	116	77	144	80	112	78	132	83	106	72	132	528	564	95	95	89	66	77	89	145	140
355	840528	1	2	1	78	88	76	96	80	89	76	100	78	90	66	96	431	892	96	97	102	76	75	99	165	189
356	840528	2	1	2	78	90	75	98	80	90	75	100	80	90	65	102	479	942	98	99	102	76	76	99	132	185
357	840528	2	2	1	78	88	76	96	79	89	74	100	80	90	72	96	592	1241	95	96	90	75	71	90	156	182
358	840528	2	3	2	79	90	76	96	80	90	76	102	80	90	70	102	451	1213	94	97	90	72	75	90	145	221
359	840528	3	1	1	84	88	76	98	80	89	73	100	80	90	66	96	478	877	95	96	108	73	75	114	112	184
360	840528	3	2	2	85	99	87	138	86	104	84	130	85	99	76	138	527	724	94	97	84	74	76	84	123	123
361	840528	3	2	1	84	90	86	144	85	112	87	132	85	106	75	132	563	922	95	98	84	75	77	87	99	128
362	840528	3	3	2	84	116	86	138	86	104	82	130	86	99	76	138	497	693	96	98	88	71	74	87	130	150
363	840528	3	1	1	85	99	85	144	85	112	80	132	86	106	76	132	499	780	99	94	88	73	77	87	153	160
364	840528	3	3	1	84	116	84	138	86	104	84	130	86	99	75	132	482	780	100	95	88	72	74	88	124	165
365	840528	4	1	2	82	99	88	144	85	112	84	132	82	106	80	134	527	985	92	96	88	70	75	88	147	154
366	840528	4	2	1	80	108	86	146	82	113	84	148	83	118	79	129	619	1274	93	95	79	87	85	79	201	143
367	840528	4	2	2	82	114	84	144	82	120	83	138	84	114	80	134	649	1299	91	96	84	85	84	79	178	168
368	840528	4	3	1	80	108	84	141	82	113	84	148	82	118	79	134	633	1144	95	98	84	80	80	82	172	132
369	840528	4	3	2	82	114	85	146	83	120	83	138	82	118	79	134	615	1217	95	99	82	81	81	82	172	176
370	840528	3	1	2	81	114	85	141	82	120	82	138	80	114	76	129	717	1395	95	96	82	81	82	80	147	192

CBS	DATE	SEC	LOC	REP	M20	T20	MH20	TW20	M40	T40	MH40	TW40	M60	T60	MH60	TW60	SAP	SIP	PTIL	PTIT	TP	PTIHL	PTIHT	TPH	CTL	CTT
373	840604	1	1	1	82	74	74	74	85	74	72	74	90	74	66	74	408	806	95	99	68	68	67	68	119	121
374	840604	1	1	2	84	74	76	74	84	74	72	74	90	73	62	73	478	796	98	97	68	67	67	68	107	151
375	840604	1	2	1	82	74	76	74	84	74	72	74	90	73	64	73	406	595	94	96	69	65	61	69	101	140
376	840604	1	2	2	85	74	76	74	84	74	72	74	90	74	60	73	424	660	101	94	69	62	61	69	128	117
377	840604	1	2	3	82	74	76	74	84	74	70	74	88	74	65	74	435	657	98	94	68	64	64	68	136	149
378	840604	2	1	1	84	74	76	74	84	80	70	80	80	79	61	79	452	802	97	94	68	64	65	68	144	172
379	840604	2	1	2	80	81	71	80	81	82	70	80	80	82	70	80	466	815	97	93	81	66	65	81	116	147
380	840604	2	2	1	80	81	72	80	80	82	68	80	82	81	62	79	418	869	80	85	81	62	63	82	124	155
381	840604	2	2	2	79	81	72	80	82	82	71	80	82	81	64	80	424	794	92	85	82	65	64	81	106	151
382	840604	2	2	3	80	81	72	80	81	82	68	80	81	81	65	80	439	765	85	88	81	66	62	81	141	140
383	840604	2	3	1	79	81	72	80	81	82	71	80	81	81	62	80	400	752	83	90	67	70	60	81	153	199
384	840604	3	1	1	86	74	76	74	86	74	70	74	91	74	66	74	414	702	100	92	66	66	60	67	116	163
385	840604	3	1	2	84	74	76	74	86	74	74	74	90	74	64	74	379	583	97	95	66	70	60	66	114	152
386	840604	3	2	1	84	74	76	74	86	74	74	74	90	74	63	73	386	662	101	94	67	65	62	67	153	141
387	840604	3	2	2	86	78	77	74	86	74	74	74	91	74	69	73	355	760	98	95	66	62	61	67	119	181
388	840604	3	3	1	85	77	73	74	81	73	74	74	82	73	67	73	373	617	85	70	67	63	61	66	129	157
389	840604	3	3	2	80	74	74	72	80	73	72	72	82	74	64	73	339	598	75	73	66	68	60	66	96	123
390	840604	4	1	1	82	73	74	73	82	73	70	74	82	73	60	73	391	542	93	80	66	59	60	66	144	144
391	840604	4	2	1	82	74	73	73	82	73	72	74	82	74	65	73	426	815	82	80	66	68	64	66	139	166
392	840604	4	2	2	83	75	73	74	83	73	74	72	82	73	60	73	394	572	90	80	66	61	64	66	153	173
393	840604	4	3	1	82	74	74	73	82	73	72	74	84	73	64	73	414	544	75	80	66	62	60	66	150	159
396	840604	4	4	1	82	77	73	77	82	73	74	72	84	74	64	73	485	653	—	—	66	62	61	66	169	138

OBS	DATE	SEC	LOC	REP	M20	T20	MH20	TW20	M40	T40	MH40	TW40	M60	T60	MH60	TW60	SAP	SIP	PTIL	PTIT	TP	PTIHL	PTIHT	TPH	CTL	CTT
397	840915	1	1	1	84	68	75	65	84	68	56	65	86	68	42	65	149	361	84	85	75	54	55	75	103	94
398	840915	1	1	2	84	68	75	65	83	68	60	65	88	68	42	65	125	325	84	85	75	55	54	75	98	116
399	840915	1	2	1	84	69	69	65	84	68	54	65	84	68	40	65	159	554	81	82	72	50	49	72	110	112
401	840915	1	2	2	84	68	70	65	84	68	55	65	87	68	40	65	142	396	79	85	72	50	56	71	140	126
401	840915	1	2	3	84	68	76	65	83	68	56	65	86	86	43	65	93	218	88	87	71	55	58	71	127	127
402	840915	2	1	1	84	68	76	65	78	68	58	65	86	100	40	95	174	404	72	73	78	56	58	81	104	103
403	840915	2	1	2	78	100	68	95	79	100	54	95	80	100	40	95	140	281	71	70	78	57	57	80	99	106
404	840915	2	2	1	80	100	72	95	76	100	56	95	80	100	40	95	137	292	75	75	76	52	53	80	107	162
405	840915	2	2	2	77	100	65	95	78	100	49	95	79	100	40	95	134	433	74	70	76	50	53	81	151	176
406	840915	2	3	1	78	100	68	95	78	100	50	65	80	100	40	95	130	421	85	75	76	56	59	81	118	138
407	840915	2	3	2	79	68	70	65	80	68	54	65	82	68	42	65	120	299	80	83	76	55	56	83	114	126
408	840915	3	1	1	85	68	73	65	85	68	50	65	84	68	40	65	134	426	87	89	76	53	55	87	103	107
409	840915	3	1	2	84	68	71	65	84	68	52	65	86	68	40	65	206	419	85	85	76	51	52	87	155	82
410	840915	3	2	1	84	68	76	65	83	68	64	65	83	68	50	65	222	396	87	89	76	54	55	80	110	94
411	840915	3	2	2	84	70	73	70	84	70	52	70	84	70	40	70	123	266	78	87	70	50	56	87	114	91
412	840915	3	3	1	84	70	72	70	83	70	64	70	86	70	39	70	138	289	75	78	72	50	57	90	94	94
413	840915	3	3	2	84	70	76	70	84	70	55	70	84	70	50	70	99	302	80	78	70	45	56	70	95	109
415	840915	4	1	1	82	70	78	70	83	70	64	70	82	70	44	70	192	445	81	80	72	46	45	72	109	120
416	840915	4	2	1	84	70	72	70	83	70	58	70	84	70	40	70	163	436	75	81	72	50	47	72	91	114
419	840915	4	3	1	82	70	72	70	83	70	54	70	84	70	38	70	113	319	82	75	71	55	51	71	74	69
420	840915	4	3	2	83	70	74	70	83	70	50	70	86	70	36	70	146	248	81	80	71	55	55	71	82	88

75
(The reverse of this page is blank.)

APPENDIX D
DERIVATION OF SAMPLE VARIABILITY

Due to the small sample size, the test variability cannot be expressed as a single value but must be expressed as a range of values. A brief derivation and discussion of how this range is determined is presented for clarity.

Assuming that the variability is constant between sample cells, the variability for each cell of two samples can be computed by the following:

$$S_i = (X_1 - \overline{X})^2 + (X_2 - \overline{X})^2$$

where S_i is the variance within a cell

X_1, X_2 are cell data values.

$\overline{X}$ is cell mean

This equation may be arranged and expressed in terms of the range by the following:

Since $\overline{X} = (X_1 + X_2)/2$

Then $S_i = [(X_1 - X_2)/2]^2 + [(X_2 - X_1)/2]^2$

rearranging and collecting like terms yields

$$S_i = (X_1 - X_2)^2/2$$

Once the cell variance is known, the overall population variance can be estimated by determining the mean of the cell variances, or

$$\sigma^2 = (\Sigma \, S_i)/n$$

As the number of cells times the estimated variance is distributed as a multiple of a Chi Square distribution, namely

$$n \cdot \sigma^2 \sim \sigma^2 \cdot \chi^2_{n,\alpha}$$

where n is number of cells

σ^2 is estimated variance

σ^2 is population variance

$\chi^2_{n,\alpha}$ is Chi Square distribution at n degrees of freedom and α confidence level.

77

A confidence interval may be determined for the population variance. This interval is given by the relationship

$$(n \cdot \sigma^2)/\chi^2_{n,\alpha} < \sigma^2 < (n \cdot \sigma^2)/\chi^2_{n,1-\alpha}$$

FREQUENCY HISTOGRAMS OF COLLECTED DATA
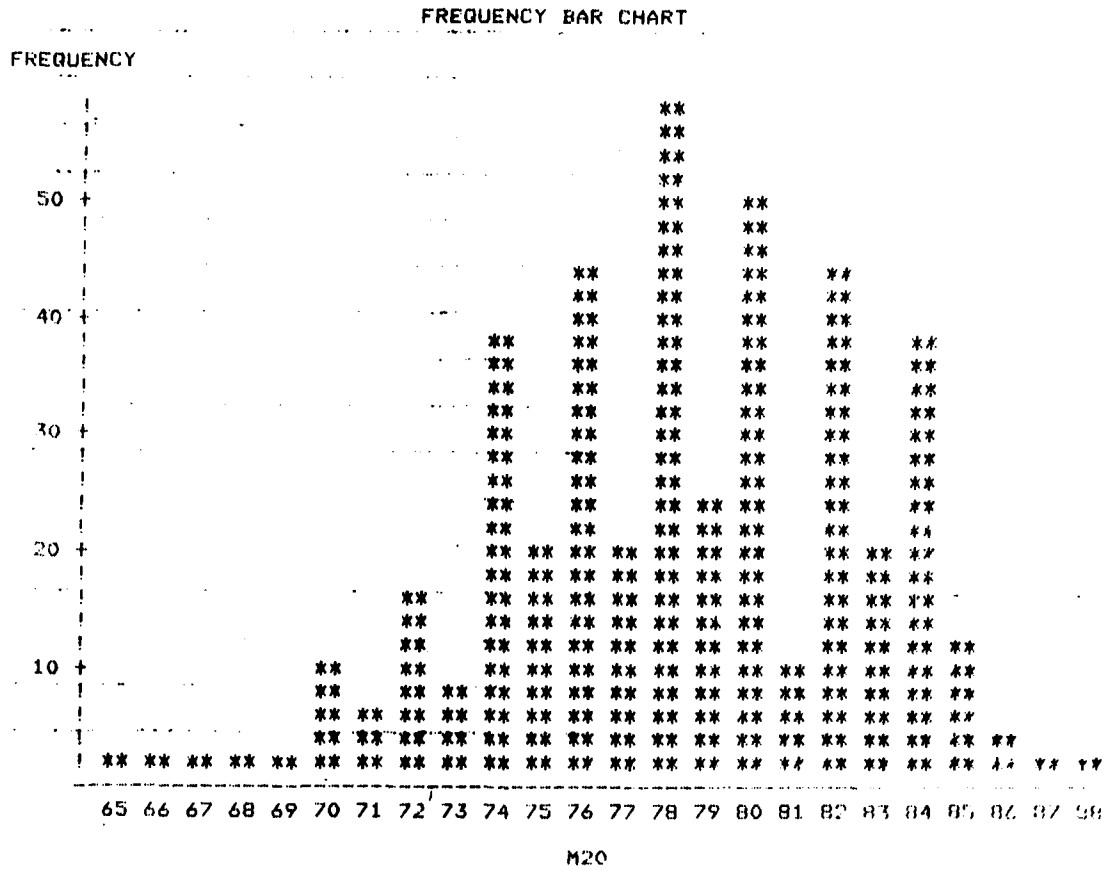
FIGURE E-1. 32 km/h (20 mi/h) DRY MU METER TESTS

FREQUENCY BAR CHART
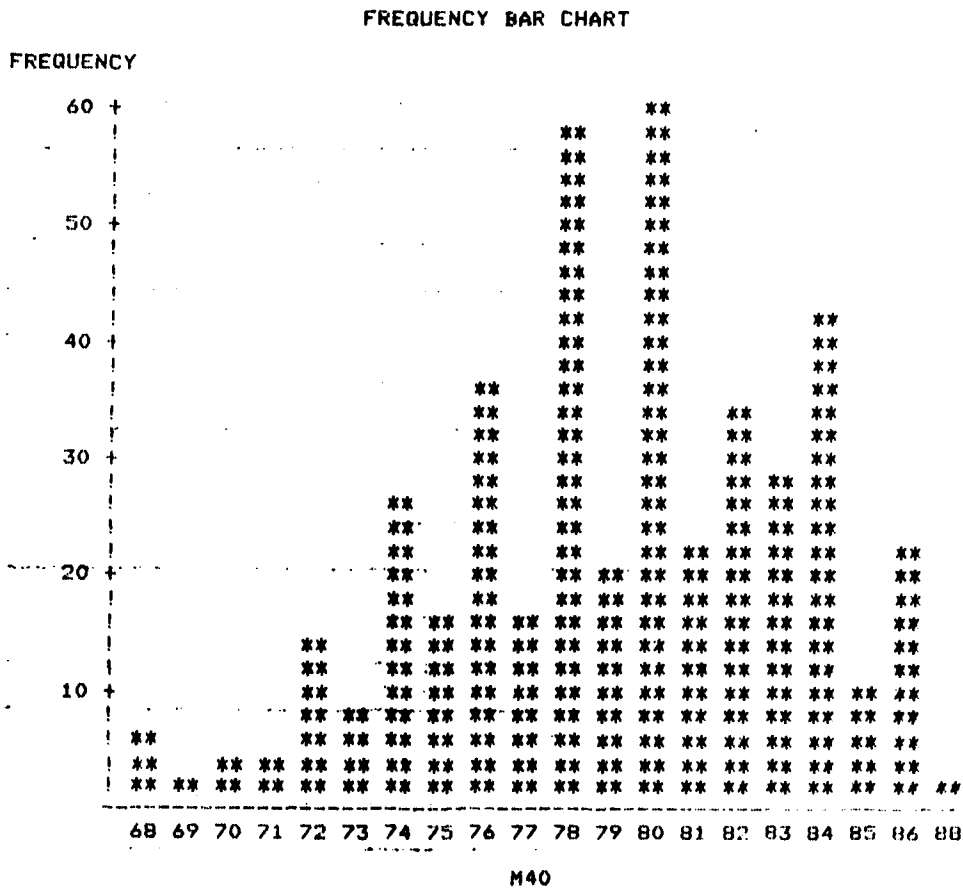
FIGURE E-2. 64 km/h (40 mi/h) DRY MU METER TESTS

FREQUENCY BAR CHART

FIGURE E-3. 96 km/h (60 mi/h) DRY MU METER TESTS

81

FREQUENCY BAR CHART

FREQUENCY

```
          !                                                          **
          !                                                          **
    90 +                                                             **
          !                                                          **
          !                                                          **
          !                                                          **
          !                                                          **
    80 +                                                             **
          !                                                          **
          !                                                          **
          !                                                          **
    70 +                                               **            **
          !                                            **            **
          !                                            **            **
          !                                            **            **
          !                                            **            **
    60 +                                            **  **  **
          !                                         **  **  **
          !                                         **  **  **
          !                                         **  **  **
          !                                         **  **  **
    50 +                                            **  **  **
          !                                         **  **  **
          !                                         **  **  **
          !                                         **  **  **
    40 +                                     **     **  **  **
          !                                  **     **  **  **
          !                                  **     **  **  **
          !                                  **     **  **  **  **
    30 +                                     **     **  **  **  **
          !                                  **     **  **  **  **
          !                                  **     **  **  **  **
          !                           **  **  **  **  **  **  **  **
          !                           **  **  **  **  **  **  **  **
    20 +                              **  **  **  **  **  **  **
          !                           **  **  **  **  **  **  **  **  **
          !                           **  **  **  **  **  **  **  **  **
          !                           **  **  **  **  **  **  **  **  **
    10 +                  **        **  **  **  **  **  **  **  **  **
          !               **        **  **  **  **  **  **  **  **  **
          !           **  **  **  **  **  **  **  **  **  **  **  **  **
          !           **  **  **  **  **  **  **  **  **  **  **  **  **
          !        **  **  **  **  **  **  **  **  **  **  **  **  **  **
          !  **  **  **        **  **  **  **  **  **  **  **  **  **  **  **  **
    --------------------------------------------------------------------------------
       30  33  36  39  42  45  48  51  54  57  60  63  66  69  72  75  78  81  84  87
```

MW20 MIDPOINT

FIGURE E-4.   32 km/h (20 mi/h) WET MU METER TESTS

FREQUENCY BAR CHART

FREQUENCY

```
          !                                               **
          !                                               **
     50 + !                                            .  **
          !                                               **
          !                                               **
     40 + !                                  **          **
          !                               ** ** ** ** ** **
          !                            ** ** ** ** ** ** **
          !                            ** ** ** ** ** ** ** **
          !                            ** ** ** ** ** ** ** **
     30 + !                         ** ** ** ** ** ** ** ** **
          !                         ** ** ** ** ** ** ** ** **
          !                         ** ** ** ** ** ** ** ** **
          !                         ** ** ** ** ** ** ** ** **
          !                         ** ** ** ** ** ** ** ** **
     20 + !                ** ** ** ** ** ** ** ** ** ** ** **
          !                ** ** ** ** ** ** ** ** ** ** ** **
          !                ** ** ** ** ** ** ** ** ** ** ** **
          !                ** ** ** ** ** ** ** ** ** ** ** **
     10 + ! ** ** ** ** ** ** ** ** ** ** ** ** ** ** ** ** **
          !    ** ** ** ** ** ** ** ** ** ** ** ** ** ** ** **
          !    ** ** ** ** ** ** ** ** ** ** ** ** ** ** ** **
          !    ** ** ** ** ** ** ** ** ** ** ** ** ** ** ** **
          ! ** ** ** ** ** ** ** ** ** ** ** ** ** ** ** ** ** **
         --------------------------------------------------------
          12 16 20 24 28 32 36 40 44 48 52 56 60 64 68 72 76 80 84 88
```

MW40 MIDPOINT
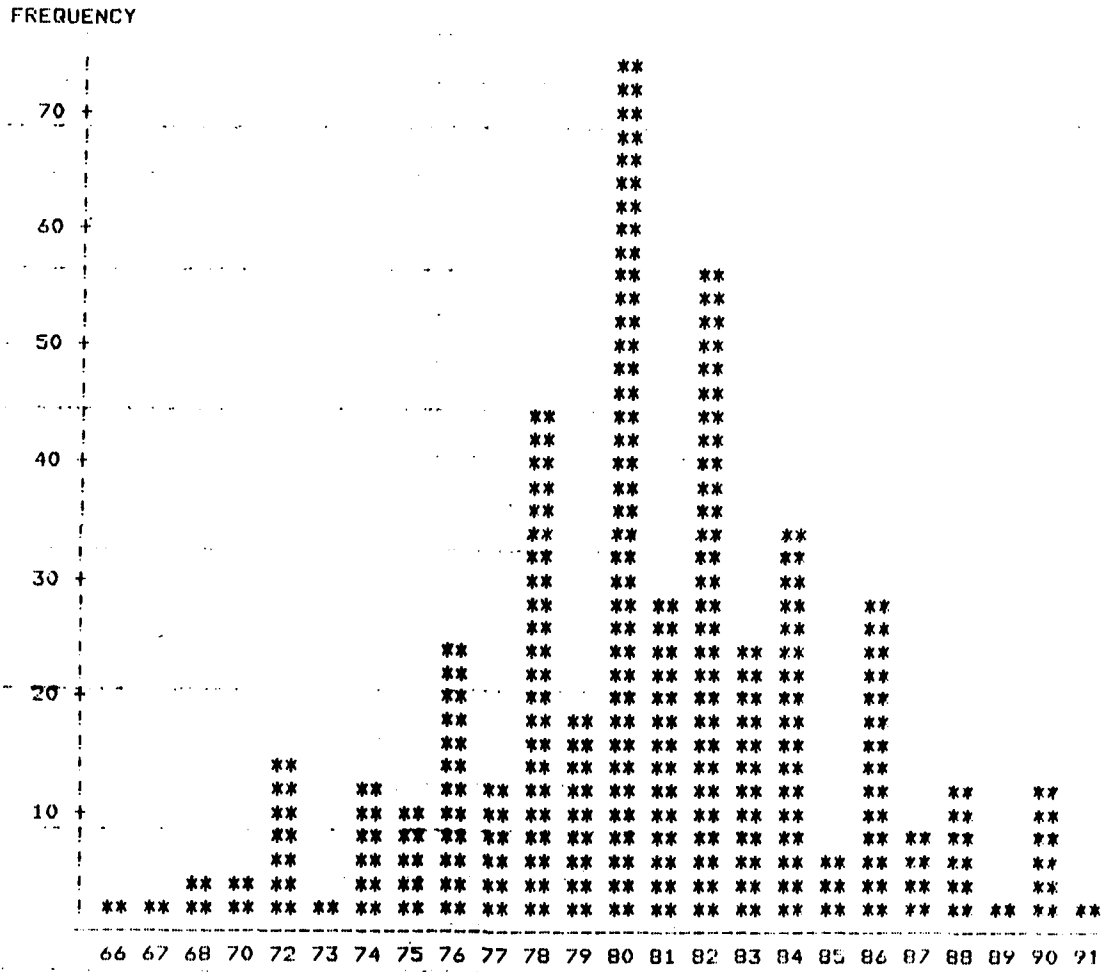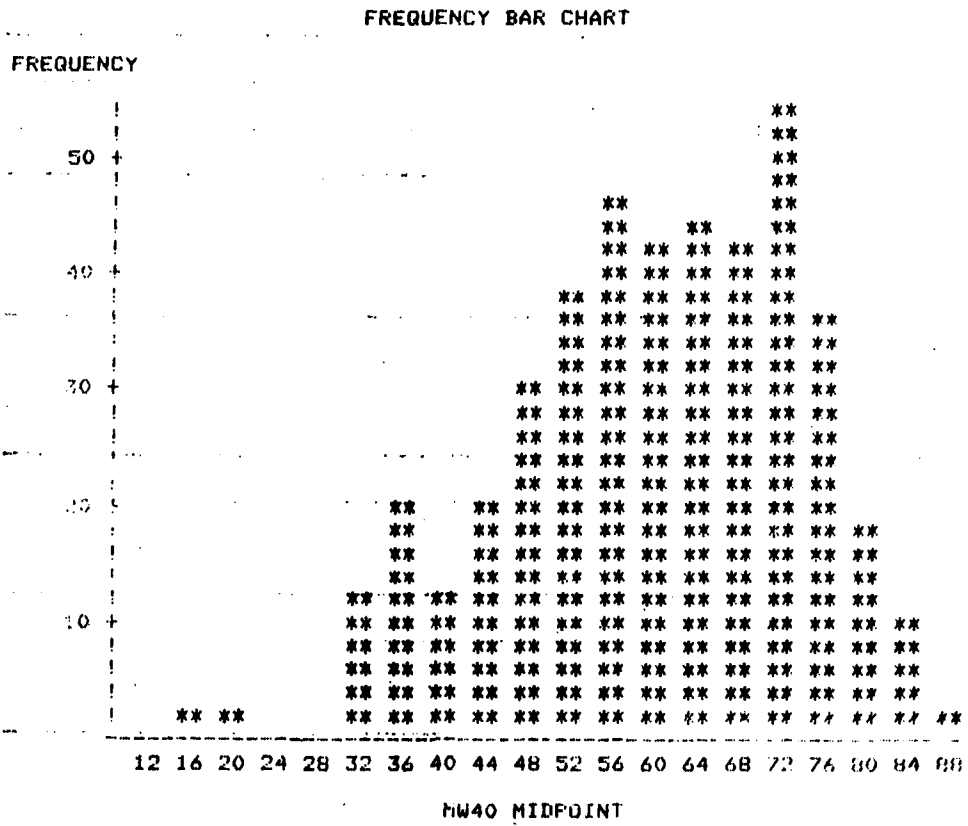
FIGURE E-5.   64 km/h (40 mi/h) WET MU METER TESTS

83

FREQUENCY BAR CHART

FREQUENCY

```
      !                              **
      !                              **
 45  +                              **
      !                              **
      !                              **
      !                              **
      !                              **            **
 40  +                              **            **
      !                              **            **
      !                              **            **      **
      !                              **            **      **
      !                              **            **      **
 35  +                              **            **      **
      !                        **  **            **      **      **
      !                        **  **            **      **      **
      !                        **  **            **      **      **
      !                        **  **            **      **      **
 30  +                        **  **            **  **  **      **
      !                        **  **  **        **  **  **      **
      !                        **  **  **        **  **  **      **
      !                        **  **  **        **  **  **      **
      !                        **  **  **        **  **  **  **  **
 25  +                **  **  **  **        **  **  **  **  **
      !                **  **  **  **        **  **  **  **  **  **
      !                **  **  **  **        **  **  **  **  **  **
      !                **  **  **  **        **  **  **  **  **  **
      !                **  **  **  **        **  **  **  **  **  **
 20  +                **  **  **  **        **  **  **  **  **  **
      !                **  **  **  **        **  **  **  **  **  **
      !                **  **  **  **        **  **  **  **  **  **
      !                **  **  **  **        **  **  **  **  **  **
 15  +        **  **  **  **  **  **  **  **  **  **  **  **  **
      !        **  **  **  **  **  **  **  **  **  **  **  **  **
      !        **  **  **  **  **  **  **  **  **  **  **  **  **  **
      !        **  **  **  **  **  **  **  **  **  **  **  **  **  **
      !        **  **  **  **  **  **  **  **  **  **  **  **  **  **
 10  +    **  **  **  **  **  **  **  **  **  **  **  **  **  **  **
      !    **  **  **  **  **  **  **  **  **  **  **  **  **  **  **
      !    **  **  **  **  **  **  **  **  **  **  **  **  **  **  **
      !    **  **  **  **  **  **  **  **  **  **  **  **  **  **  **
      !    **  **  **  **  **  **  **  **  **  **  **  **  **  **  **
  5  +    **  **  **  **  **  **  **  **  **  **  **  **  **  **  **
      !    **  **  **  **  **  **  **  **  **  **  **  **  **  **  **  **
      !    **  **  **  **  **  **  **  **  **  **  **  **  **  **  **  **
      !**  **  **  **  **  **  **  **  **  **  **  **  **  **  **  **  **
      !**  **  **  **  **  **  **  **  **  **  **  **  **  **  **  **  **  **
    --------------------------------------------------------------------
      8  12 16 20 24 28 32 36 40 44 48 52 56 60 64 68 72 76 80 84
```

MW60 MIDPOINT

FIGURE E-6.   96 km/h (60 mi/h) WET MU METER TESTS

FREQUENCY BAR CHART

FREQUENCY

```
          !  **
          !  **
     100 +  **
          !  **
          !  **
          !  **
      90 +  **
          !  **
          !  **
          !  **
      80 +  **
          !  **
          !  **
          !  **
      70 +  **
          !  **
          !  **
          !  **
      60 +  **
          !  **
          !  **
          !  **
      50 +  **  **
          !  **  **              **
          !  **  **              **
          !  **  **      **      **
      40 +  **  **      **      **
          !  **  **      **      **
          !  **  **  **  **  **  **
          !  **  **  **  **  **  **
      30 +  **  **  **  **  **  **
          !  **  **  **  **  **  **  **  **
          !  **  **  **  **  **  **  **  **
          !  **  **  **  **  **  **  **  **
      20 +  **  **  **  **  **  **  **  **
          !  **  **  **  **  **  **  **  **
          !  **  **  **  **  **  **  **  **  **
          !  **  **  **  **  **  **  **  **  **      **
      10 +  **  **  **  **  **  **  **  **  **  **  **
          !  **  **  **  **  **  **  **  **  **  **  **
          !  **  **  **  **  **  **  **  **  **  **  **  **
          !  **  **  **  **  **  **  **  **  **  **  **  **      **              **
```

```
                                                            1   1   1
          1   2   2   3   3   4   4   5   5   6   6   7   7   8   8   9   9   0   0   1
          5   0   5   0   5   0   5   0   5   0   5   0   5   0   5   0   5   0   5   0
          0   0   0   0   0   0   0   0   0   0   0   0   0   0   0   0   0   0   0   0
```
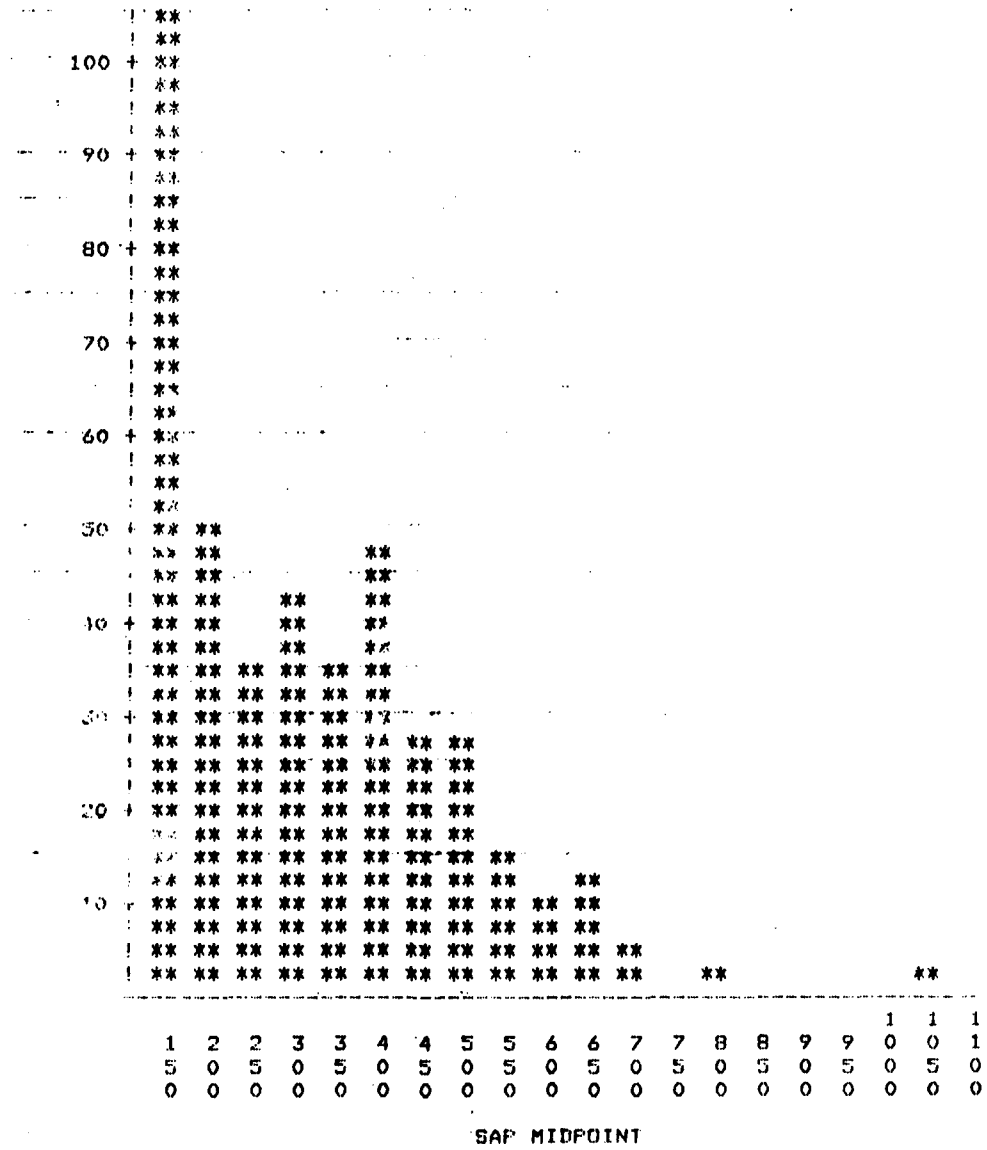
SAP MIDPOINT

FIGURE E-7. AVERAGE TEXTURE DEPTH MEASURED BY THE SAND PATCH
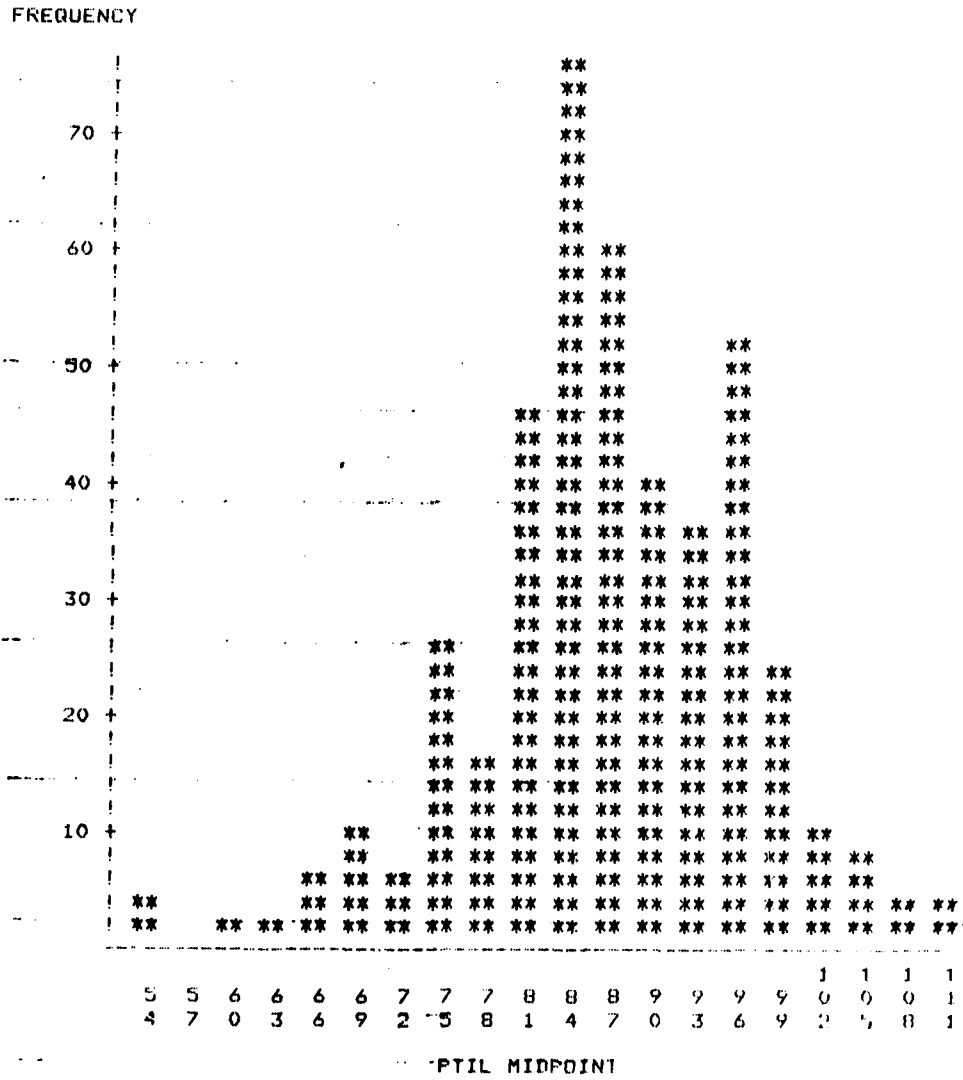PROCEDURE EXPRESSED IN 10^{-4} in

FREQUENCY BAR CHART

FREQUENCY

```
         !                   **
         !             ** ** **
         !             ** ** **
         !             ** ** **
    50 + !          ** ** ** **
         !          ** ** ** **
         !          ** ** ** **
         !       ** ** ** ** **
         !       ** ** ** ** **
    40 + !    ** ** ** ** ** **
         !    ** ** ** ** ** ** ** **
         ! ** ** ** ** ** ** ** **
         ! ** ** ** ** ** ** ** ** **
         ! ** ** ** ** ** ** ** **
    30 + ! ** ** ** ** ** ** ** **
         ! ** ** ** ** ** ** ** **
         ! ** ** ** ** ** ** ** ** **
         ! ** ** ** ** ** ** ** ** **
         ! ** ** ** ** ** ** ** **
    20 + ! ** ** ** ** ** ** ** **
         ! ** ** ** ** ** ** ** **
         ! ** ** ** ** ** ** ** **    **
         ! ** ** ** ** ** ** ** **  ** **
         ! ** ** ** ** ** ** ** ** ** ** **
    10 + ! ** ** ** ** ** ** ** ** ** ** **
         ! ** ** ** ** ** ** ** ** ** ** **
         ! ** ** ** ** ** ** ** ** ** ** ** **
         ! ** ** ** ** ** ** ** ** ** ** ** ** **
         ! ** ** ** ** ** ** ** ** ** ** ** ** **      **              **
```

```
                                    1  1  1  1  1  1  1  1  1  1  2  2
        2  3  4  5  6  7  8  9  0  1  2  3  4  5  6  7  8  9  0  1
        0  0  0  0  0  0  0  0  0  0  0  0  0  0  0  0  0  0  0  0
        0  0  0  0  0  0  0  0  0  0  0  0  0  0  0  0  0  0  0  0
```

SIP MIDPOINT

FIGURE E-8.   AVERAGE TEXTURE DEPTH MEASURED BY THE SILICONE PUTTY
             PROCEDURE EXPRESSED IN 10-⁴ in

FIGURE E-9. RAW DRAG TEST NUMBERS MEASURED DRY IN THE LONGITUDINAL DIRECTION

FIGURE E-10. RAW DRAG TEST NUMBERS MEASURED DRY IN THE TRANSVERSE DIRECTION

1.0 ▊▊▊
4.5
5.0
5.6
6.3
7.1
2.8
3.2
3.6
4.0
2.5
2.2
2.0
1.8
1.1 ▊▊▊
1.25 ▊▊▊ 1.4 ▊▊▊ 1.6 ▊▊▊
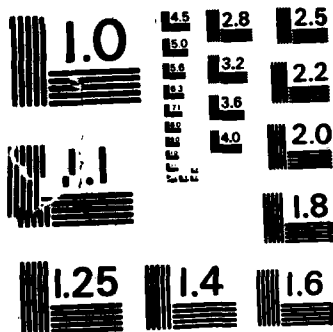
MICROCOPY RESOLUTION TEST CHART
NATIONAL BUREAU OF STANDARDS – 1963 – A

FREQUENCY BAR CHART

FREQUENCY

```
        !                          **
     70 +                          **
        !                          **
        !                          **
        !                          **
        !                          **
     60 +                          **
        !                          **
        !                          **
        !                          **
        !                          **
     50 +                          **
        !                  **       **       **
        !                  **       **       **
        !                  **       ** ** **
     40 +            ** ** ** ** ** **
        !            ** ** ** ** ** **
        !            ** ** ** ** ** **
        !            ** ** ** ** ** **
        !            ** ** ** ** ** **
        !            ** ** ** ** ** ** **
     30 +            ** ** ** ** ** ** **
        !            ** ** ** ** ** ** **
        !            ** ** ** ** ** ** **
        !            ** ** ** ** ** ** **
        !            ** ** ** ** ** ** **
        !            ** ** ** ** ** ** **
     20 +            ** ** ** ** ** ** **
        !      **    ** ** ** ** ** ** ** **
        !      **    ** ** ** ** ** ** ** **
        !      ** ** ** ** ** ** ** ** ** **
        !      ** ** ** ** ** ** ** ** ** **
     10 +      ** ** ** ** ** ** ** ** ** ** **       **
        !   ** ** ** ** ** ** ** ** ** ** ** ** **    **
        ! ** ** ** ** ** ** ** ** ** ** ** ** **    **
        ! ** ** ** ** ** ** ** ** ** ** ** ** ** ** ** **
        ! ** ** ** ** ** ** ** ** ** ** ** ** ** ** ** ** **
```

   30 33 36 39 42 45 48 51 54 57 60 63 66 69 72 75 78 81 84 87

                    PTIWL MIDPOINT
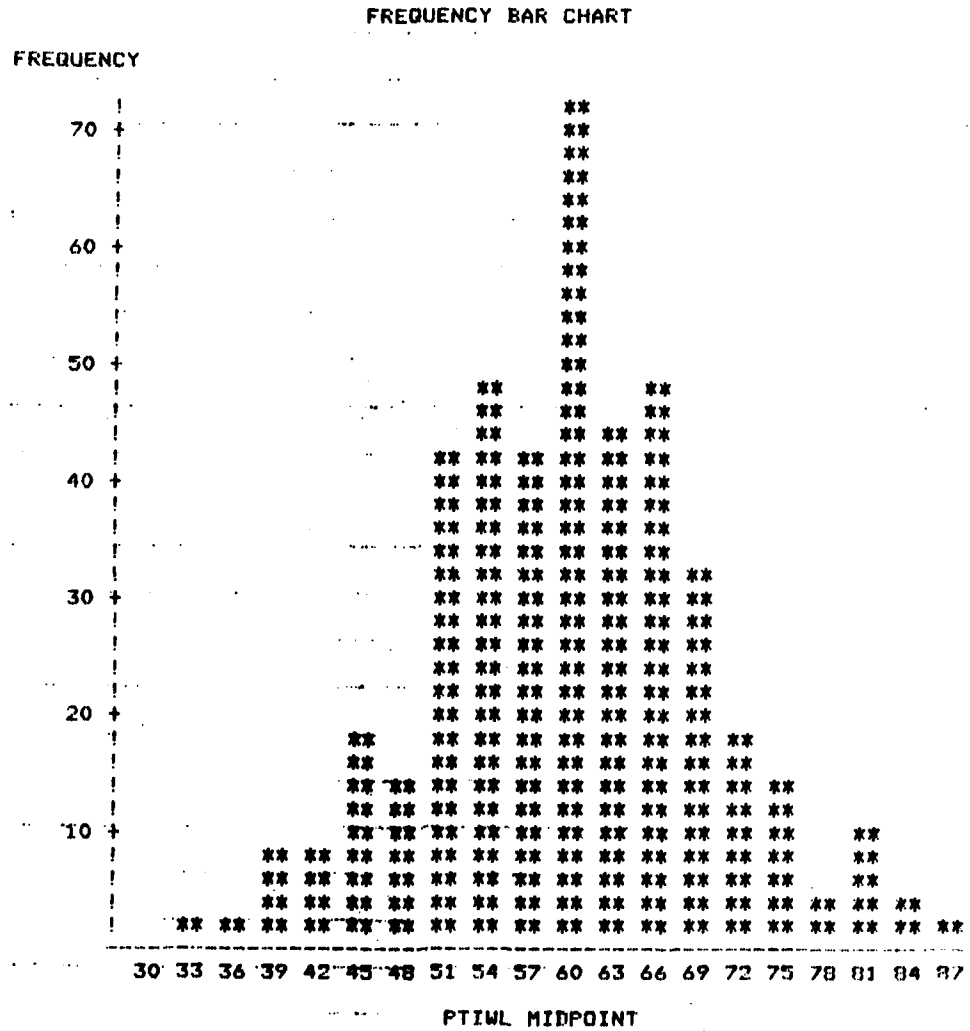
FIGURE E-11. RAW DRAG TEST NUMBERS MEASURED WET IN THE LONGITUDINAL
             DIRECTION

89

FIGURE E-12. RAW DRAG TEST NUMBERS MEASURED WET IN THE TRANSVERSE DIRECTION

FIGURE E-13. CHALK WEAR COEFFICIENT MEASURED IN THE LONGITUDINAL
DIRECTION EXPRESSED IN 10^{-4} in/ft

91

FREQUENCY BAR CHART

FREQUENCY

CTT MIDPOINT

FIGURE E-14. CHALK WEAR COEFFICIENT MEASURED IN THE TRANSVERSE DIRECTION EXPRESSED IN 10^{-4} in/ft

92

APPENDIX F
COMPARISON PLOTS OF PREDICTED VERSUS MEASURED FRICTION VALUES

PLOT OF P1*MW40   SYMBOL USED IS *
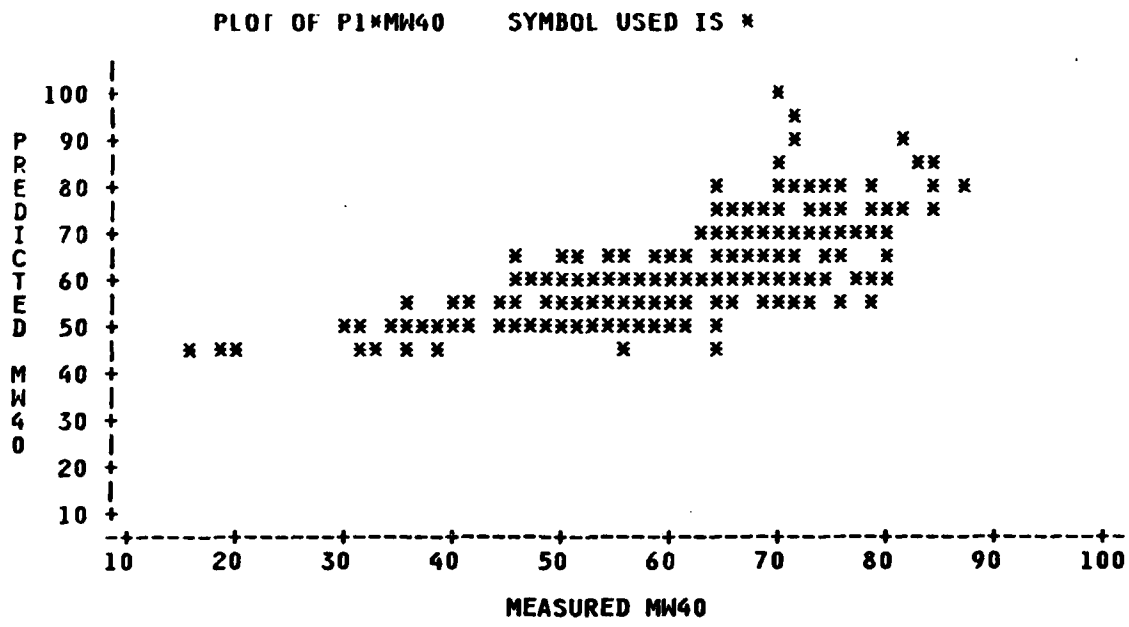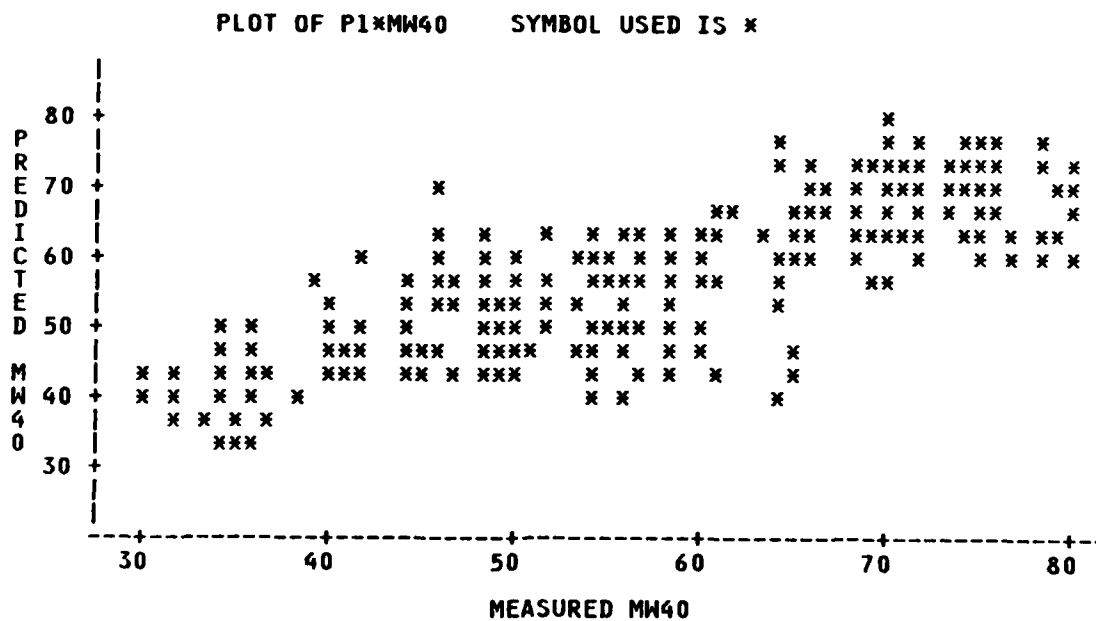
FIGURE F-1. MW40 PREDICTED BY REGRESSION MODEL EQUATION 5
             COMPARED WITH MEASURED MW40 VALUES

PLOT OF P*MW40   SYMBOL USED IS *
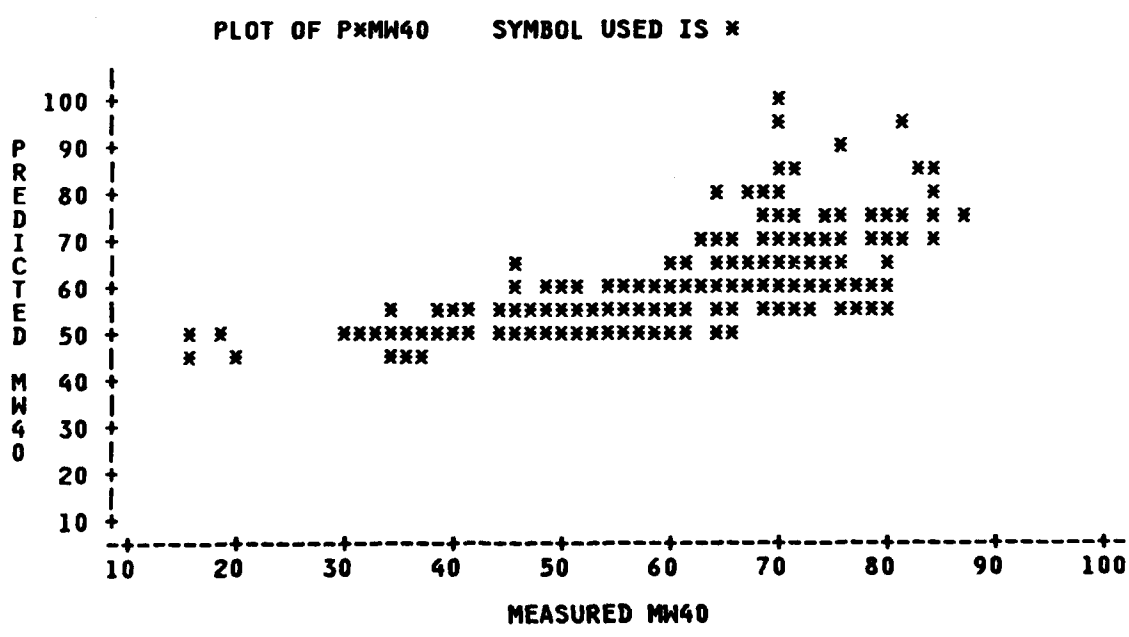
FIGURE F-2. MW40 PREDICTED BY REGRESSION MODEL EQUATION 6
             COMPARED WITH MEASURED MW40 VALUES

PLOT OF P*M   SYMBOL USED IS *
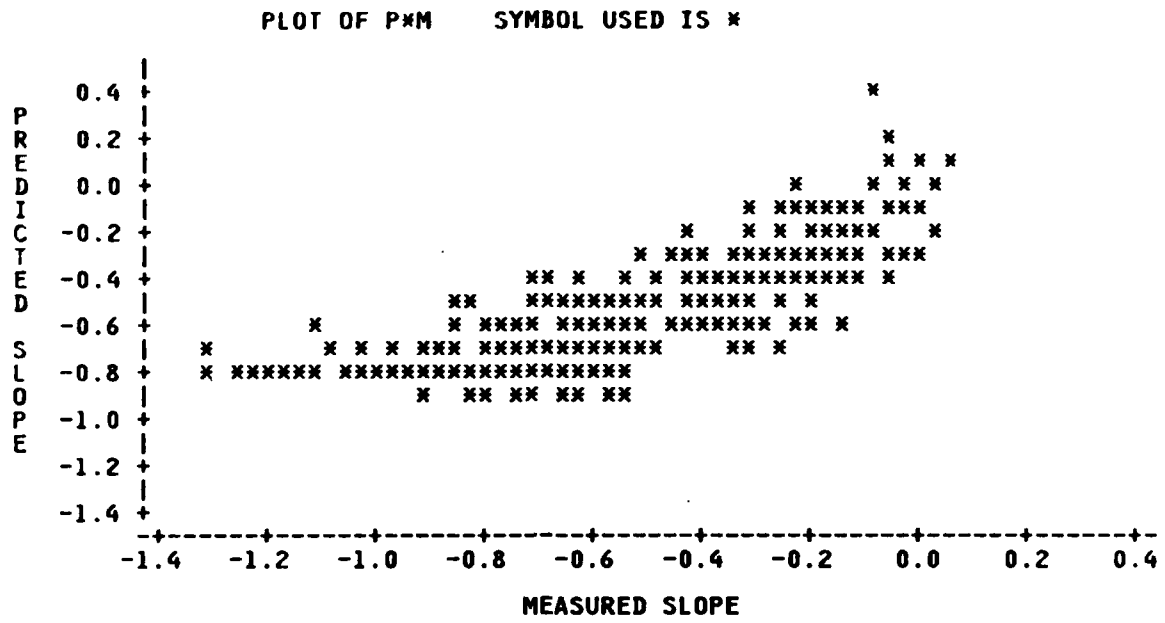
MEASURED SLOPE

FIGURE F-3.   SLOPE PREDICTED BY REGRESSION MODEL EQUATION 7
             COMPARED WITH MEASURED SLOPE VALUES

PLOT OF P1*M   SYMBOL USED IS *
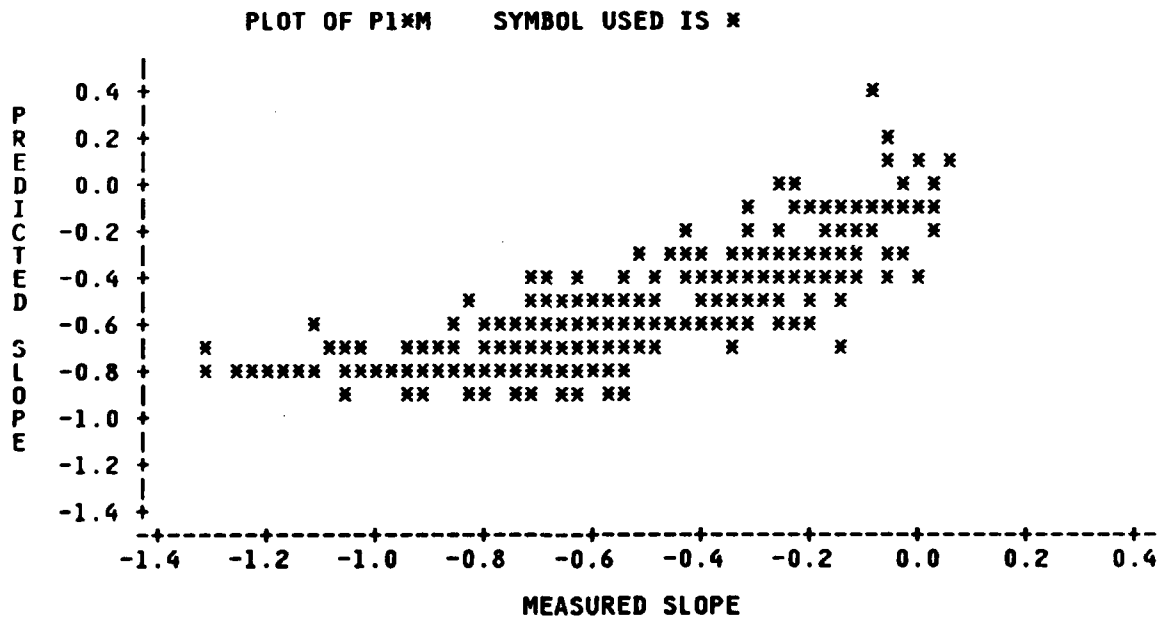
MEASURED SLOPE

FIGURE F-4.   SLOPE PREDICTED BY REGRESSION MODEL EQUATION 8
             COMPARED WITH MEASURED SLOPE VALUES

95

PLOT OF P2×M   SYMBOL USED IS ×
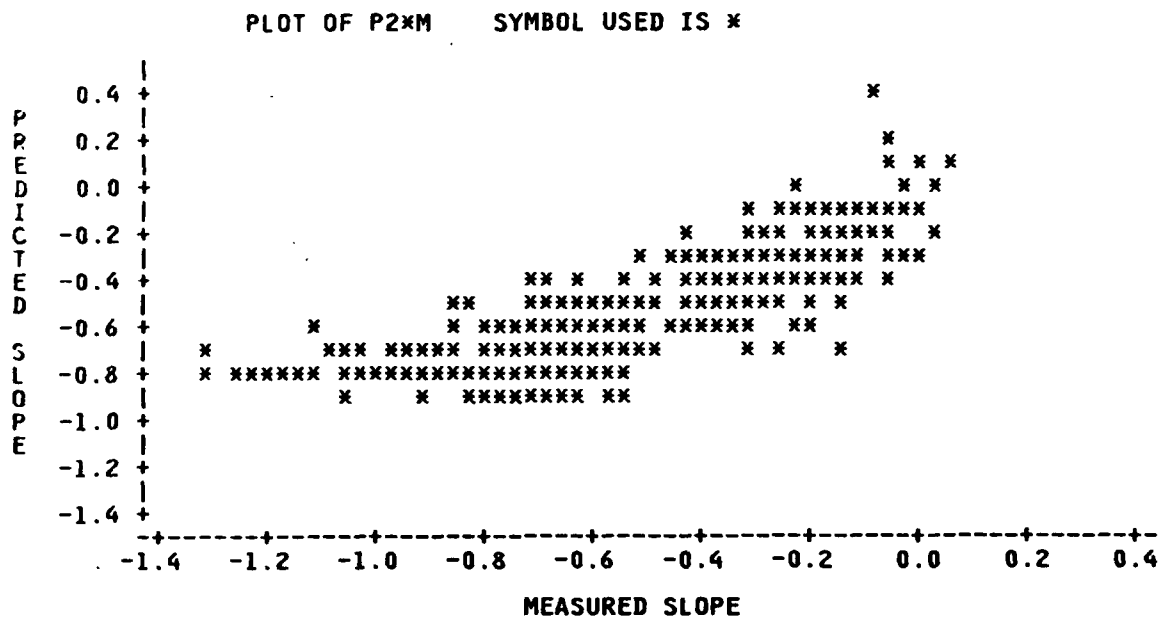
FIGURE F-5.   SLOPE PREDICTED BY REGRESSION MODEL EQUATION 9
              COMPARED WITH MEASURED SLOPE VALUES

PLOT OF P3×B   SYMBOL USED IS ×
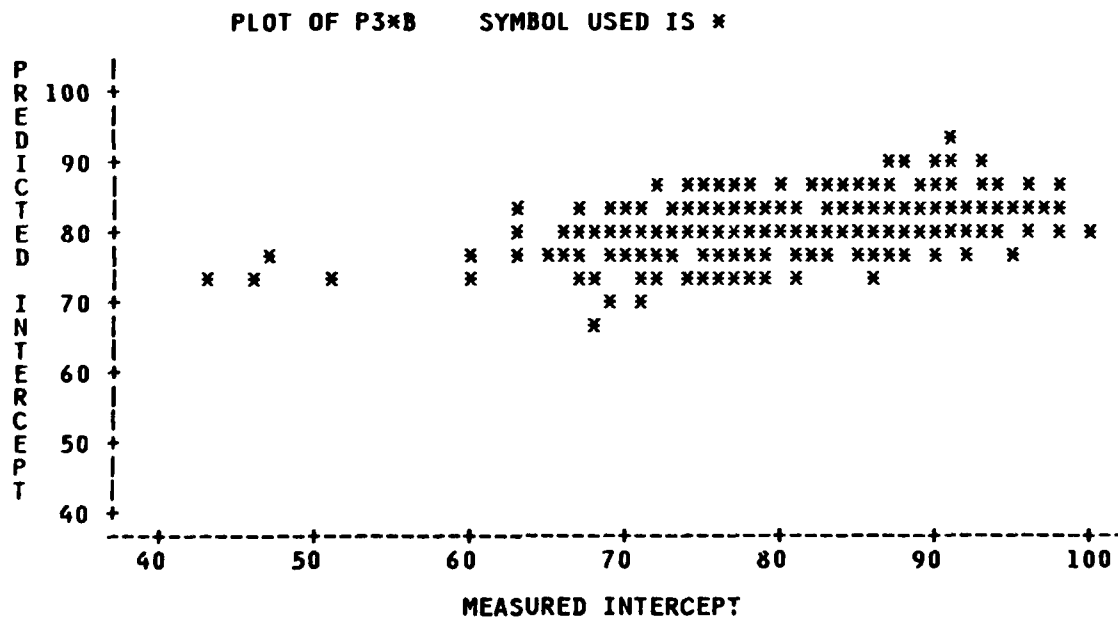
FIGURE F-6.   INTERCEPT PREDICTED BY REGRESSION MODEL EQUATION 10
              COMPARED WITH MEASURED INTERCEPT VALUES
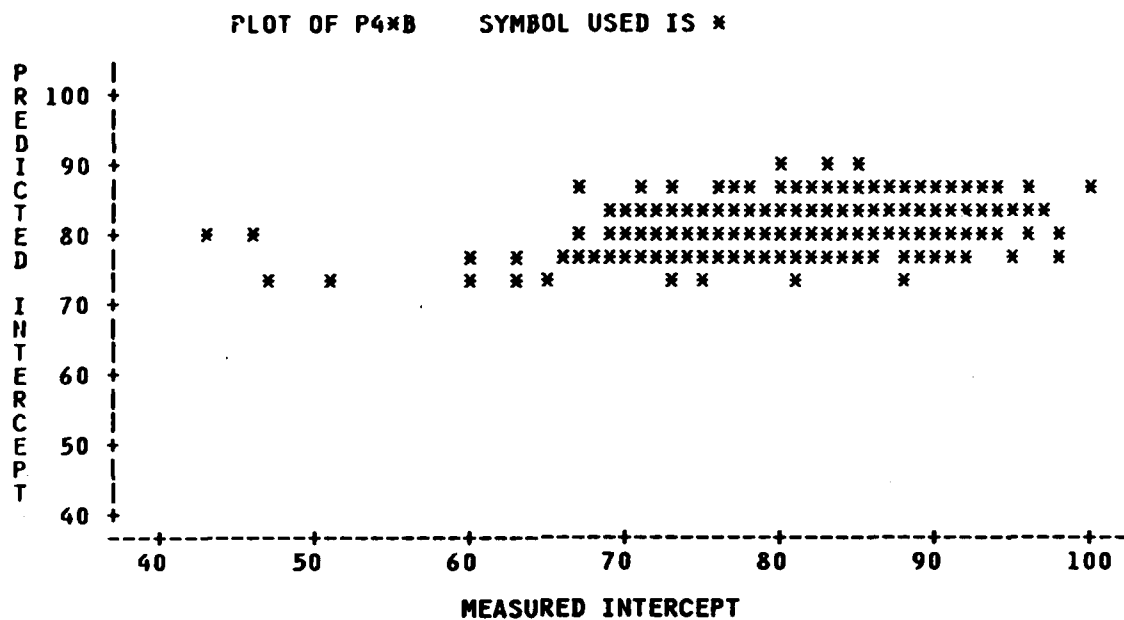
FIGURE F-7. INTERCEPT PREDICTED BY REGRESSION MODEL EQUATION 11
COMPARED WITH MEASURED INTERCEPT VALUES
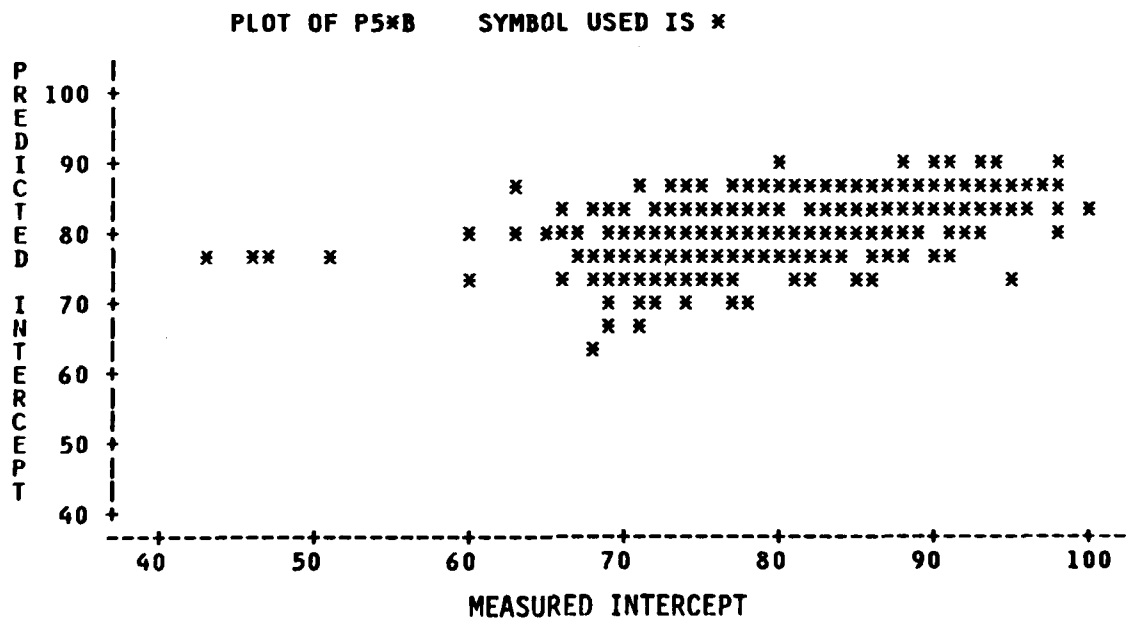
FIGURE F-8. INTERCEPT PREDICTED BY REGRESSION MODEL EQUATION 12
COMPARED WITH MEASURED INTERCEPT VALUES

PLOT OF P6*CMAC   SYMBOL USED IS *
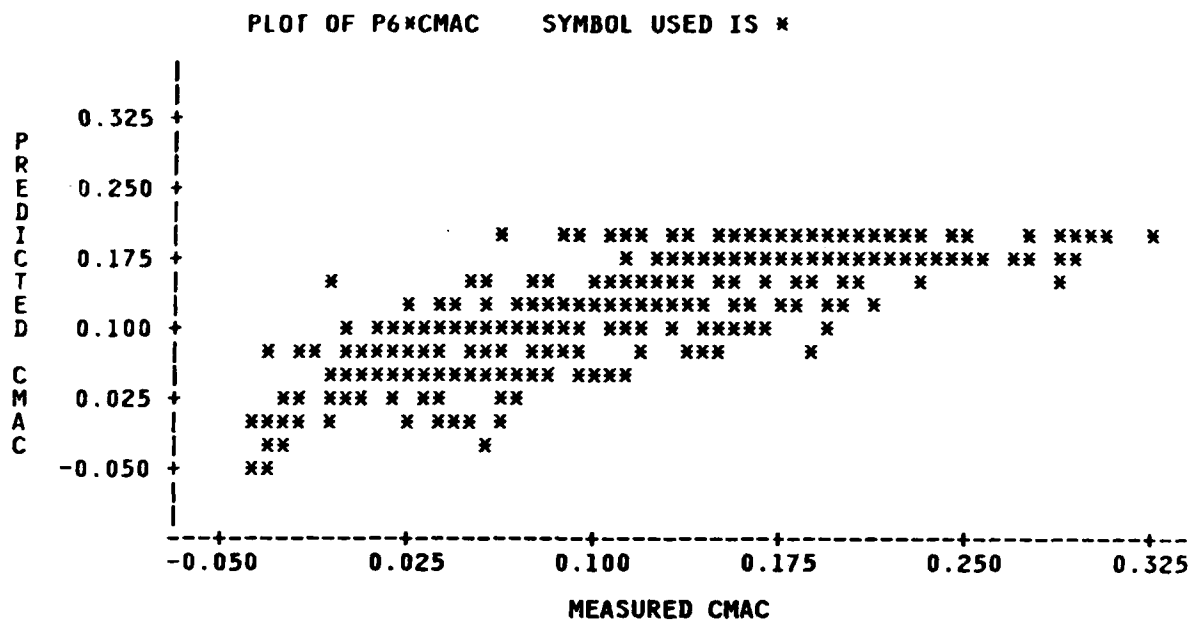
FIGURE F-9. C_{mac} PREDICTED BY REGRESSION MODEL EQUATION 21
COMPARED WITH C_{mac} VALUES

PLOT OF P7*CMIC   SYMBOL USED IS *
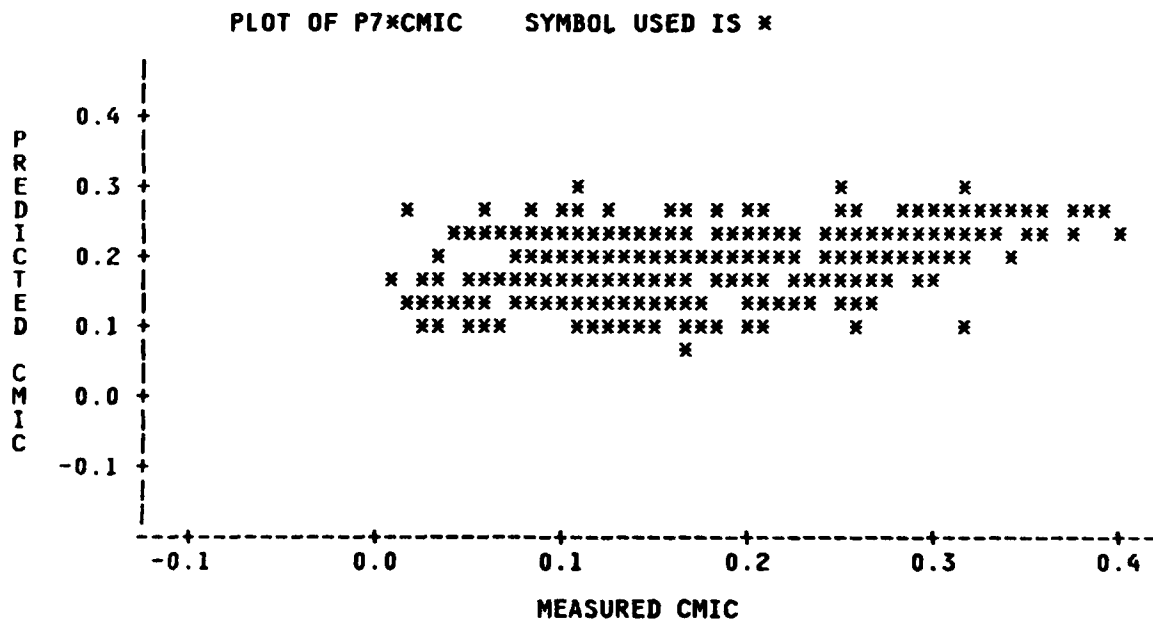
FIGURE F-10. C_{mic} PREDICTED BY REGRESSION MODEL EQUATION 22
COMPARED WITH MEASURED C_{mic} VALUES

98

PLOT OF P*MW40   SYMBOL USED IS *
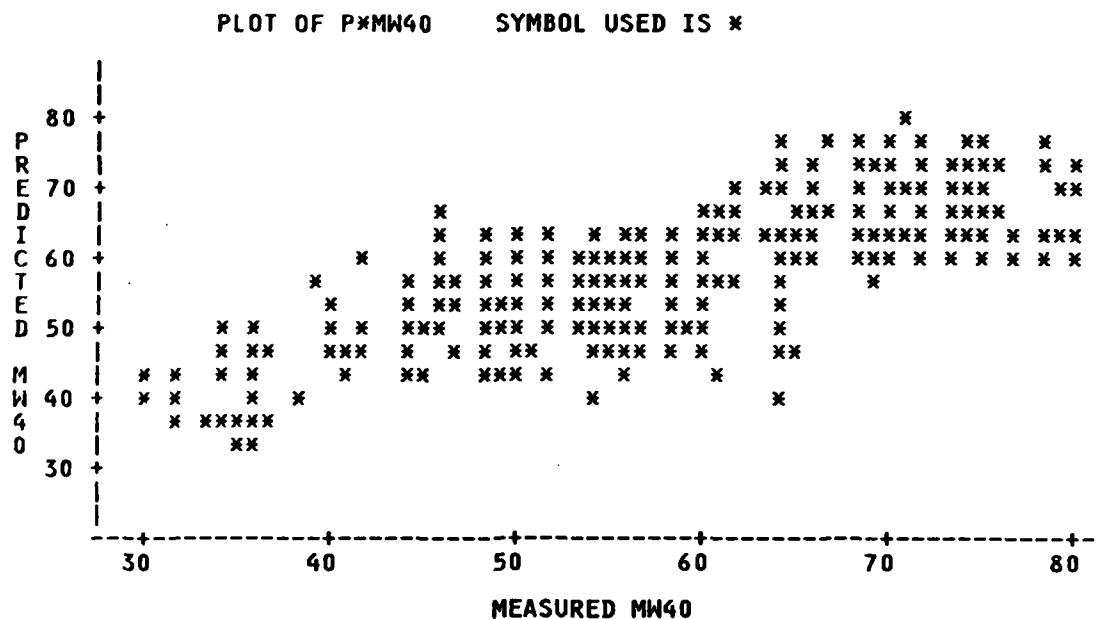
FIGURE F-11. MW40 PREDICTED BY REGRESSION MODEL EQUATION 23
COMPARED WITH MEASURED MW40 VALUES
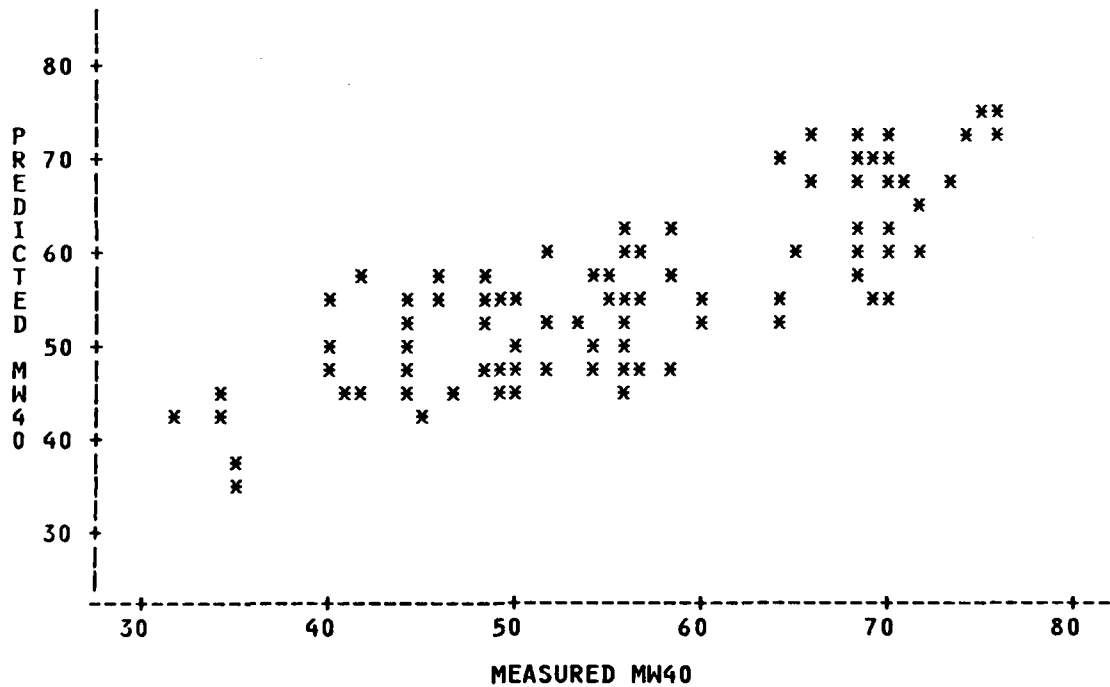
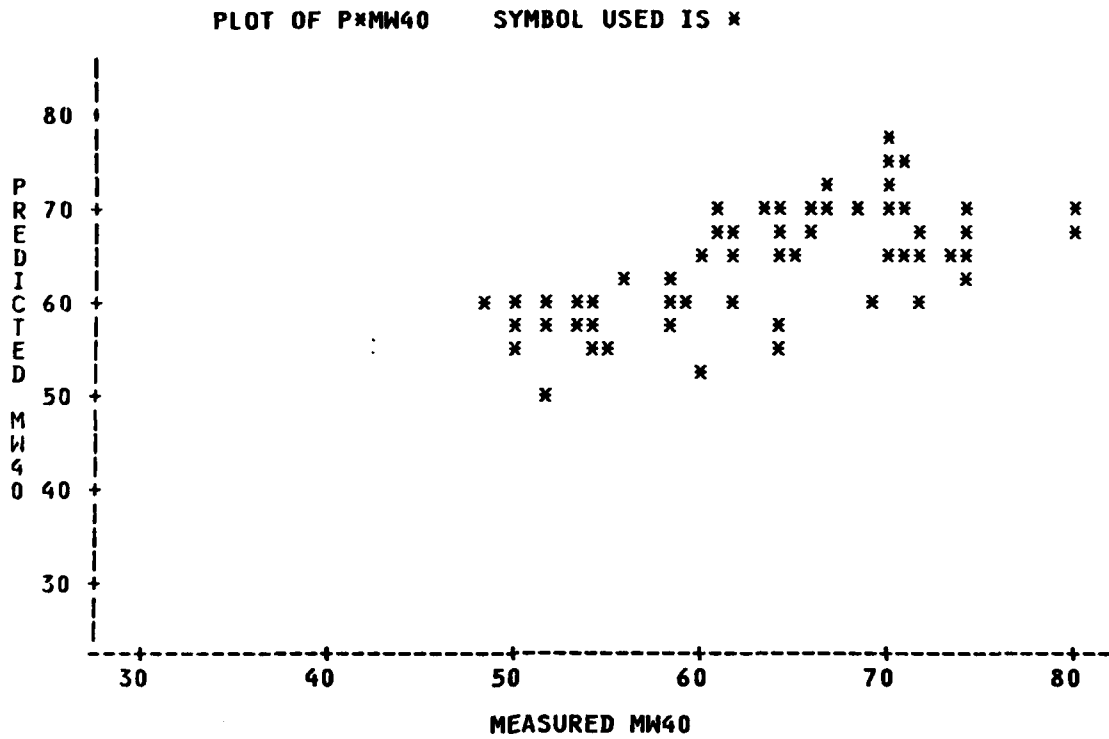PLOT OF P1*MW40   SYMBOL USED IS *

FIGURE F-12. MW40 PREDICTED BY REGRESSION MODEL EQUATION 24
COMPARED WITH MEASURED MW40 VALUES
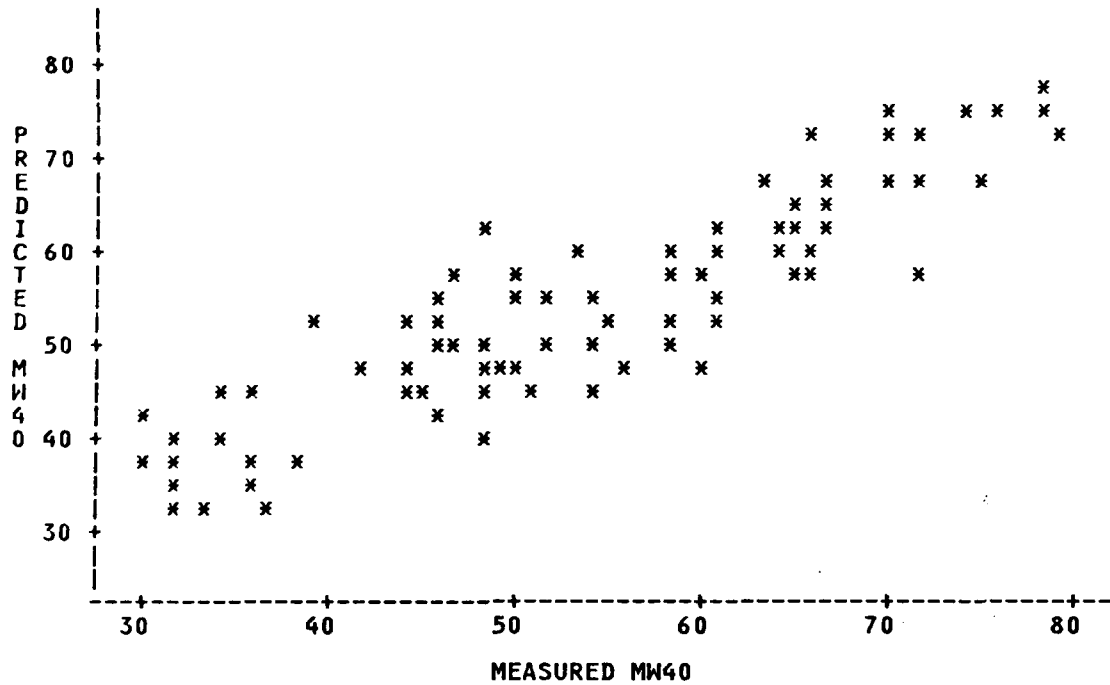
FIGURE F-13. MW40 PREDICTED BY REGRESSION MODEL EQUATION 25
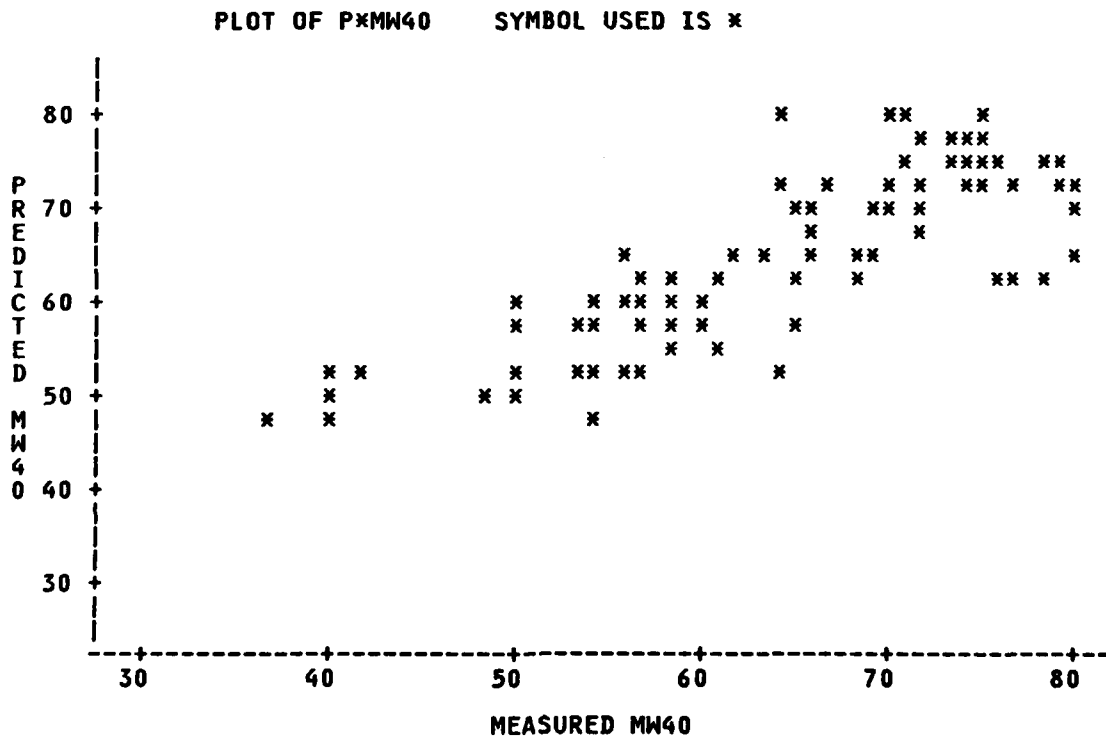COMPARED WITH MEASURED MW40 VALUES

FIGURE F-14. MW40 PREDICTED BY REGRESSION MODEL EQUATION 26
COMPARED WITH MEASURED MW40 VALUES

100

PLOT OF P*MW40   SYMBOL USED IS *

FIGURE F-15. MW40 PREDICTED BY REGRESSION MODEL EQUATION 27
COMPARED WITH MEASURED MW40 VALUES

PLOT OF P*MW40   SYMBOL USED IS *

FIGURE F-16. MW40 PREDICTED BY REGRESSION MODEL EQUATION 28
COMPARED WITH MEASURED MW40 VALUES

101

END

DTIC

6 — 86